


May 2019

Part I: An Investigation of Calcitroic Acid and Its Phase II Conjugates. Part II: Toward the Development of a Novel Orally-available Asthma Treatment Targeting Gabaa Receptors in the Lungs

Olivia B. Yu

University of Wisconsin-Milwaukee

Follow this and additional works at: <https://dc.uwm.edu/etd>

 Part of the [Biochemistry Commons](#), and the [Organic Chemistry Commons](#)

Recommended Citation

Yu, Olivia B., "Part I: An Investigation of Calcitroic Acid and Its Phase II Conjugates. Part II: Toward the Development of a Novel Orally-available Asthma Treatment Targeting Gabaa Receptors in the Lungs" (2019). *Theses and Dissertations*. 2146.
<https://dc.uwm.edu/etd/2146>

This Dissertation is brought to you for free and open access by UWM Digital Commons. It has been accepted for inclusion in Theses and Dissertations by an authorized administrator of UWM Digital Commons. For more information, please contact open-access@uwm.edu.

PART I: AN INVESTIGATION OF CALCITROIC ACID AND ITS PHASE II CONJUGATES

PART II: TOWARD THE DEVELOPMENT OF A NOVEL ORALLY-AVAILABLE ASTHMA

TREATMENT TARGETING GABA_A RECEPTORS IN THE LUNGS

by

Olivia B. Yu

A Dissertation Submitted in
Partial Fulfillment of the
Requirements for the Degree of

Doctor of Philosophy
in Chemistry

at

The University of Wisconsin—Milwaukee

May 2019

ABSTRACT

PART I: AN INVESTIGATION OF CALCITROIC ACID AND ITS PHASE II CONJUGATES

by

Olivia B. Yu

The University of Wisconsin-Milwaukee, 2019
Under the Supervision of Professor Alexander Arnold

Calcitroic acid (CTA) was isolated and characterized more than four decades ago.⁵ Radiolabeled calcitriol (1,25-dihydroxyvitamin D₃) was used at that time to enable the identification of radioactive CTA formed *in vivo*, which was subsequently extracted and characterized by derivatization.⁷ CTA was found to be predominantly formed in the liver and secreted into the gut through the bile duct via enterohepatic circulation, leading to fairly high concentrations of this metabolite of vitamin D in the intestine.⁸ However, assuming it was only a catabolic product of calcitriol, it was ignored thereafter.

Recently, novel experiments showed that CTA can bind the vitamin D receptor (VDR) and initiate gene regulation of certain metabolic enzymes.⁴ The VDR is a nuclear hormone receptor and is present in many tissues.⁹ VDR is a biological sensor with the ability to bind several endogenous ligands. Calcitriol has the highest known affinity for VDR and has been very thoroughly investigated. In contrast to that, very little is known about the main final metabolite of vitamin D: calcitroic acid. Because its binding to VDR is weaker than calcitriol, it was presumed to be biologically inactive at the time of its discovery.

Gene regulation in the presence of CTA has now been demonstrated in epithelia, keratinocytes, and prostate cancer cells.⁸ One assumed function of VDR in the intestine is the regulation of P450 enzymes. These are important enzymes for detoxification, especially with respect to harmful accumulation of toxic endogenous small molecules, such as lithocholic acid. Our hypothesis is that CTA regulates this process in conjunction with VDR for the purpose of preventing the development of inflammation-based gastrointestinal diseases such as irritable bowel syndrome, or even colorectal cancer.

My research has been focused on producing CTA synthetically and testing its effects *in vitro* and *in vivo*. Due to it being unavailable for purchase at a reasonable price and the difficulty of its synthesis, much of my research was focused on modifying and optimizing a lengthy synthetic route to the final product. Secondly, I generated ¹³C-labeled CTA to be used as an isotopic standard to enable the quantification of CTA in bodily fluids. Several proposed phase two conjugates of CTA and the recently discovered other final vitamin D metabolite calcioic acid were also synthesized following novel synthetic routes. We confirmed the binding between these analogs and VDR. The availability of CTA conjugates will support their quantification *in vivo* in future studies using LCMS/MS and MALDI-TOF/TOF. Additionally, VDR's expression in leukocytes has shown immune suppression influence with calcitriol as its ligand. Studies with CTA and its conjugates also have indicated similar anti-inflammatory effects. Further studies will be conducted to determine whether CTA or its conjugates have any of the suspected detoxification properties in the gut.

ABSTRACT

PART II: TOWARD THE DEVELOPMENT OF A NOVEL ORALLY-AVAILABLE ASTHMA TREATMENT TARGETING GABA_A RECEPTORS IN THE LUNGS

by

Olivia B. Yu

The University of Wisconsin-Milwaukee, 2019
Under the Supervision of Professor Alexander Arnold

The treatment and control of asthma remains a persistent modern clinical problem, despite being recognized for decades and occurrence across the globe.¹⁰ The central hallmarks of asthma are chronically inflamed airways, hypersensitivity to certain external stimuli, and obstruction of the airways.¹¹ These characteristics lead to clinical features that include persistent cough, shortness of breath, wheezing, coughing, and chest tightness.¹²

Our laboratory, in collaboration with the Cook laboratory at UWM, is seeking an alternate therapy to combat multiple symptoms associated with living with acute asthma.^{1, 13} Currently available treatments have multiple factors that could be improved upon, from the imprecise dosages of treatment delivered via inhaler¹⁴ to the adverse side effects of systemically administered corticosteroids.¹⁵⁻¹⁹ A better asthma drug alternative would be orally administered to improve patient compliance and eliminate dosage irregularity. Furthermore, unwanted central nervous system effects should be avoided at all cost. Finally, the alternative drug should alleviate a full range of asthma symptoms, such as relaxing the smooth muscle constriction and decreasing inflammation in the airways, rendering combination treatments obsolete.²⁰

Central to achieving those goals is a new therapeutic target for asthma, which is the family of gamma-aminobutyric acid A receptors (GABA_AR). GABA_ARs are ligand-gated chloride ion channels, whose primary function is to regulate intracellular chloride concentrations, especially in neurons. The GABA_ARs consists of five subunits combined into a heteropentamer.²¹ In recent decades, the Cook group has introduced GABA_AR ligands based on the imidazobenzodiazepine scaffold that are selective to certain subtypes of GABA_ARs.²² With recent confirmation that distinct populations of GABA_AR subtypes are present in lung tissue, our collaboration is keen to develop molecules that can target these subtypes. Further investigations have shown that these ligands mediate distinct pharmacological properties including relaxation of airway smooth muscle and anti-inflammation. Proof of concept that GABA_AR ligands can alleviate asthma symptoms was first shown with plant-based positive allosteric modulator honokiol by Munroe et al.²³ Our group has since developed imidazobenzodiazepine-based compounds that target relevant GABA_AR subtypes expressed in the lung with pronounced efficacy in several asthmatic mouse models.^{1, 13, 20, 24} Achieving targeted asthmatic relief with oral medication and thus eliminating the use of corticosteroids is seen as a significant step forward in asthma treatment.

1. Yu, O. B.; Arnold, L. A., Calcitroic Acid—A Review. *ACS Chemical Biology* **2016**, *11* (10), 2665-2672.
2. Esvelt, R. P.; Schnoes, H. K.; DeLuca, H. F., Isolation and characterization of 1.alpha.-hydroxy-23-carboxytetranorvitamin D: a major metabolite of 1,25-dihydroxyvitamin D3. *Biochemistry* **1979**, *18* (18), 3977-3983.
3. Onisko, B. L.; Esvelt, R. P.; Schnoes, H. K.; DeLuca, H. F., Metabolites of 1 alpha, 25-dihydroxyvitamin D3 in rat bile. *Biochemistry* **1980**, *19* (17), 4124-30.
4. Teske, K. A.; Bogart, J. W.; Sanchez, L. M.; Yu, O. B.; Preston, J. V.; Cook, J. M.; Silvaggi, N. R.; Bikle, D. D.; Arnold, L. A., Synthesis and evaluation of vitamin D receptor-mediated activities

- of cholesterol and vitamin D metabolites. *European journal of medicinal chemistry* **2016**, *109*, 238-46.
5. Pike, W. S., N. K., In *Vitamin D*, 2005; Vol. 2nd Ed.
 6. Trends in Asthma Morbidity and Mortality. . Services., A. L. A. E. S. U. R. a. P., Ed.
 7. Pascual, R. M.; Peters, S. P., Airway remodeling contributes to the progressive loss of lung function in asthma: an overview. *The Journal of allergy and clinical immunology* **2005**, *116* (3), 477-86; quiz 487.
 8. Moorman, J. E.; Rudd, R. A.; Johnson, C. A.; King, M.; Minor, P.; Bailey, C.; Scalia, M. R.; Akinbami, L. J., National surveillance for asthma--United States, 1980-2004. *Morbidity and mortality weekly report. Surveillance summaries (Washington, D.C. : 2002)* **2007**, *56* (8), 1-54.
 9. Forkuo, G. S.; Nieman, A. N.; Yuan, N. Y.; Kodali, R.; Yu, O. B.; Zahn, N. M.; Jahan, R.; Li, G.; Stephen, M. R.; Guthrie, M. L.; Poe, M. M.; Hartzler, B. D.; Harris, T. W.; Yocum, G. T.; Emala, C. W.; Steeber, D. A.; Stafford, D. C.; Cook, J. M.; Arnold, L. A., Alleviation of Multiple Asthmatic Pathologic Features with Orally Available and Subtype Selective GABAA Receptor Modulators. *Molecular pharmaceuticals* **2017**, *14* (6), 2088-2098.
 10. Jahan, R.; Stephen, M. R.; Forkuo, G. S.; Kodali, R.; Guthrie, M. L.; Nieman, A. N.; Yuan, N. Y.; Zahn, N. M.; Poe, M. M.; Li, G.; Yu, O. B.; Yocum, G. T.; Emala, C. W.; Stafford, D. C.; Cook, J. M.; Arnold, L. A., Optimization of substituted imidazobenzodiazepines as novel asthma treatments. *European journal of medicinal chemistry* **2017**, *126*, 550-560.
 11. *Guidelines for the Diagnosis and Management of Asthma*; National Heart, Lung, and Blood Institute: August 2007.
 12. Cates, C. J.; Cates, M. J., Regular treatment with formoterol for chronic asthma: serious adverse events. *The Cochrane database of systematic reviews* **2012**, (4), Cd006923.
 13. Cates, C. J.; Cates, M. J., Regular treatment with salmeterol for chronic asthma: serious adverse events. *The Cochrane database of systematic reviews* **2008**, (3), Cd006363.
 14. Dahl, R., Systemic side effects of inhaled corticosteroids in patients with asthma. *Respiratory medicine* **2006**, *100* (8), 1307-17.
 15. Kelly, H. W.; Sternberg, A. L.; Lescher, R.; Fuhlbrigge, A. L.; Williams, P.; Zeiger, R. S.; Raissy, H. H.; Van Natta, M. L.; Tonascia, J.; Strunk, R. C., Effect of inhaled glucocorticoids in childhood on adult height. *The New England journal of medicine* **2012**, *367* (10), 904-12.
 16. Lipworth, B. J., Systemic adverse effects of inhaled corticosteroid therapy: A systematic review and meta-analysis. *Archives of internal medicine* **1999**, *159* (9), 941-55.
 17. Forkuo, G. S.; Nieman, A. N.; Kodali, R.; Zahn, N. M.; Li, G.; Rashid Roni, M. S.; Stephen, M. R.; Harris, T. W.; Jahan, R.; Guthrie, M. L.; Yu, O. B.; Fisher, J. L.; Yocum, G. T.; Emala, C. W.; Steeber, D. A.; Stafford, D. C.; Cook, J. M.; Arnold, L. A., A Novel Orally Available Asthma Drug Candidate That Reduces Smooth Muscle Constriction and Inflammation by Targeting GABAA Receptors in the Lung. *Molecular pharmaceuticals* **2018**, *15* (5), 1766-1777.

18. Olsen, R. W.; Sieghart, W., International Union of Pharmacology. LXX. Subtypes of gamma-aminobutyric acid(A) receptors: classification on the basis of subunit composition, pharmacology, and function. Update. *Pharmacological reviews* **2008**, *60* (3), 243-60.
19. Sieghart, W.; Savic, M. M., International Union of Basic and Clinical Pharmacology. CVI: GABAA Receptor Subtype- and Function-selective Ligands: Key Issues in Translation to Humans. *Pharmacological reviews* **2018**, *70* (4), 836-878.
20. Munroe, M. E.; Businga, T. R.; Kline, J. N.; Bishop, G. A., Anti-Inflammatory Effects of the Neurotransmitter Agonist Honokiol in a Mouse Model of Allergic Asthma. *The Journal of Immunology* **2010**, *185* (9), 5586-5597.
21. Forkuo, G. S.; Guthrie, M. L.; Yuan, N. Y.; Nieman, A. N.; Kodali, R.; Jahan, R.; Stephen, M. R.; Yocum, G. T.; Treven, M.; Poe, M. M.; Li, G.; Yu, O. B.; Hartzler, B. D.; Zahn, N. M.; Ernst, M.; Emala, C. W.; Stafford, D. C.; Cook, J. M.; Arnold, L. A., Development of GABAA Receptor Subtype-Selective Imidazobenzodiazepines as Novel Asthma Treatments. *Molecular pharmaceutics* **2016**, *13* (6), 2026-38.

© Copyright by Olivia B. Yu, 2019
All Rights Reserved

TABLE OF CONTENTS

LIST OF FIGURES.....	x
LIST OF SCHEMES	xiv
LIST OF ABBREVIATIONS	xv
PART I: AN INVESTIGATION OF CALCITROIC ACID AND ITS PHASE II CONJUGATES.....	1
1.1 A Brief History of Vitamin D	2
1.2 The Structure and Function of the Vitamin D Receptor	6
1.3 The Phase I Metabolism of Vitamin D and Calcitroic Acid	13
1.4 The Synthesis of Calcitroic Acid	20
1.5 Synthetic Strategy for Production of Calcitroic Acid.....	26
1.6 Characterization of Calcitroic Acid Synthesis Compounds	43
1.7 Biological Characterization of Calcitroic Acid	58
1.8 The Phase II Metabolism of Calcitroic Acid.....	87
1.9 Synthetic Strategy for the Production of Calcitroic Acid Conjugates	93
1.10 Characterization of Calcitroic Acid Conjugates.....	102
1.11 A Brief Biological Characterization of Calcitroic Acid Conjugates.....	109
PART II: TOWARD THE DEVELOPMENT OF A NOVEL ORALLY-AVAILABLE ASTHMA TREATMENT TARGETING GABA _A RECEPTORS IN THE LUNGS	119
2.1 A Brief Introduction to Asthma.....	120
2.2 Mucin Volume Density as a Marker of Asthmatic Disease State.....	126
References	138
Curriculum Vitae	148

LIST OF FIGURES

Figure 1: (a) The 12 α -helices of VDR represented as cylinders, with the activating domain helix shown in its closed position (pink) and its native ligand bound (yellow ball-and-stick). (b) The binding pocket cavity (blue mesh) and the anchoring interactions with surrounding residues that hold $1,25(\text{OH})_2\text{D}_3$ in the binding cavity.

Figure 2: A schematic and crystal structure outlining the general domains of a nuclear receptor. Structures adapted courtesy of the Protein Data Bank and Brzozowski AM, et.al.³

Figure 3: Crystal structure of the DBDs of both VDR (left) and its typical heterodimer partner RXR (right) bound to their respective DNA hexameric half-sites.⁶ The light blue alpha helices in both structures bind to the major groove of the DNA. The Zn^{2+} ions taking part in coordination with cysteine residues are shown in gray. (PDB: 1YNW)

Figure 4: A crystal structure of the LBD of VDR. Within the binding pocket resides the calcitriol analogue VitIII 17-20Z (gray ball-and-stick). The short helical peptide in the upper left is the NR2 box of coactivator peptide DRIP 205 complexed to the LBD by way of the coactivator recognition sequence LxxLL. (PDB: 204J)

Figure 5: The flash-frozen RXR-VDR structure in complex with a DNA response element, as imaged by electron microscopy and overlaid with individual crystal structures.² A) Side view shows the ligand binding domains of VDR (orange, facing) and RXR (green, far side) at $\sim 90^\circ$ angle from where they are bound to DNA. B) The DBDs encapsulate the response element DNA, the two recognition helices positioned at about 45° from each other due to the 3 base-pair spacer between the half-sites. Helix 12 is shown on VDR in red, in its closed position with ligands bound (shown in yellow for VDR; blue for RXR).

Figure 6: To identify metabolic products from $1,25(\text{OH})_2\text{D}_3$, the ^{14}C and ^3H analogues were administered. The resulting organ extracts contained an enriched ^3H -labeled material, indicating modification to the side chain in calcitriol's metabolites.

Figure 7: CYP24A1 gene regulation by VDR ligands (7.5 mM) in DU145 cells after 18 hrs. Stars represent $P < 0.001$ (***) compared to vehicle DMSO. Graph courtesy of Teske KA et al.⁴

Figure 8: Saturated with ozone, the MeOH/pyridine solution turns blue

Figure 9: Concentrated doubly-protected C,D-ring takes on a slightly pink hue

Figure 10: Nitrile reaction turns red as we attempt to get salts into solution. When sonicated/heated, sometimes it turned green when everything was in solution

Figure 11: Fluffy quenched DIBAL following aq. NH_4Cl addition and TBME dilution is ready for drying

Figure 12: Faintly seen aqueous and organic layers as reaction turns yellow in Pinnick oxidation

Figure 13: Trimethylsilyldiazo-methane turns the methylating reaction yellow

Figure 14: Finely ground, oxidized PDC turning black during the reaction

Figure 15: Wittig-Horner reaction at different stages. From left to right: the deprotonation of organophosphine oxide by *n*-BuLi; reaction color darkened upon brief removal from dry ice bath to ensure full consumption of *n*-BuLi; an unsuccessful reaction turned peach color when quenched by water.

Figure 16: CYP24A1 upregulation by synthetic phase 2 metabolites of lithocholic acid, LCA, and CTA (7.5 μM) in DU145 prostate cancer cells, with $1,25(\text{OH})_2\text{D}_3$ (20nM) as a positive control and DMSO as a negative control.

Figure 17: Modulation of binding of SRC2-3 to VDR-LBD in presence of LG190178 as a function of displacement by CTA (A) and CTA methyl ester (B).

Figure 18: Other nuclear receptors and their fluorescently labeled peptide sequences did not depolarize light in the presence of CTA, providing evidence that CTA's binding to VDR is specific.

Figure 19: Stick-figure overlays of calcitriol (cyan) and CTA (yellow) within the binding pocket of VDR.

Figure 20: Protein-ligand interactions between CTA and VDR. Green arrows indicate side-chain donation/acceptance.

Figure 21: CTA in the binding pocket of zVDR LBD. The two OH residues on the A-ring (lower left, red) are anchored by donor/acceptor interactions with Tyr, Ser, and Arg residues, while the acid function (upper right, red) interacts with histidine.

Figure 22: Protein crystals of (A) human LBD-VDR and (B) zebrafish LBD-VDR

Figure 23: Detailed view of donor/acceptor interactions. (A) The acid functionality on CTA's side chain interacts through solvent contact with His 423. (B) On the other end of the molecule and binding pocket, the two hydroxyl groups make both donor and acceptor contacts with Ser 306, Tyr 175, Ser 265, and Arg 302.

Figure 24: (A) The PXR-BODIPY FL vindoline interaction was not inhibited in the presence of CTA. (B) The CAR-PGC1 α interaction was not inhibited in the presence of CTA.

Figure 25: Combined dose response curves showing partial agonistic activity (teal) and competitive inhibition in the presence of calcitriol (pink) of CTA with VDR.

Figure 26: Transcriptional activity was absent in assays of other nuclear receptors treated with CTA.

Figure 27: (A) Nitric oxide suppression as measured by Griess assay following stimulation with 150units/mL IFN γ and 50ng/mL LPS in RAW264.7 murine macrophages. 1,25(OH) $_2$ D $_3$ and CTA exhibited a decrease in NO, along with the positive control dexamethasone. (B) Downregulation of mRNA of inflammatory species in the presence of CTA and calcitriol, along with positive control dexamethasone.

Figure 28: CYP3A4 upregulation by CTA (6 μ M) in Caco2 cells. DMSO is a negative control. No upregulation of other CYP mRNA was seen under these conditions.

Figure 29: Gel of CYP3A4 primer, which is differentially upregulated by CTA and calcitriol.

Figure 30: Upregulation by CTA and lithocholic acid (both 10 μ M) in HIEC6 human normal intestinal epithelial cells, with 1,25(OH) $_2$ D $_3$ (20nM) as a positive control and DMSO at a negative control, against CYP3A4 (A) and CYP24A1 (B).

Figure 31: Microsomal digestion of CTA (A), calcitriol (B), and both CTA and calcitriol (C).

Figure 32: Binding curves for conjugates by FP analysis. EC $_{50}$ values: calcioic acid (71 \pm 4 μ M), CTA taurine (145 \pm 25 μ M), CTA glycine (92 \pm 17 μ M), CTA mono sulfate (92 \pm 5 μ M), CTA bis sulfate (139 \pm 20 μ M).

Figure 33: Transcription activation of CTA and its conjugates and related compounds, shown as percentages of full calcitriol activation at 60nM. EC $_{50}$ of CTA taurine is 49 \pm 21 μ M.

Figure 34: Significant deviation from stimulated macrophage (DMSO-treated) NO production seen at 12.5 μ M, with trends increasing in significance at higher concentrations

Figure 35: Toxicity assay for macrophages. No toxicity was seen up to 100 μ M for any of the compounds

Figure 36: Goblet cells adopted from <https://www.histology.leeds.ac.uk>

Figure 37: Overlay of GFP and RFP filtered images of ovalbumin sensitized and challenged mouse airway epithelium

Figure 38: Using ROI manager to quantify data concerning drawn line segments in airway epithelium image opened in ImageJ

Figure 39: (a) Representative control: vehicle-only mouse airway epithelium; (b) Representative positive control/treatments: ovalbumin sensitized and challenged mouse airway epithelium. Note that all mice tested with small molecules also had the same appearance; (c) Representative negative control: the corticosteroid dexamethasone decreased mucin quantities.

Figure 40: Mucin volume densities of mouse lungs treated with compound 1. CTL: Non-challenged; vehicle (3 % DMSO, 20% propylene glycol and 77% water) given i.p. twice a day for 5 days; Dexamethasone (Dex) 4 mg/kg/day i.p. (5 days); Cmpd1: 20 mg/kg b.i.d., i.p. for 5 days or 40 minutes before euthanasia; osmotic mini-pumps that release 20 mg/kg/day for 7 days. Data is represented as mean \pm SEM, n = 7. ANOVA repeated measured was used for statistical analysis; *, **, *** indicates $p < 0.05$ with reference to the vehicle injection/pumps mice.

Figure 41: Mucin volume densities for Compound 2.1 CTL: non-challenged; vehicle gavage: vehicle (3 % DMSO, 20% propylene glycol and 77% water) administered twice daily for 5 days by oral gavage; Cmpd 2 gavage: 100 mg/kg administered twice daily for 5 days by oral gavage. Data is represented as mean \pm SEM, n = 7. ANOVA repeated measured was used for statistical analysis; *, **, *** indicates $p < 0.05$, $p < 0.01$, $p < 0.001$, respectively with reference to the vehicle gavage mice.

Figure 42: Mucin volume densities for Compound 3.1 CTL: non-challenged; vehicle injection: vehicle (3 % DMSO, 20% propylene glycol and 77% water) administered i.p. twice daily for 5 days.; Cmpd 3 inj.: 20 mg/kg b.i.d., i.p. for 5 days or 40 minutes before euthanasia. Data is represented as mean \pm SEM, n = 7. ANOVA repeated measured was used for statistical analysis; *, **, *** indicates $p < 0.05$, $p < 0.01$, $p < 0.001$, respectively with reference to the vehicle injection mice.

LIST OF SCHEMES

Scheme 1: The metabolism of various vitamin D metabolites and analogues to CTA.

Scheme 2: Synthesis of CTA starting from a cholesterol analogue precursor.

Scheme 3: Synthesis of CTA using a provitamin D precursor.

Scheme 4: Synthesis of CTA starting from a seco-steroid precursor.

Scheme 5: Synthesis of CTA starting from vitamin D₂ using a Ring A phosphine oxide synthon

LIST OF ABBREVIATIONS

1,25(OH) ₂ D ₃ : 1,25-dihydroxyvitamin D ₃ ; calcitriol	HIEC: human epithelial intestinal cells
25(OH)D ₃ : 25-hydroxyvitamin D ₃	HLM: human liver microsomes
ACN: acetonitrile	HOCl: hypochlorous acid
AF-1 or -2: activating function 1 or 2	IC ₅₀ : 50% inhibitory concentration
CAR: constitutive androgen receptor	IFN γ : interferon gamma
CHCl ₃ : chloroform	IL-1b: interleukin 1beta
CMV: cytomegalovirus	iNOS: nitric oxide synthase
CSA: camphorsulfonic acid	KCN: potassium cyanide
CTA: calcitric acid	KF: potassium fluoride
CuSO ₄ : copper sulfate	KOH: potassium hydroxide
CYP: cytochrome p450	LBD: ligand binding domain
DBD: DNA binding domain	LCA: lithocholic acid
DCM: dichloromethane	LCMS: liquid chromatography-mass spectrometry
DI: deionized	IT-TOF: ion trap time-of-flight
DIBAL: diisobutylaluminum hydride	LPS: lipopolysaccharide
DMAP: 4-dimethylaminopyridine	MALDI: matrix-assisted laser desorption/ionization
DMF: dimethyl formamide	MeOH: methanol
DMSO: dimethyl sulfoxide	MgSO ₄ : magnesium sulfate
EC ₅₀ : 50% effective concentration	MRM: multiple reaction monitoring
EDCl: ethylcarbodiimide hydrochloride	mRNA: messenger ribonucleic acid
EtOAc: ethyl acetate	MS: mass spectrometry
EtOH: ethanol	NaBH ₄ : sodium borohydride
FBS: fetal bovine serum	NaClO ₂ : sodium chlorite
FP: fluorescence polarization	NaH ₂ PO ₄ : monosodium phosphate
FRET: fluorescence resonance energy transfer	NaHCO ₃ : sodium bicarbonate
GABA _A : gamma-aminobutyric acid A	NaOH: sodium hydroxide
GABA _A R: gamma-aminobutyric acid A receptor	<i>n</i> -BuLi: <i>n</i> -butyl lithium
GFP: green fluorescent protein	NH ₄ Cl: ammonium chloride
H ₂ SO ₄ : sulfuric acid	NH ₄ OH: ammonium hydroxide
HCl: hydrochloric acid	NMM: <i>n</i> -methyl morpholine
Hex: hexanes	NMR: nuclear magnetic resonance
	NO: nitric oxide

O₃: ozone
Ova S/C: ovalbumin sensitized and challenged
PDC: pyridinium dichromate
PXR: pregnane X receptor
qRT-PCR: quantitative reverse transcriptase polymerase chain reaction
RBF: round bottom flask
RFP: red fluorescent protein
RNA: ribonucleic acid
RXR: retinoid X receptor
SPE: solid phase extraction
SRC-1 or 2-3: steroid receptor coactivator 1 or 2-3
TBA: tetrabutyl ammonium
TBAF: tetrabutylammonium fluoride
TBME: *tert*-butyl methyl ether
TBS: *tert*-butyl silyl
TBSOTf: *t*-butyldimethylsilyl trifluoromethanesulfonate
TEA: triethylamine
TFA: trifluoroacetic acid
THF: tetrahydrofuran
TLC: thin layer chromatography
UV: ultraviolet
UWM: University of Wisconsin—Milwaukee
VDR: vitamin D receptor
VDRE: vitamin D response elements

the only good thesis is a finished one

—@AcademicsSay

PART I: AN INVESTIGATION OF CALCITROIC ACID AND ITS PHASE II CONJUGATES

1.1 A Brief History of Vitamin D

The establishment of vitamins as essential to a complete diet is actually a surprisingly new discovery, made after the turn of the twentieth century. While certain diseases caused by vitamin-deficiency had already been discovered and were known to be treatable by supplementing one's diet,²⁵ the reasons behind the supplemental cures were unknown or incorrect at that time. The early 1900's saw the discovery of the first few "vital amines," or vitamins, in large part due to the work of Elmer McCollum. Following the 1910 demonstrations by both Hopkins²⁶ and Funk²⁷ that a diet consisting only of purified proteins, fats, salts, and carbohydrates was incapable of encouraging animal growth, McCollum isolated a lipophilic non-saponifiable compound from butter fat which was found to be necessary for growth and

prevented xerophthalmia in rats in 1914.²⁸ This “factor A” soon became known as vitamin A, and its discovery led to vitamin B’s discovery by McCollum (amongst others)²⁹ only four years later.³⁰

At the same time, in the Industrial Revolution in England in the early twentieth century, cases of rickets, especially in children, had reached epidemic proportions as polluted air blocked the sun and people living in poverty worked long hours in factories.³¹ The discovery of the first vitamins led to administration of cod liver oil, a good source of vitamin A, but which also unbeknownst contained vitamins D and E as well. The treatment with cod liver oil cured rickets, but McCollum, doubting whether it was in fact vitamin A’s action, performed a groundbreaking study. He oxidized vitamin A in cod liver oil to destroy its activity, and found that even so it could be used to cure rickets (though not the vitamin A deficiency disease xerophthalmia).³² He thus concluded that there was another vital vitamin present in cod liver oil that cured rickets, and called this vitamin D,³³ as it was the fourth vitamin to be discovered and named.

In Europe, a discovery about curing rickets from a completely different source was made by both Huldschinsky³⁴ and Chick et al.³⁵ They independently showed that rickets could also be cured by exposing ricketic children to UV light. Therapeutic exposure to sunlight was no different than cod liver oil administration in curing the disease, providing the interesting insight that vitamin D has both vitamin-like and hormone-like properties.³⁶ Steenbock, at Wisconsin, confirmed this in 1924 when he showed that he could induce vitamin D activity to cure rickets in lactating goats by irradiating both animals and diets with UV light. This showed that there was an inactive substance present that could be converted to an active form of vitamin D.

The isolation of vitamin D itself was initially in error, as Windaus in Germany accidentally first found a tachysterol/ergocalciferol adduct that was active against rickets and called it vitamin D₁.³⁷ Later, the true first isolation and structure determination of ergocalciferol (vitamin D₂) was successfully conducted by Askew in Britain,³⁸ which Windaus' group later confirmed.³⁹ Windaus and Bock went on in 1936 to isolate from skin 7-dehydrocholesterol, a precursor to vitamin D₃, and convert it to cholecalciferol.⁴⁰⁻⁴¹ Thereby the two nutritional forms of vitamin D were identified.

It was not until 1967 that Hector DeLuca showed that radiolabeled vitamin D was not in fact the active form.⁴² Polar metabolites in target tissues caused the physiological response and were far more biologically active than unmetabolized vitamin D. In 1968, his group isolated the primary circulating form of vitamin D, the metabolite 25-hydroxyvitamin D₃ (25(OH)D₃), which was temporarily thought to be its most active form.⁴³ However, DeLuca's group later demonstrated indisputably that the yet more polar molecule 1,25-dihydroxyvitamin D₃ (1,25(OH)₂D₃, trivial name calcitriol) was in fact the primary active form of vitamin D.⁴⁴

1. Rosenfeld, L., Vitamine--vitamin. The early years of discovery. *Clinical chemistry* **1997**, *43* (4), 680-5.
2. Hopkins, F. G., Feeding Experiments Illustrating the Importance of Accessory Food Factors in Normal Diets. *J. Physiol* **1912**, *44*, 425-460.
3. Funk, C., On the Chemical Nature of the Substance Which Cures Polyneuritis in Birds Induced by a Diet of Polished Rice. *J. Physiol* **1911**, *43*, 395-402.
4. McCollum, E. V.; Davis, M., The Necessity of Certain Lipins in the Diet During Growth. *J. Biol. Chem* **1913**, *15*, 167-175.

5. T. B. Osborne, L. B. M., The role of vitamins in the diet. *J. Biol. Chem.* **1917**, *31*, 149-163.
6. McCollum, E. V.; Simmonds, N.; Pitz, W., The Relation of the Unidentified Dietary Factors, the Fat-Soluble A, and Water-Soluble B, of the Diet to the Growth-Promoting Properties of Milk. *J. Biol. Chem* **1916**, *27*, 33-38.
7. Hess, A., *The history of rickets*. Lea & Febiger: Philadelphia, Pennsylvania, 1929.
8. McCollum, E. V.; Simmonds, N.; Becker, J. E., An Experimental Demonstration of the Existence of a Vitamin Which Promotes Calcium Deposition. *J Biol. Chem* **1922**, *53*, 293-298.
9. Deluca, H. F., Historical Overview of Vitamin D. In *Vitamin D, 3rd Edition*, Feldman, D.; Pike, J. W.; Adams, J. S., Eds. 2011; Vol. 1.
10. Huldschinsky, K., Heilung von Rachitis durch künstlich hohen-sonne. *Deut. Med. Wochenschr* **1919**, *45*, 712-713.
11. Chick, D. H., Study of Rickets in Vienna 1919-1922. *Medical Research Council, Special Report* **1923**.
12. Vieth, R., Why "Vitamin D" is not a hormone, and not a synonym for 1,25-dihydroxy-vitamin D, its analogs or diltanoids. *The Journal of steroid biochemistry and molecular biology* **2004**, *89-90* (1-5), 571-3.
13. A. Windaus, O. L., Vitamin D1. *Ann. Chem.* **1928**, *465*, 148.
14. Askew, F. A.; Bourdillon, R. B.; Bruce, H. M.; Jenkins, R. G. C.; Webster, T. A., The Distillation of Vitamin D. *Proc. R. Soc.* **1930**, *B107*, 76-90.
15. Windaus, A.; Linsert, O.; Lüttringhaus, A.; Weidlich, G., Über das kristallisierte Vitamin D2. *Justus Liebigs Annalen der Chemie* **1932**, *492* (1), 226-241.
16. Windaus, A.; Bock, F., Über das Provitamin aus dem Sterin der Schweineschwarte. In *Hoppe-Seyler's Zeitschrift für physiologische Chemie*, 1936; Vol. 245, p 168.
17. Windaus, A.; Schenck, F., Über das antirachitisch wirksame bestrahlungs-produkt aus 7-dehydrocholesterin. *Hoppe.-Seylers. Z. Physiol. Chem* **1936**, *241*, 100-103.
18. Morii, H.; Lund, J.; Neville, P. F.; DeLuca, H. F., Biological activity of a vitamin D metabolite. *Archives of Biochemistry and Biophysics* **1967**, *120* (3), 508-512.
19. Blunt, J. W.; DeLuca, H. F.; Schnoes, H. K., 25-Hydroxycholecalciferol. A Biologically Active Metabolite of Vitamin D₃. *Biochemistry* **1968**, *7* (10), 3317-3322.
20. Holick, M. F.; Schnoes, H. K.; DeLuca, H. F.; Suda, T.; Cousins, R. J., Isolation and Identification of 1,25-Dihydroxycholecalciferol A Metabolite of Vitamin D Acite in Intestine. *Biochemistry* **1971**, *10*, 2799-2804.

1.2 The Structure and Function of the Vitamin D Receptor

The vitamin D receptor (VDR) belongs to the superfamily of nuclear receptors and functions as a transcription factor. The receptor is responsible for the regulations of genes involved in calcium homeostasis, cell proliferation, and cell differentiation.⁴⁵ While vitamin D was rapidly isolated in 1930,⁴⁶ it took the field nearly 40 years to begin to discover that the metabolism of vitamin D was necessary to create biologically active molecules.⁴² This is due to their interactions with VDR: while VDR binds vitamin D metabolites and other molecules, the actual vitamin D₂ and D₃ molecules do not bind to the receptor.

VDR was identified in 1973⁴⁷ and cloned fourteen years later.⁴⁸ In 2000, the first portion of VDR's three-dimensional structure was elucidated by X-ray crystallography: the ligand binding domain (LBD), responsible for binding small molecules. The ligand binding domain consists of

three β -sheets and three layers of 12 α -helices in sandwich folds (Figure 1a). It undergoes a major conformational change when a ligand is bound. Helix 11 shifts over and aligns with helix 10, which allows helix 12 (pink) to swing shut to the position shown in Figure 1a and close off the binding pocket. Helix 12 is the “activating domain,” allowing the structure to stabilize by contributing to additional contacts with the ligand and overall making a more hydrophobic environment in the ligand pocket. Within the binding pocket, VDR’s native ligand calcitriol takes up only 56% of the cavity (blue mesh in Figure 1b). R274 and S278 from Helix 5, S237 from Helix 3, Y143 from loop H1-H2, H305 from loop H6-H7, and H397 from Helix 11 form the anchoring hydrogen bonds that hold $1,25(\text{OH})_2\text{D}_3$ in the binding cavity (see Figure 1).⁴⁹

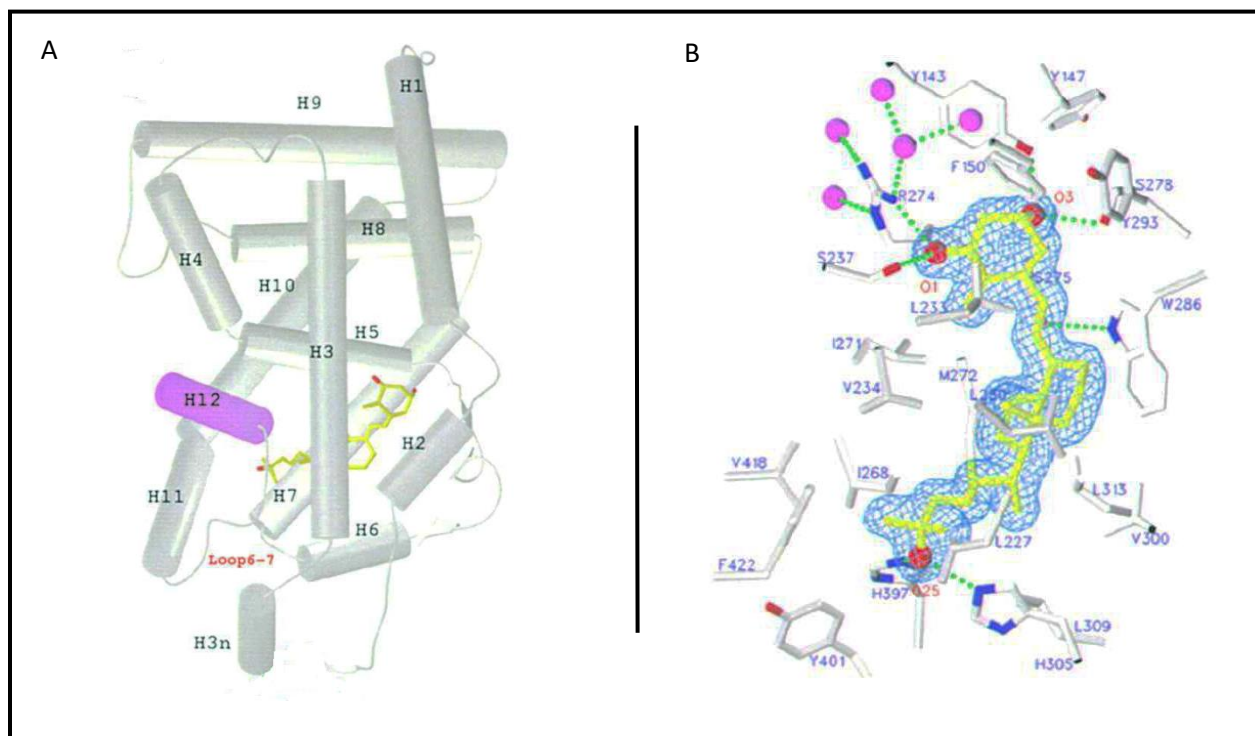


Figure 1: (a) The 12 α -helices of VDR represented as cylinders, with the activating domain helix shown in its closed position (pink) and its native ligand bound (yellow ball-and-stick). (b) The binding pocket cavity (blue mesh) and the anchoring interactions with surrounding residues that hold $1,25(\text{OH})_2\text{D}_3$ in the binding cavity.

To function as a transcription factor, VDR must in addition to binding small molecules also interact with cofactors, bind to activating DNA sequences, and take part in its heterodimer

with the retinoid X receptor (RXR). It thus has more than one domain (Figure 2). The A/B domain is at the N-terminus, and amongst nuclear receptors this domain is non-conserved as it is the part that binds various cofactors and enzymes.⁵⁰ In VDR, this domain contains activating function 1 (AF-1), which has some weak transcriptional activity in the absence of ligand.⁵⁰

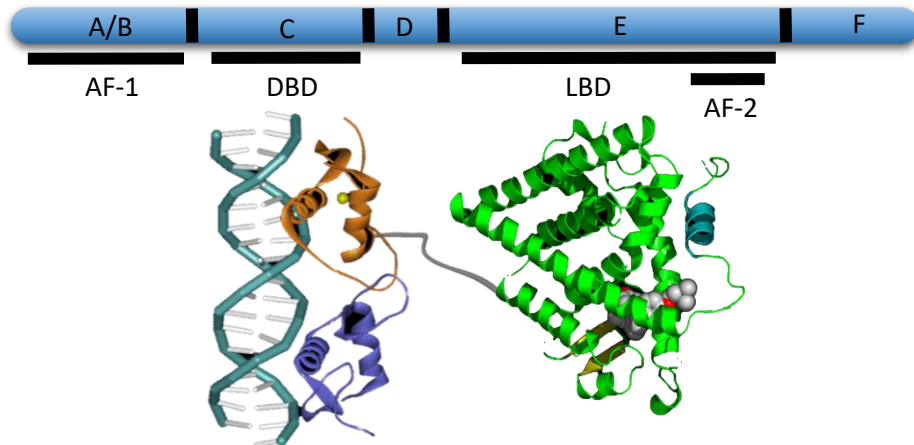


Figure 2: A schematic and crystal structure outlining the general domains of a nuclear receptor. Structures adapted courtesy of the Protein Data Bank and Brzozowski AM, et.al.³

The C domain, also known as the DNA binding domain, is highly conserved across nuclear receptors⁵¹ (Figure 3). It consists of 66 residues formed into two structures, both of which contain zinc finger motifs. The amino-terminal zinc finger region binds to the major groove of

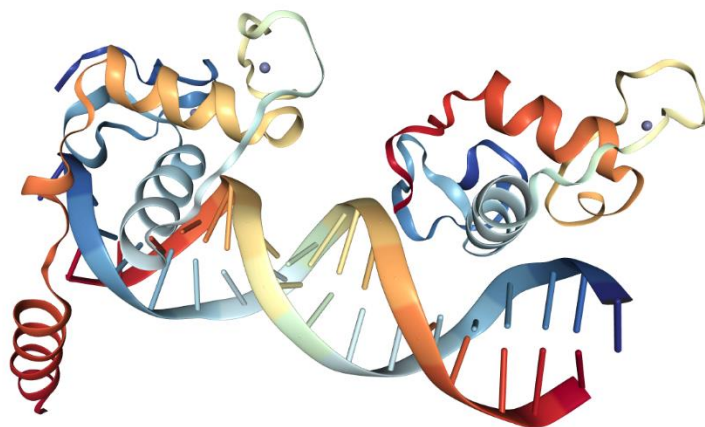


Figure 3: Crystal structure of the DBDs of both VDR (left) and its typical heterodimer partner RXR (right) bound to their respective DNA hexameric half-sites.⁶ The light blue alpha helices in both structures bind to the major groove of the DNA. The Zn^{2+} ions taking part in coordination with cysteine residues are shown in gray. (PDB: 1YNW)

DNA at certain sequences called hormone response elements. The second zinc finger region is used to heterodimerize with other proteins.⁵²⁻⁵³ A typical hormone response element for the VDR-RXR heterodimer contains two hexameric half-sites with the sequence 5'-AGGTCA-3' in a direct repeat with three neutral base pair spacers,⁵⁴ compared to other half-site combinations for various nuclear receptors which can also involve inverted, everted, and mirror repeats. VDR response elements include those for many gene targets, such as *CYP24A1*, *CYP3A4*, *SULT2A1*, *ABCB1*, *CYP2B6*, *CDKN1A*, *SPP1*, *OC*, and *OPN* genes along with a host of others.⁵⁵

The D domain is simply the highly flexible hinge region that connects the DBD and the ligand binding domain (LBD), which is located in the E domain. The E domain is well-conserved and as the name implies is responsible for binding ligands. It consists of three β -sheets and 12 α -helices in three layers of sandwich folds. This domain also interacts with coregulators (corepressors and coactivators) in a ligand dependent manner⁵⁶ (Figure 4). When a ligand is

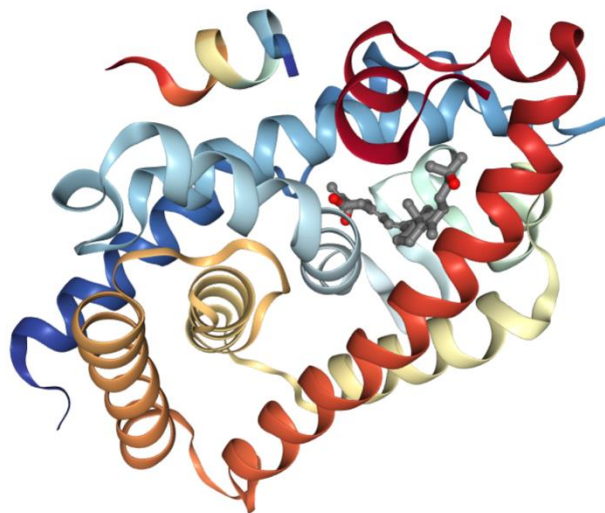


Figure 4: A crystal structure of the LBD of VDR. Within the binding pocket resides the calcitriol analogue VitIII 17-20Z (gray ball-and-stick). The short helical peptide in the upper left is the NR2 box of coactivator peptide DRIP 205 complexed to the LBD by way of the coactivator recognition sequence LxxLL. (PDB: 204J)

bound, a major conformational change occurs wherein Helix 12 swings shut over the binding pocket, stabilizing the structure through additional contacts with the ligand and creating a more hydrophobic environment in the binding pocket. Once helix 12 is in place, it provides a new exterior surface with a hydrophobic cleft and the two charged residues K246 and E420 on either end, forming a “charge clamp” with which coregulators and heterodimers interact.⁵⁷

This ability to regulate activity based on the presence of ligands, coactivators, and corepressors is known as the activating function 2 (AF-2) of the nuclear receptor: ligand dependent activity, as opposed to the ligand-independent activity of AF-1. The ligand-binding domain is thus the control center of VDR, regulating both DNA binding and transcription modification.⁵⁸ Within the LBD is the essential ligand “cave” known as the activating function 2

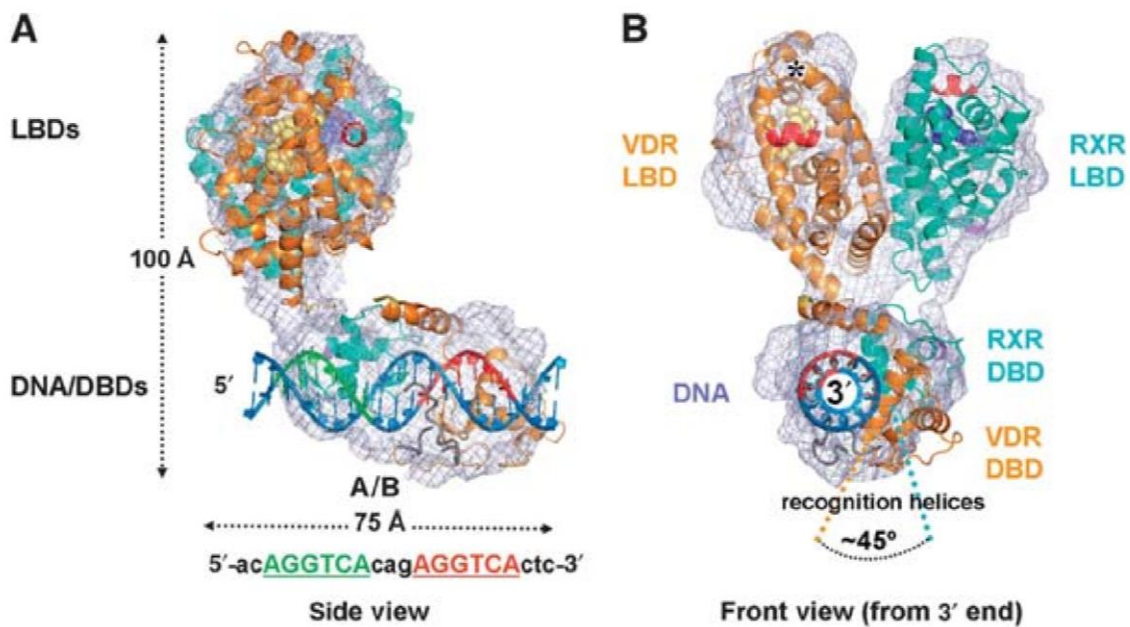


Figure 5: The flash-frozen RXR-VDR structure in complex with a DNA response element, as imaged by electron microscopy and overlaid with individual crystal structures.² A) Side view shows the ligand binding domains of VDR (orange, facing) and RXR (green, far side) at $\sim 90^\circ$ angle from where they are bound to DNA. B) The DBDs encapsulate the response element DNA, the two recognition helices positioned at about 45° from each other due to the 3 base-pair spacer between the half-sites. Helix 12 is shown on VDR in red, in its closed position with ligands bound (shown in yellow for VDR; blue for RXR).

(AF-2) wherein binding with VDR's many ligands occurs. Once a ligand has bound, AF-2 also completes the interface for binding with the retinoid X receptor as well as other coactivators and corepressors (Figure 5). When heterodimerized with the retinoid X receptor (VDR's most common dimeric partner), the two bind sequences on DNA known as "vitamin D-responsive elements" (VDRE) on VDR target genes and recruit additional coactivators.⁵⁹

The specificity of the target binding sequences allows for promoter-selective gene transcription, and ultimately determines the rate of protein production via RNA polymerase II transcription. Once the VDR-RXR heterodimer is bound, additional coactivators are recruited including the RNA polymerase II and other transcriptional proteins with histone acetyl transferases activity to mediate priming and eventual transcription of DNA.⁶⁰

The F domain, which is entirely variable across nuclear receptors, is absent in VDR.⁶¹⁻⁶²

1. Orlov, I.; Rochel, N.; Moras, D.; Klaholz, B. P., Structure of the full human RXR/VDR nuclear receptor heterodimer complex with its DR3 target DNA. *The EMBO journal* **2012**, *31* (2), 291-300.
2. Brzozowski, A. M.; Pike, A. C.; Dauter, Z.; Hubbard, R. E.; Bonn, T.; Engstrom, O.; Ohman, L.; Greene, G. L.; Gustafsson, J. A.; Carlquist, M., Molecular basis of agonism and antagonism in the oestrogen receptor. *Nature* **1997**, *389* (6652), 753-8.
3. Pike, J. W.; Meyer, M. B.; Lee, S.-M.; Onal, M.; Benkusky, N. A., The vitamin D receptor: contemporary genomic approaches reveal new basic and translational insights. *The Journal of Clinical Investigation* **2017**, *127* (4), 1146-1154.
4. Shaffer, P. L.; Gewirth, D. T., Structural analysis of RXR-VDR interactions on DR3 DNA. *The Journal of steroid biochemistry and molecular biology* **2004**, *89-90* (1-5), 215-9.
5. Askew, F. A.; Bourdillon, R. B.; Bruce, H. M.; Jenkins, R. G. C.; Webster, T. A., The Distillation of Vitamin D. *Proceedings of the Royal Society. Series B.* **1930**, *107*, 76-90.
6. Morii, H.; Lund, J.; Neville, P. F.; DeLuca, H. F., Biological activity of a vitamin D metabolite. *Archives of Biochemistry and Biophysics* **1967**, *120* (3), 508-512.
7. Brumbaugh, P. F.; Haussler, M. R., $1\alpha,25$ -dihydroxyvitamin D3 receptor: competitive binding of vitamin D analogs. *Life Sciences* **1973**, *13* (12), 1737-1746.

8. McDonnell, D. P.; Mangelsdorf, D. J.; Pike, J. W.; Haussler, M. R.; O'Malley, B. W., Molecular cloning of complementary DNA encoding the avian receptor for vitamin D. *Science (New York, N.Y.)* **1987**, *235* (4793), 1214-7.
9. Rochel, N.; Wurtz, J. M.; Mitschler, A.; Klaholz, B.; Moras, D., The crystal structure of the nuclear receptor for vitamin D bound to its natural ligand. *Molecular cell* **2000**, *5* (1), 173-9.
10. Wärnmark, A.; Treuter, E.; Wright, A. P. H.; Gustafsson, J.-A. k., Activation Functions 1 and 2 of Nuclear Receptors: Molecular Strategies for Transcriptional Activation. *Molecular Endocrinology* **2003**, *17* (10), 1901-1909.
11. Kumar, R.; Thompson, E. B., The structure of the nuclear hormone receptors. *Steroids* **1999**, *64* (5), 310-319.
12. (a) Pike, W.; Shevde, N. K., The Vitamin D Receptor. In *Vitamin D, 2nd Edition*, Feldman, D.; Pike, J. W.; Glorieux, F. H., Eds. Elsevier Academic Press: 2005; Vol. 1, pp 167-191; (b) Whitfield, G. K.; Jurutka, P. W.; Haussler, C. A.; Hsieh, J.-C.; Barthel, T. K.; Jacobs, E. T.; Dominguez, C. E.; Thatcher, M. L.; Haussler, M. R., Nuclear Vitamin D Receptor: Structure-Function, Molecular Control of Gene Transcription, and Novel Bioactions. In *Vitamin D Receptor, 2nd Edition*, Feldman, D.; Pike, J. W.; Glorieux, F. H., Eds. Elsevier Academic Press: Burlington, MA, 2005; Vol. 1, pp 219-261.
13. Kurokawa, R.; Yu, V. C.; Naar, A.; Kyakumoto, S.; Han, Z.; Silverman, S.; Rosenfeld, M. G.; Glass, C. K., Differential orientations of the DNA-binding domain and carboxy-terminal dimerization interface regulate binding site selection by nuclear receptor heterodimers. *Genes Dev.* **1993**, *7*, 1423-1435.
14. Pike, W. M., M; Lee, S.M., The Vitamin D Receptor: Biochemical, Molecular, Biological, and Genomic Era Investigations. In *Vitamin D*, Pike, W. S., N. K., Ed. 2011; Vol. 3rd Ed, pp 97-135.
15. Blanco, J. C.; Wang, I. M.; Tsai, S. Y.; Tsai, M. J.; O'Malley, B. W.; Jurutka, P. W.; Haussler, M. R.; Ozato, K., Transcription factor TFIIB and the vitamin D receptor cooperatively activate ligand-dependent transcription. *Proceedings of the National Academy of Sciences of the United States of America* **1995**, *92* (5), 1535-1539.
16. Rochel, N.; Moras, D., Structural Basis for Ligand Activity in VDR. In *Vitamin D, 3rd Edition*, Feldman, D.; Pike, J. W.; Adams, J. S., Eds. Elsevier Inc: 2011; Vol. II, pp 171-191.
17. Moras, D.; Gronemeyer, H., The Nuclear Receptor Ligand-binding Domain: Structure and Function. *Current Opinion in Cell Biology* **1998**, *10* (3), 384-91.
18. Umesono, K.; Murakami, K. K.; Thompson, C. C.; Evans, R. M., Direct repeats as selective response elements for the thyroid hormone, retinoic acid, and vitamin D3 receptors. *Cell* **1991**, *65* (7), 1255-1266.
19. Bikle, D., Vitamin D: Production, Metabolism, and Mechanisms of Action. . Vitamin D: Production, M., and Mechanisms of Action. , Ed. Endotext: South Dartmouth (MA), 2000.
20. (a) Mangelsdorf, D. J.; Thummel, C.; Beato, M.; Herrlich, P.; Schutz, G.; Umesono, K.; Blumberg, B.; Kastner, P.; Mark, M.; Chambon, P.; Evans, R. M., The Nuclear Receptor Superfamily: The Second Decade. *Cell* **1995**, *83*, 835-839; (b) Pike, J. W.; Meyer, M. B.; Lee, S. M., The Vitamin D Receptor. In *The Vitamin D Receptor, 3rd Edition*, Feldman, D.; Pike, J. W.; Adams, J. S., Eds. Elsevier: 2011; Vol. 1.

1.3 The Phase I Metabolism of Vitamin D and Calcitric Acid

As noted previously, it took some time before scientists determined that it was not vitamin D₂ or D₃ that acted on the vitamin D receptor, but instead its metabolites. This work was pioneered in 1961 by Kodicek and Chalk with *in vivo* dosing of ¹⁴C-labeled vitamin D₂ which showed that metabolism of

the labeled vitamin was occurring.⁶³ However, it was the administration of ³H-labeled vitamin analogs in the 1960s that led to the first identification of a

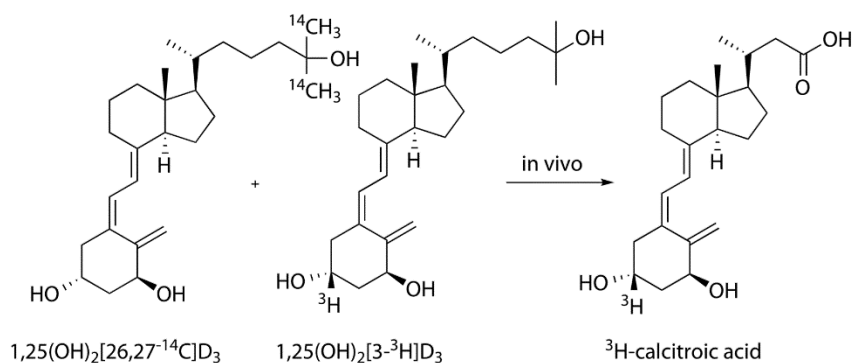
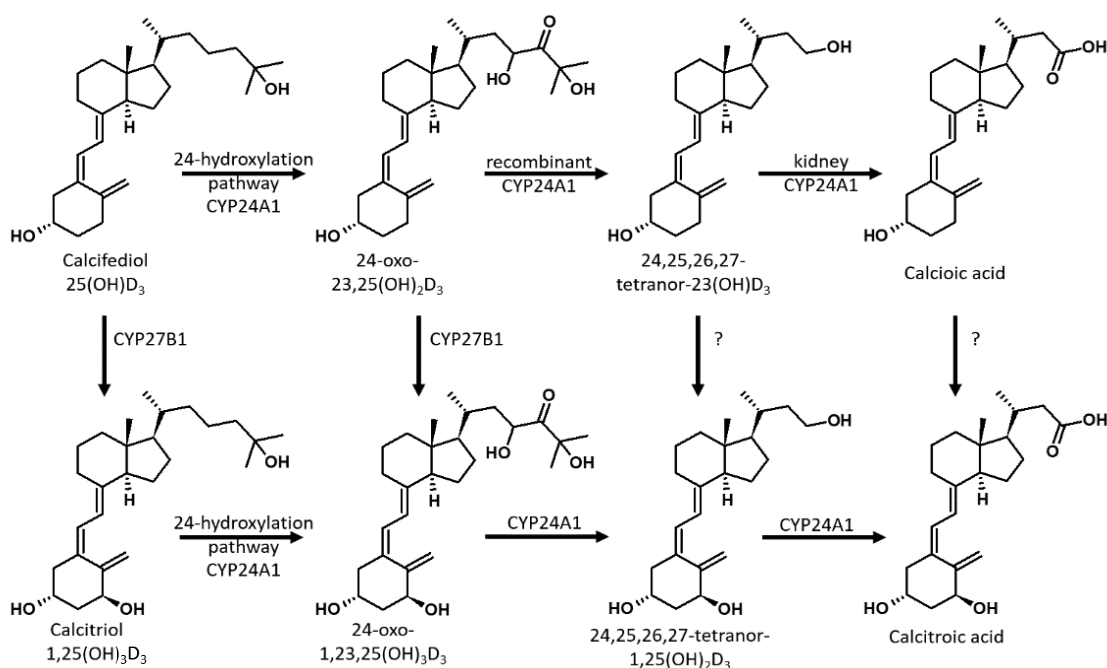


Figure 6: To identify metabolic products from 1,25(OH)₂D₃, the ¹⁴C and ³H analogues were administered. The resulting organ extracts contained an enriched ³H-labeled material, indicating modification to the side chain in calcitriol's metabolites.

vitamin D analog with significant biological activity, 25(OH)D₃.⁴³ The same group also discovered the most active vitamin D analog known, 1,25(OH)₂D₃, in 1971.⁶⁴ These discoveries initiated many research programs in the fields of medicine, biochemistry, physiology, chemistry, and pharmacology, especially once the vitamin D receptor was identified⁶⁵ and eventually cloned.⁴⁸

A near miss to uncovering CTA occurred in 1965, when it was observed that significant radioactivity was present in the aqueous extracts of the bile and intestines of 1 α -³H-D₃ dosed rats; however, none of these radioactive species were analyzed further.⁶⁶ With improvement in rat bile duct cannulation, the same group collected bile for 24 hours and separated it chromatographically into five fractions including “fraction D,” which after acid hydrolysis separated into polar and less polar fractions.⁶⁷ A glucuronide conjugate of a vitamin D analog was identified as a major component, which masked CTA; however, separation methods for acidic metabolites such as anion-exchange chromatography and derivatization with diazomethane were established. Although researchers repeatedly reported large amounts of radioactivity for aqueous extracts of liver and intestine from ³H-25(OH)D₃ treated animals,⁶⁸ it would take another 10 years until the first isolation of CTA took place.⁷ In their study, rats were treated with a combination of ¹⁴C- and ³H- labeled 1,25(OH)₂D₃ (Figure 6) and after 4 hours, soluble contents of liver and intestine (with contents) were separated as a chloroform fraction and methanol/water fraction. The aqueous layers of both tissues were enriched in ³H over ¹⁴C, indicating that the side chain of 1,25(OH)₂D₃ was shortened during metabolism—a key finding. Fractions of negatively charged compounds after diethylaminoethyl cellulose separation (anion exchange) had especially significant amounts of radioactivity. ³H-CTA was then isolated as methyl

ester after esterification with diazomethane and characterized by mass spectrometry.⁷ Blood was found to contain a small amount of ³H-CTA; however, much larger amounts were found in the liver and especially in the intestine plus content. Thus, the hypothesis that CTA is part of the enterohepatic circulation was subsequently confirmed with the identification of ³H-CTA in the bile duct.⁸ A more detailed analysis of tissue distribution of CTA with the techniques stated above using bolus administration of 1,25(OH)₂-[3α-³H]D₃ demonstrated a more complex metabolism.⁶⁹ Primarily, other acidic metabolites were found that were suggested to be polar CTA conjugates, and secondarily, CTA was found in the intestine of bile duct-cannulated rats, which suggests endogenous mucosal synthesis of CTA. In addition, only up to 50% of the radioactive material could be extracted from dried liver, another indication of complex metabolite formation.



Scheme 1: The metabolism of various vitamin D metabolites and analogues to CTA.

Due to the attention that the organ chloroform extracts received, however, several less abundant metabolites were identified long before CTA, uncovering one of the most pronounced pathways for vitamin D metabolism. The first evidence of the 24-hydroxylation of vitamin D was found in the blood of [1,2-³H]D₃-treated chicks, with the product initially believed to be 21,25(OH)₂D₃,⁷⁰ but later identified as 24,25(OH)₂D₃ in chick kidney homogenates.⁷¹ It was further discovered that 1,25(OH)₂D₃ increases the production of 24,25(OH)₂D₃, suggesting for the first time an upregulation of 24-hydroxylase (*CYP24A1*) by 1,25(OH)₂D₃.⁷² *CYP24A1* was first identified in chick kidneys,⁷³ and further characterization of the purified enzyme found in kidney mitochondria was accomplished by several groups⁷⁴⁻⁷⁵ and eventually led to cloning and expression of mitochondrial kidney *CYP24A1*.⁷⁶

In the meantime, several new vitamin D metabolites were identified *in vivo* or with perfused rat kidney: 24,25,26,27-tetranor-23(OH)D₃⁷⁷ and 24,25,26,27-tetranor-1,23(OH)₂D₃,⁷⁸ which were assumed to be the most likely precursors for CTA (Scheme 1). The conversion of 24,25,26,27-tetranor-1,23(OH)₂D₃ into CTA was then reported by two groups in the same year using perfused rat kidney.⁷⁹⁻⁸⁰ It had already been shown that cultured bone cells mediated the same metabolism in addition to the earlier reported conversion of 25-(OH)D₃ to 24,25(OH)₂D₃.⁸¹ As such, it was known that the expression of *CYP24A1* was not limited to the kidney. Analysis of recombinant human *CYP24A1* confirmed that a single P450 enzyme catalyzed the six-step pathway from 1,25(OH)₂D₃ to CTA,⁸² confirming the most pronounced CTA-generating route, the C-24 hydroxylation pathway. In addition, it was demonstrated that *CYP24A1* also mediated the alternative C-23 hydroxylation pathway, a four-step monooxygenation from 25-(OH)D₃ to

25(OH)D₃-26,23-lactone, which interestingly was not observed for rat CYP24A1.⁸³ Human recombinant CYP24A1 was also able to catalyze the conversion of 25(OH)D₃ to 24,25,26,27-tetranor-23(OH)D₃,⁸⁴ however complete oxidation to calcioic acid was only observed in perfused rat kidney.⁸⁵ In addition, CTA was found in perfused kidney when treated with supplement-derived 1,25(OH)₂D₂,⁸⁶ although CYP24A1 seemed not to be the only enzyme involved in this process.⁸⁷ CTA was also identified in the bile of rats treated with 1,25(OH)₂D₄.⁸⁸

Vitamin D analogs bearing an α1 hydroxyl functionality, such as 1,25(OH)₂D₃, bind more strongly to VDR compared to their non-1α-hydroxylated counterpart (such as 25(OH)D₃) and are therefore biologically more active at the same concentration. The identification, purification, and characterization of the responsible enzyme, 25-hydroxyvitamin D₃ 1α-hydroxylase (CYP27B1), has been ongoing for five decades.⁸⁹ Just as with *CYP24A1*, *CYP27B1* expression is not limited to kidney mitochondria. Only recently was it shown that CYP27B1 is able to convert most vitamin D metabolites of the 24-hydroxylation pathway to their corresponding 1α-hydroxyl products; however, the conversion of 24,25,26,27-tetranor-23(OH)D₃ to 24,25,26,27-tetranor-1,23(OH)₂D₃ and calcioic acid to CTA have not been investigated yet.⁹⁰

1. Chalk, K. J.; Kodicek, E., The association of 14C-labelled vitamin D₂ with rat serum proteins. *The Biochemical journal* **1961**, *79* (1), 1-7.
2. Blunt, J. W.; DeLuca, H. F.; Schnoes, H. K., 25-Hydroxycholecalciferol. A biologically active metabolite of vitamin D₃. *Biochemistry* **1968**, *7* (10), 3317-3322.
3. DeLuca, H. F.; Holick, M. F.; Schnoes, H. K.; Suda, T.; Cousins, R. J., Isolation and identification of 1,25-dihydroxycholecalciferol. A metabolite of vitamin D active in intestine. *Biochemistry* **1971**, *10* (14), 2799-2804.

4. Brumbaugh, P. F.; Haussler, M. R., 1 α ,25-dihydroxyvitamin D₃ receptor: competitive binding of vitamin D analogs. *Life Sci* **1973**, *13* (12), 1737-46.
5. McDonnell, D. P.; Mangelsdorf, D. J.; Pike, J. W.; Haussler, M. R.; O'Malley, B. W., Molecular cloning of complementary DNA encoding the avian receptor for vitamin D. *Science (New York, N.Y.)* **1987**, *235* (4793), 1214-7.
6. Callow Robert, K.; Kodicek, E.; Thompson, G. A., Metabolism of tritiated vitamin D. *Proceedings of the Royal Society of London. Series B. Biological Sciences* **1966**, *164* (994), 1-20.
7. Bell, P. A.; Kodicek, E., Investigations on metabolites of vitamin D in rat bile. Separation and partial identification of a major metabolite. *The Biochemical journal* **1969**, *115* (4), 663-669.
8. Tsai, H. C.; Wong, R. G.; Norman, A. W., Studies on Calciferol Metabolism: IV. SUBCELLULAR LOCALIZATION OF 1,25-DIHYDROXY-VITAMIN D₃ IN INTESTINAL MUCOSA AND CORRELATION WITH INCREASED CALCIUM TRANSPORT. *Journal of Biological Chemistry* **1972**, *247* (17), 5511-5519.
9. Esvelt, R. P.; Schnoes, H. K.; DeLuca, H. F., Isolation and characterization of 1.alpha.-hydroxy-23-carboxytetranorvitamin D: a major metabolite of 1,25-dihydroxyvitamin D₃. *Biochemistry* **1979**, *18* (18), 3977-3983.
10. Onisko, B. L.; Esvelt, R. P.; Schnoes, H. K.; DeLuca, H. F., Metabolites of 1 alpha, 25-dihydroxyvitamin D₃ in rat bile. *Biochemistry* **1980**, *19* (17), 4124-30.
11. Esvelt, R. P.; De Luca, H. F., Calcitroic acid: biological activity and tissue distribution studies. *Arch Biochem Biophys* **1981**, *206* (2), 403-13.
12. Suda, T.; DeLuca, H. F.; Schnoes, H. K.; Ponchon, G.; Tanaka, Y.; Holick, M. F., 21,25-Dihydroxycholecalciferol. A metabolite of vitamin D₃ preferentially active on bone. *Biochemistry* **1970**, *9* (14), 2917-2922.
13. Holick, M. F.; Schnoes, H. K.; DeLuca, H. F.; Gray, R. W.; Boyle, I. T.; Suda, T., Isolation and identification of 24,25-dihydroxycholecalciferol, a metabolite of vitamin D₃ made in the kidney. *Biochemistry* **1972**, *11* (23), 4251-4255.
14. Tanaka, Y.; DeLuca, H. F., Stimulation of 24,25-Dihydroxyvitamin D₃ Production by 1,25-Dihydroxyvitamin D₃. *Science (New York, N.Y.)* **1974**, *183* (4130), 1198-1200.
15. Knutson, J. C.; DeLuca, H. F., 25-Hydroxyvitamin D₃-24-hydroxylase. Subcellular location and properties. *Biochemistry* **1974**, *13* (7), 1543-1548.
16. (a) Burgos-Trinidad, M.; Brown, A. J.; DeLuca, H. F., Solubilization and reconstitution of chick renal mitochondrial 25-hydroxyvitamin D₃ 24-hydroxylase. *Biochemistry* **1986**, *25* (9), 2692-2696; (b) Ohyama, Y.; Okuda, K., Isolation and characterization of a cytochrome P-450 from rat kidney mitochondria that catalyzes the 24-hydroxylation of 25-hydroxyvitamin D₃. *Journal of Biological Chemistry* **1991**, *266* (14), 8690-8695.
17. Ohyama, Y.; Noshiro, M.; Okuda, K., Cloning and expression of cDNA encoding 25-hydroxyvitamin D₃ 24-hydroxylase. *FEBS Letters* **1991**, *278* (2), 195-198.
18. Jones, G.; Kung, M.; Kano, K., The isolation and identification of two new metabolites of 25-hydroxyvitamin D₃ produced in the kidney. *The Journal of biological chemistry* **1983**, *258* (21), 12920-8.

19. Reddy, G. S.; Tserng, K. Y.; Thomas, B. R.; Dayal, R.; Norman, A. W., Isolation and identification of 1,23-dihydroxy-24,25,26,27-tetranorvitamin D₃, a new metabolite of 1,25-dihydroxyvitamin D₃ produced in rat kidney. *Biochemistry* **1987**, *26* (1), 324-31.
20. (a) Reddy, G. S.; Tserng, K. Y., Calcitroic acid, end product of renal metabolism of 1,25-dihydroxyvitamin D₃ through C-24 oxidation pathway. *Biochemistry* **1989**, *28* (4), 1763-9; (b) Makin, G.; Lohnes, D.; Byford, V.; Ray, R.; Jones, G., Target cell metabolism of 1,25-dihydroxyvitamin D₃ to calcitroic acid. Evidence for a pathway in kidney and bone involving 24-oxidation. *Biochem J* **1989**, *262* (1), 173-80.
21. Turner, R. T.; Puzas, J. E.; Forte, M. D.; Lester, G. E.; Gray, T. K.; Howard, G. A.; Baylink, D. J., In vitro synthesis of 1 alpha,25-dihydroxycholecalciferol and 24,25-dihydroxycholecalciferol by isolated calvarial cells. *Proceedings of the National Academy of Sciences of the United States of America* **1980**, *77* (10), 5720-5724.
22. Sakaki, T.; Sawada, N.; Komai, K.; Shiozawa, S.; Yamada, S.; Yamamoto, K.; Ohyama, Y.; Inouye, K., Dual metabolic pathway of 25-hydroxyvitamin D₃ catalyzed by human CYP24. *European journal of biochemistry* **2000**, *267* (20), 6158-65.
23. Sakaki, T.; Sawada, N.; Nonaka, Y.; Ohyama, Y.; Inouye, K., Metabolic studies using recombinant escherichia coli cells producing rat mitochondrial CYP24 CYP24 can convert 1alpha,25-dihydroxyvitamin D₃ to calcitroic acid. *European journal of biochemistry* **1999**, *262* (1), 43-8.
24. Inouye, K.; Sakaki, T., Enzymatic studies on the key enzymes of vitamin D metabolism; 1 alpha-hydroxylase (CYP27B1) and 24-hydroxylase (CYP24). *Biotechnology annual review* **2001**, *7*, 179-94.
25. Reddy, G. S.; Omdahl, J. L.; Robinson, M.; Wang, G.; Palmore, G. T.; Vicchio, D.; Yergey, A. L.; Tserng, K. Y.; Uskokovic, M. R., 23-carboxy-24,25,26,27-tetranorvitamin D₃ (calcioic acid) and 24-carboxy-25,26,27-trinorvitamin D₃ (cholacalcioic acid): end products of 25-hydroxyvitamin D₃ metabolism in rat kidney through C-24 oxidation pathway. *Arch Biochem Biophys* **2006**, *455* (1), 18-30.
26. Zimmerman, D. R.; Reinhardt, T. A.; Kremer, R.; Beitz, D. C.; Reddy, G. S.; Horst, R. L., Calcitroic acid is a major catabolic metabolite in the metabolism of 1 alpha-dihydroxyvitamin D(2). *Arch Biochem Biophys* **2001**, *392* (1), 14-22.
27. Horst, R. L.; Omdahl, J. A.; Reddy, S., Rat cytochrome P450C24 (CYP24) does not metabolize 1,25-dihydroxyvitamin D₂ to calcitroic acid. *Journal of cellular biochemistry* **2003**, *88* (2), 282-5.
28. Tachibana, Y.; Tsuji, M., Study on the metabolites of 1alpha,25-dihydroxyvitamin D₄. *Steroids* **2001**, *66* (2), 93-97.
29. Sakaki, T.; Kagawa, N.; Yamamoto, K.; Inouye, K., Metabolism of vitamin D₃ by cytochromes P450. *Frontiers in bioscience : a journal and virtual library* **2005**, *10*, 119-34.
30. Tang, E. K. Y.; Tieu, E. W.; Tuckey, R. C., Expression of human CYP27B1 in Escherichia coli and characterization in phospholipid vesicles. *The FEBS journal* **2012**, *279* (19), 3749-3761.

1.4 The Synthesis of Calcitroic Acid

As these findings have shown, CTA is the most significant final metabolite of vitamin D. When CTA was discovered by DeLuca in 1974, however, it was quickly characterized and then mostly forgotten for forty years because it was believed that no specific biological activity was mediated by CTA. Recently, however, a study in our lab unexpectedly found CTA to be active in cells.⁴ For a VDR-mediated transcription assay, our group found VDR target gene CYP24A1 upregulated in DU145 cells in the presence of CTA (Figure 7). The focus of this project has

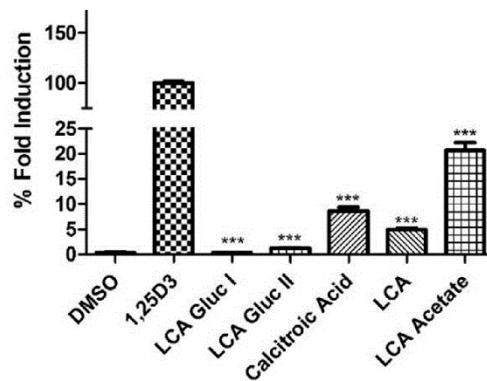
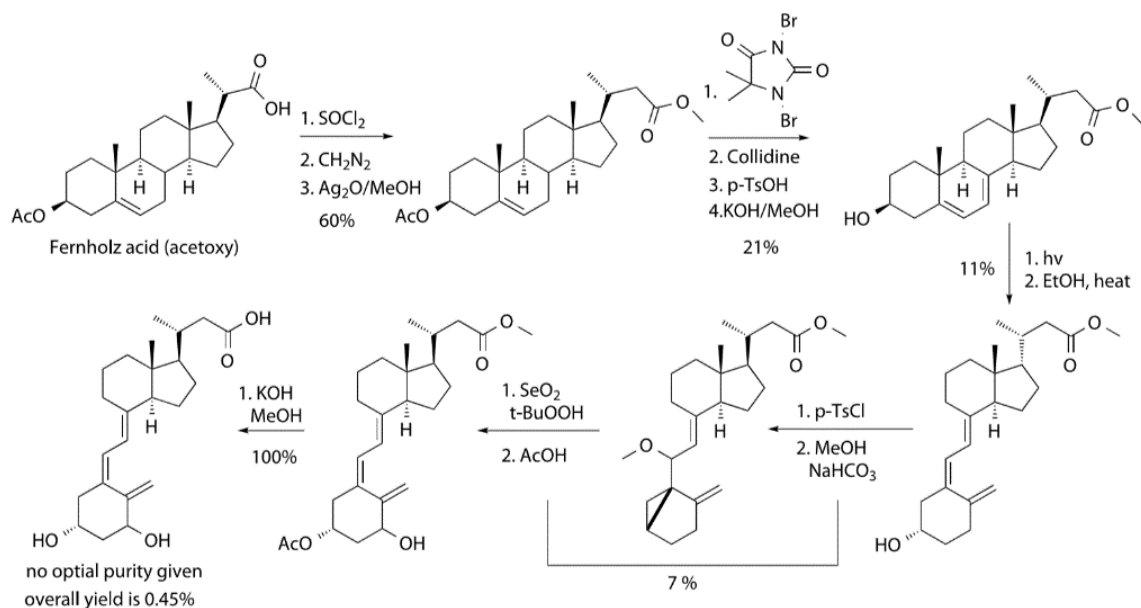
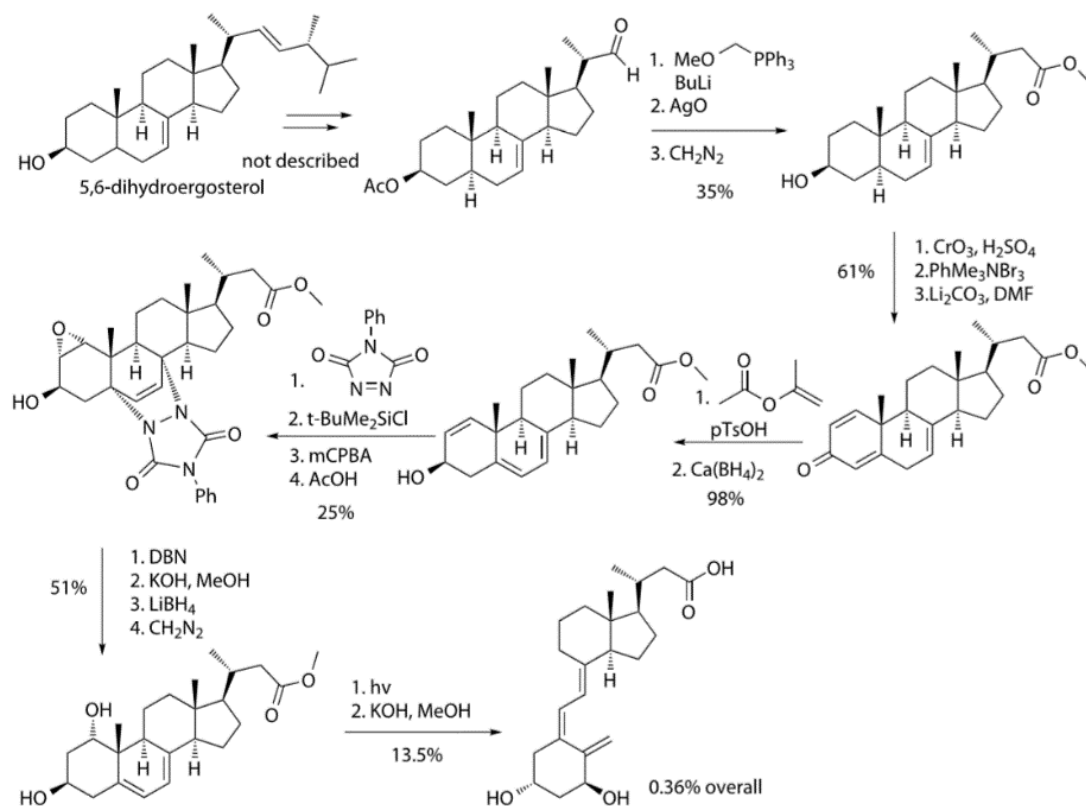


Figure 7: CYP24A1 gene regulation by VDR ligands (7.5 mM) in DU145 cells after 18 hrs. Stars represent 0.001 $P < (***)$ compared to vehicle DMSO. Graph courtesy of Teske KA et al.⁴



Scheme 2: Synthesis of CTA starting from a cholesterol analogue precursor



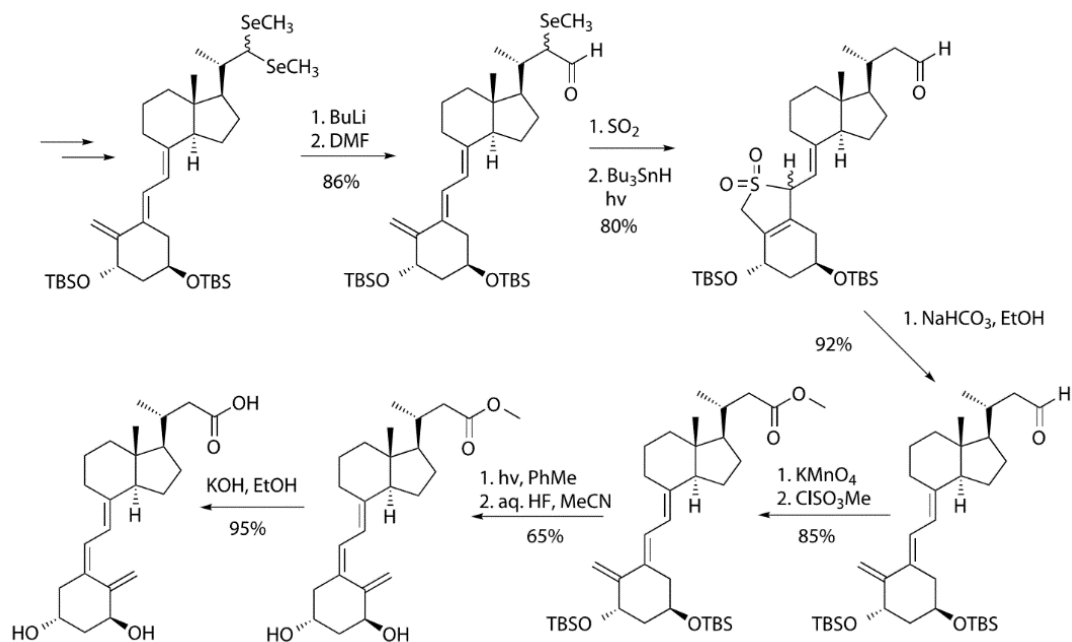
Scheme 3: Synthesis of CTA using a provitamin D precursor

thus been to evaluate the biological activity of CTA in order to assess its function. Unfortunately, CTA is not available commercially in the quantities required to study it fully, and is prohibitively expensive even in small amounts (~\$4000/mg).

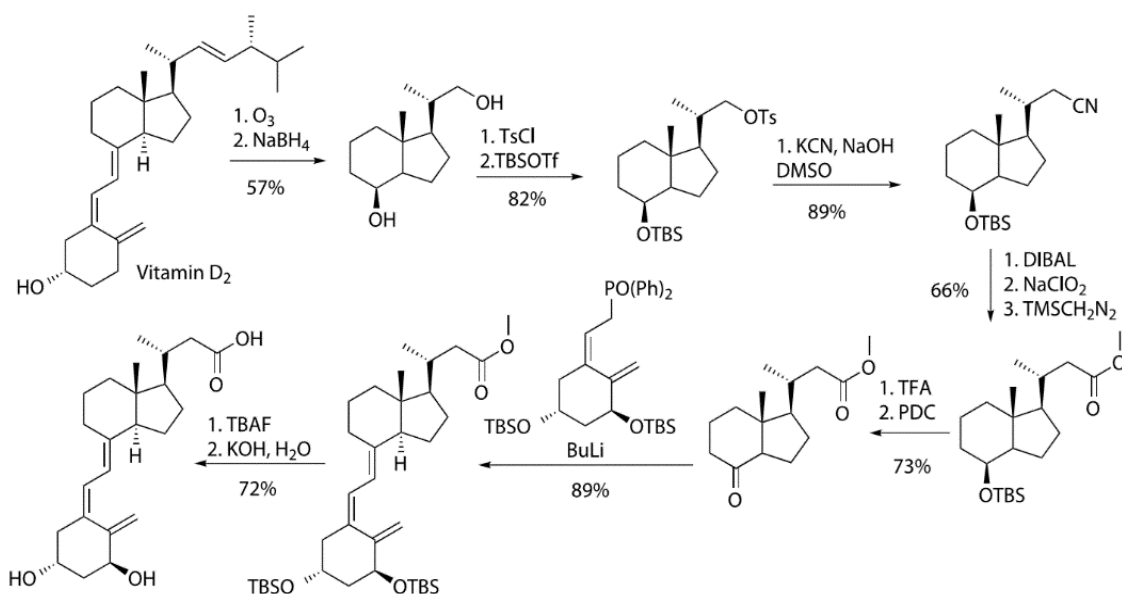
The reason for the high price of CTA is that its isolation by both synthetic and enzymatic methods have very low overall yields. The first CTA synthesis was reported in 1981 (Scheme 2).⁹¹ The acetoxy derivative of Fernholz acid, which is commercially available from Steraloids, was used as starting material and converted using an Arndt-Eistert reaction to the corresponding higher carboxy homologue. Allylic bromination and subsequent elimination installed the diene, which was converted in low yield under photochemical and thermal conditions to the methyl ester of calcioic acid. 1 α -hydroxylation was achieved by synthesizing a cyclovitamin D derivative followed by allylic oxidation and cycloreversion with acetic acid. Hydrolysis gave CTA in an overall yield of 0.09%. The optical rotation was not given, but the corresponding methyl ester coeluted in HPLC with the derivatized material isolated from rat livers. Small improvements to this route increased the overall yield to 0.28%.⁹²

Two years later, a new route based on a previous synthesis of vitamin D analogs was reported with an overall yield of 0.36% (Scheme 3).⁹³ The synthesis started with 5,6-dihydroergosterol, which was used to prepare the corresponding aldehyde. The carbon chain elongation was carried out by a Wittig reaction followed by demethylation, oxidation, and esterification. A quinone-like structure was generated by oxidation, α -carbon bromination, and elimination, which was subsequently isomerized and reduced to the allylic alcohol. The diene and alcohol function were protected, followed by oxidation and subsequent deprotection. The

retro Diels–Alder reaction recreated the diene, and conversion of the ester to the acid enabled a selective reduction of the epoxide followed by esterification. Finally, the seco-steroid scaffold



Scheme 5: Synthesis of CTA starting from a seco-steroid precursor



Scheme 4: Synthesis of CTA starting from vitamin D₂ using a Ring A phosphine oxide synthon

was produced by light and subsequent saponification, generating CTA in 0.36% overall yield. Importantly, the light-induced ring opening reaction reduced significantly the overall yield of both described methods.

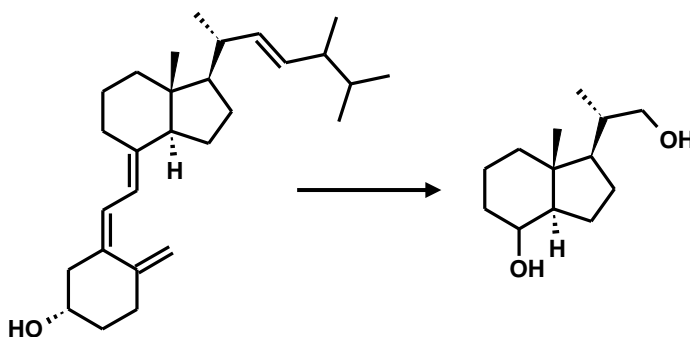
During the 1980s and 1990s, many different synthetic strategies were explored to generate other vitamin D analogs, which led to the availability of many new synthons for their synthesis.⁹⁴ The carbon chain elongation using a seco-steroid as a starting material to produce CTA was introduced in 1990 (Scheme 4).⁹⁵ The starting material was a seleno acetal, which was generated from the corresponding 1 α -hydroxy vitamin D aldehyde derivative. Formylation gave a lithio-demethylseleno derivative as a carbon homologue, which was protected as a hetero Diels–Alder product with sulfur dioxide followed by radical deselenation induced by light. A retro Diels–Alder reaction was achieved under mild conditions followed by oxidation and esterification to the corresponding ester. Photoisomerization installed the natural Z-configuration of methyl ester of the protected CTA, which was subsequently deprotected and hydrolyzed to give CTA. The reactions described in Scheme 4 achieved high yields; however, the route has many steps if the synthesis of the precursor would be included.

Very recently, a synthesis using commercially available chemicals was reported, that for the first time enabled the synthesis of gram quantities of CTA (Scheme 5).⁹⁶ Originally developed to generate ¹³C-labeled CTA for metabolic research, this synthesis used the Inhoffen Lythgoe diol, which is both commercially available and readily synthesized from vitamin D₂.⁹⁷ This new route was the foundation for our CTA production, which we modified in several ways to improve reaction yields.

1. Teske, K. A.; Bogart, J. W.; Sanchez, L. M.; Yu, O. B.; Preston, J. V.; Cook, J. M.; Silvaggi, N. R.; Bikle, D. D.; Arnold, L. A., Synthesis and evaluation of vitamin D receptor-mediated activities of cholesterol and vitamin D metabolites. *European journal of medicinal chemistry* **2016**, *109*, 238-46.
2. Hector F. DeLuca, H. K. S., Robert P. Esvelt Processes for preparing calcitroic acid and esters thereof. 1981.
3. Esvelt, R. P.; Fivizzani, M. A.; Paaren, H. E.; Schnoes, H. K.; DeLuca, H. F., Synthesis of calcitroic acid, a metabolite of 1.alpha.,25-dihydroxycholecalciferol. *The Journal of Organic Chemistry* **1981**, *46* (2), 456-458.
4. de Costa, B. R.; Makk, N.; Midgley, J. M.; Modi, N. T.; Watt, R. A.; Whalley, W. B., Unsaturated steroids. Part 12. Synthesis of 1 α ,3 β -dihydroxy-24-nor-9,10-secochola-5,7,10(19)trien-23-oic (calcitroic) acid and of the cholic-and 25-homocholeic acid analogues. *Journal of the Chemical Society, Perkin Transactions 1* **1985**, (0), 1331-1336.
5. Zhu, G.-D.; Okamura, W. H., Synthesis of Vitamin D (Calciferol). *Chemical Reviews* **1995**, *95* (6), 1877-1952.
6. Calverley, M. J., The Seleno-Acetal Route to Side-Chain Modified 1-Alpha-Hydroxy-Vitamin-D Analogs - Stereoselective Synthesis of the New 22z Isomer of Mc903 (Calcipotriol). *Synlett* **1990**, *1990*, 157-159.
7. Meyer, D.; Rentsch, L.; Marti, R., Efficient and scalable total synthesis of calcitroic acid and its 13C-labeled derivative. *RSC Advances* **2014**, *4* (61), 32327-32334.
8. Posner, G. H.; Lee, J. K.; White, M. C.; Hutchings, R. H.; Dai, H.; Kachinski, J. L.; Dolan, P.; Kensler, T. W., Antiproliferative Hybrid Analogs of the Hormone 1alpha,25-Dihydroxyvitamin D(3): Design, Synthesis, and Preliminary Biological Evaluation. *J Org Chem* **1997**, *62* (10), 3299-3314.

1.5 Synthetic Strategy for Production of Calcitric Acid

Synthesis of Inhoffen Lythgoe diol:⁹⁸



The Meyer synthesis used purchased Inhoffen Lythgoe diol.⁹⁶ While we did initially purchase some diol, we quickly decided that it would be less expensive to produce the diol using ozonolysis from the much cheaper ergocalciferol (vitamin D₂). We initially planned to use a

reductive workup to isolate the aldehyde and convert it to the diol in a separate step. This proved difficult because the aldehyde was difficult to purify and the yield was low. After we learned from a collaborator that the reduction to the diol could be done in one-pot using sodium borohydride, we changed our route to a one-pot two-step reaction to generate the Inhoffen Lythgoe diol.

Even so, perfecting this reaction was quite challenging. There were multiple issues, starting with finding the balance between enough MeOH to support the ozonolysis process and enough pyridine to dissolve ergocalciferol. We were also unable to

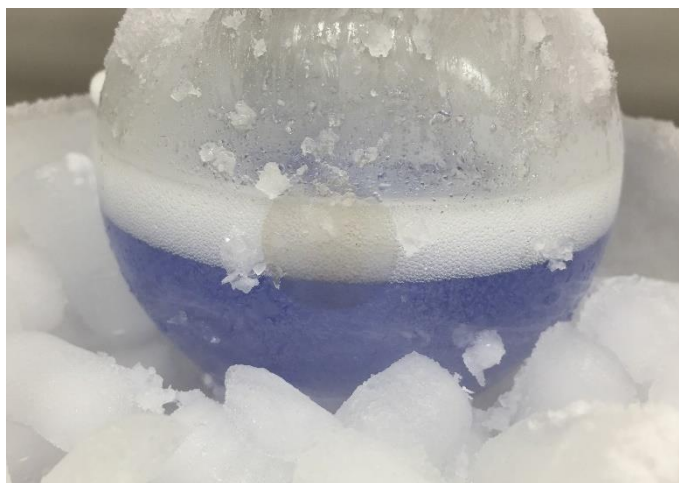


Figure 8: Saturated with ozone, the MeOH/pyridine solution turns blue

get the reaction to reliably turn blue (saturate with O_3) and needed to acquire a “fizzer” gas dispersion fitting to bubble O_3 through the solution with high surface area, allowing it to saturate. Once those had been solved, there were additional issues realized as we attempted to scale the reaction up; namely, we were unsuccessful scaling it up past the 3 g scale. A specific round bottom flask (500mL, with a narrow outlet for used gas to escape) filled halfway was the only way to get a balance between enough solvent in the proper proportions to dissolve 3 g of vitamin D_2 , and having a large enough surface area-to-volume ratio to be able to keep the solution at $-78^\circ C$ so the ozone could saturate the solution. Running the reaction for a full 7 hours at that temperature was generally the best way to ensure that all double bonds are

oxidized. After allowing the reaction to warm up overnight, we added NaBH₄ in tablet form one at a time to limit the surface area and ensure that the solution did not overheat.

The workup remained a problematic issue for nearly the entire time that the diol was being produced. After evaporation of the methanol, we were left with a large amount of pyridine, which had been required to keep ergocalciferol in solution during the ozonolysis. We were not able to evaporate pyridine or use azeotropic distillation to remove it from the product. During the workup, the extracted DCM layer was washed multiple times with 1M HCl in an attempt to protonate pyridine and dissolve it in the aqueous layer. This worked somewhat, but still left plenty behind. Because pyridine and the diol were nearly overlapping via TLC plate, full separation was never achieved via flash chromatography. We resorted to dealing with its presence throughout the next step, until the tosylate protection rendered the product sufficiently nonpolar to enable separation via flash chromatography.

However, on the final round of diol production, we used 10% CuSO₄ for washing the organic layer. This single wash removed all pyridine from the organic layer. As such, it is highly recommended for eliminating pyridine in future syntheses.

Synthesis of O-silylated C,D-ring tosylate:

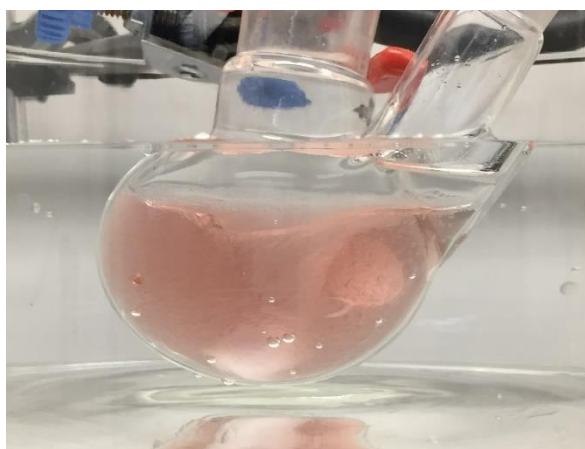
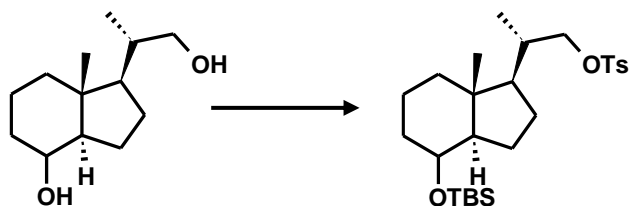
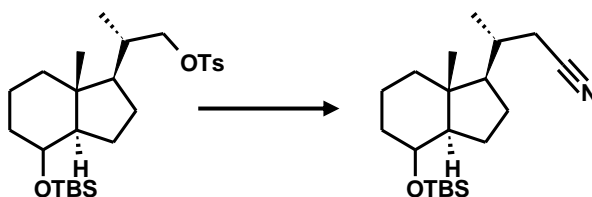


Figure 9: Concentrated doubly-protected C,D-ring takes on a slightly pink hue

The Meyer synthesis was followed for the protection of the two alcohol functions independently. The tosylate group on the primary alcohol was carried out first, as it is the more accessible alcohol. Thus, with one equivalent of Ts-Cl, the primary alcohol will be selectively protected in the presence of the secondary

alcohol. This reaction was reliable and gave the tosylated C,D-ring in high yield. The silyl ether protecting group was added with a t-butyldimethylsilyl trifluoromethanesulfonate (TBSOTf). This protecting group is stable under weak acidic conditions, very stable under basic conditions and readily removed in the presence of fluorine ions.

Synthesis of O-silylated C,D-ring nitrile:



The Meyer synthesis' carbon elongation utilizes a classic route wherein the side chain's tosylate is a good leaving group for substitution by potassium cyanide. In our lab, this reaction was challenging and unreliable from the start. The Meyer synthesis heated the reaction to 90°C, but we found that this heat was sufficient to lose a moderate portion of the product by loss of the silyl protecting group (20-60%), even if closely monitored and quenched as soon as the starting material was gone. Even reactions with minimal degradation faced a more severe problem: loss of product during workup. Initially, the reaction was

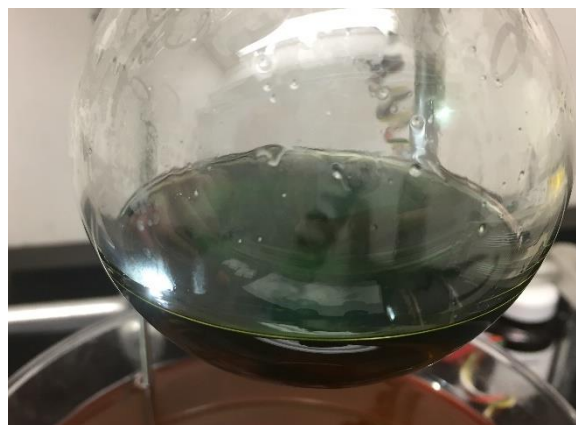


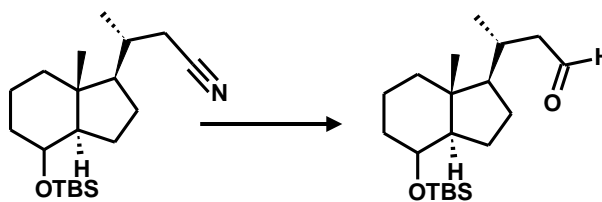
Figure 10: Nitrile reaction turns red as we attempt to get salts into solution. When sonicated/heated, sometimes it turned green when everything was in solution

carried out in DMSO—a necessary concession when dealing with organic compounds that need to react with inorganic salts (NaOH and KCN). For the workup, the reaction was dissolved in 10-50x the volume of water and extracted with ethyl acetate, but it still resulted in a large amount

of DMSO in the organic layer. Excessive washing of the organic layer with water until the DMSO disappeared resulted in unacceptably low yields. This was observed across the many different workup procedures we tried, which included: extraction with many solvents, especially ones known not to dissolve DMSO very well; using an excessive amount of water to dilute DMSO; using a recursive extract/wash system with a series of separatory funnels to get progressively less DMSO and more organic product; using DMF instead of DMSO (similar problems) and using ACN instead of DMSO (no conversion).

Unable to produce good results, we changed the method. ACN on its own was unable to solubilize the salts enough for the reaction to proceed at any temperature. However, a polar but volatile solvent would change the difficulty of this reaction workup entirely, so we tried another method: crown ethers. It is well-known that 18-crown-6 readily solubilizes K^+ ions. While potassium wasn't the ion of interest for purposes of substitution, the strong affinity of 18-crown-6 for K^+ causes the "naked ion" effect for CN^- , wherein it becomes an even better nucleophile in the absence of its balancing cation. This altered reaction was highly successful when run at $75^\circ C$, with no trouble during the workup and an improved yield around 93%.

Synthesis of O-silylated C,D-ring aldehyde:



The side-chain modification continues, converting the nitrile in three steps to the aldehyde, to the acid, and then to the ester. The reduction of the nitrile to the aldehyde was carried out with DIBAL in dry DCM at 0°C.

During the quench it should be noted that the reaction needs to be kept at 0°C throughout. The addition of aqueous NH₄Cl to quench the DIBAL is extremely exothermic and prone to bubbling over, especially during the first few drops. We found that the quenched reaction does

need to stir for at least a half hour before breaking up the viscous

solution with t-butyl methyl ether (TBME). Once TBME was added, the reaction needed to stir at 0°C for as long as necessary until the aqueous layer separated more thoroughly, forming a white

fluffy gelatin that typically balled up and adhered to the flask somewhere (Figure 11). Rushing

these steps results in loss of product, possibly because intermediate imines are not fully

hydrolyzed to the aldehyde. Only then is it appropriate to begin drying off the aqueous layer,

which is done simply by adding a large amount of MgSO₄ until a dry solution is achieved.

Breaking up the solidified MgSO₄ as best as possible is advised in order to allow any product

trapped within the gelatin to dissolve into the organic layer. Because the nitrile and aldehyde are

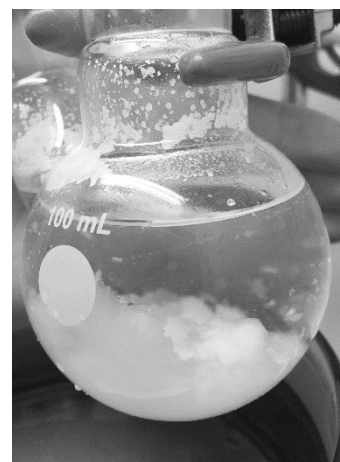
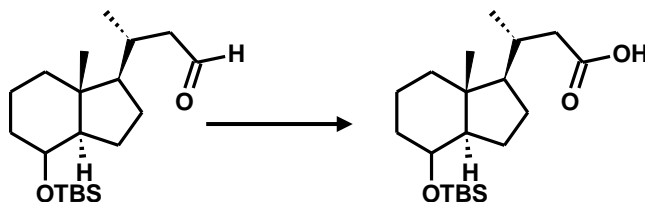


Figure 11: Fluffy quenched DIBAL following aq. NH₄Cl addition and TBME dilution is ready for drying

almost overlapping via TLC, it is important that this reaction run to completion before it is quenched; otherwise separation between the two is impossible by chromatography.

In the case that the ^{13}C labeling will not lead to a compound distinguishable by MS from non-labeled CTA, a secondary plan to label the compound with an ^{18}O during this step is proposed. In this reaction, DIBAL reacts with the nitrile to form an intermediate imine. The intermediate imine is hydrolyzed by water to form an aldehyde, acquiring the oxygen molecule from the water. As such, quenching the reaction using ^{18}O heavy water would add another label to the final product.

Synthesis of O-silylated C,D-ring acid:



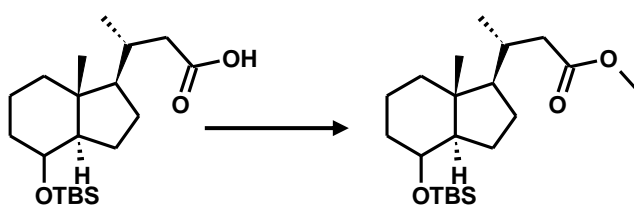
The conversion of the aldehyde to the acid is a Pinnick oxidation. In this reaction, chlorous acid is formed from chlorite under acidic conditions as the oxidant. Chlorous acid adds to the aldehyde and then undergoes pericyclic fragmentation to produce the acid function and hypochlorous acid (HOCl). The presence of



Figure 12: Faintly seen aqueous and organic layers as reaction turns yellow in Pinnick oxidation

the HOCl scavenger 2-methyl-2-butene then ensures that the species will not go on to destroy other NaClO₂ ions (which would prevent them from completing the oxidation) or produce other unwanted byproducts.⁹⁹ This reaction is a little unusual in that it uses mixed aqueous and organic phases. The starting material is dissolved in *t*-butanol, with the 2-methyl-2-butene hypochlorous acid byproduct scavenger added. The NaClO₂ is then dissolved separately in water containing the stabilizer/buffer NaH₂PO₄. The water layer is then added to the organic, and a yellow-green solution is immediately observed. The color fades as the reaction proceeds. While this reaction can be separated via chromatography, we found that all byproducts were easily removed during the workup: upon extraction, NaH₂PO₄, NaClO₂, HOCl and its scavenger byproduct went into the aqueous layer while *t*-butanol and 2-methyl-2-butene were removed through concentration. Thus, by proceeding directly to the next reaction, we returned higher yields.

Synthesis of O-silylated C,D-ring ester:



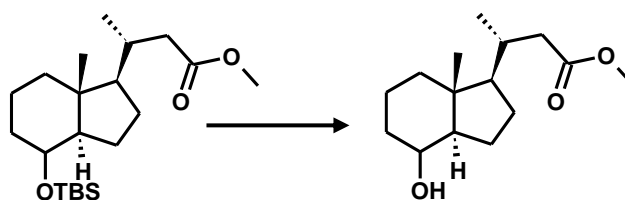
For the esterification, the methylating agent trimethylsilyldiazomethane was used, which was added dropwise through a septum into the dry toluene/MeOH reaction mixture. The mixture turns



Figure 13: Trimethylsilyldiazomethane turns the methylating reaction yellow

yellow to indicate the presence of the diazo compound, and when complete it can be quenched with acetic acid, turning the solution clear again. The solution is then concentrated and purified directly via column (quantitative yield).

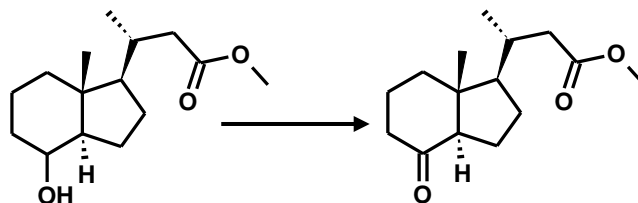
Synthesis of C,D-ring alcohol:



The reaction to deprotect the silyl group to an alcohol group using TFA worked fine during the first rounds of synthesis. However, when we were reacting more material, a previously trace byproduct spot took over about half of the reaction yield. While we were unable to identify this byproduct, we inadvertently discovered how to convert it to the desired C,D-alcohol product. We separated the desired deprotected alcohol product from the rest of the crude (which contained both unreacted silyl-protected C,D-ring alcohol and the unknown byproduct). The crude was then re-reacted with TBAF, anticipating that what remained unreacted would instead form product, and the byproduct would just be a loss. Instead, we saw the byproduct spot disappear to form the desired C,D-ring alcohol product, while the unreacted starting material remained untouched. Continued reactions made clear that this was the best

way to manage the large amount of byproduct that formed: first, the reaction was run with TFA to form both anticipated product and byproduct, and then a second reaction was run to convert the byproduct to the anticipated product. Eventually, all the silyl-protected substrate was converted to the alcohol in an overall improved yield across the two reactions (89%).

Synthesis of C,D-ring ketone:



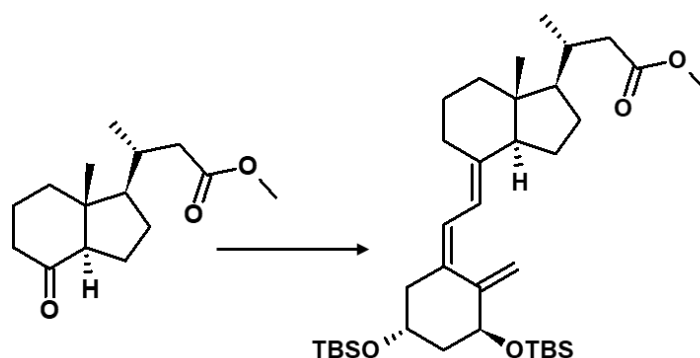
Following the Meyer synthesis again, we then oxidized the alcohol to the ketone. The reaction is best run under nitrogen at room temperature and proceeds fairly well as long as the DCM is dry. It is important for the PDC to be very freshly ground prior to the reaction to expose the unoxidized surface, which is orange instead of brown or black. As PDC does not dissolve in DCM, a suspension will form that turns black as the reaction proceeds. The reaction appears to be complete within 3 hours, but it is best to run overnight to ensure complete conversion, as both starting material and product have the same R_f and thus cannot be



Figure 14: Finely ground, oxidized PDC turning black during the reaction

separated by chromatography. Completion can be confirmed by NMR. It is important to remove all product off the solid PDC. Filtering over celite, then re-suspending the solids in fresh DCM with vigorous stirring at least three more times led to improved yields (up to 20% improvement).

Synthesis of O-Bis-silylated calcitroic acid methyl ester:



The Wittig-Horner ligation was the most challenging reaction in the synthesis of CTA, and prone to failure and low yields. Successful, moderate-yield reactions required extensive planning, careful controlled execution, and extremely dry conditions. To begin with, solid ketone and solid commercially-acquired organophosphine oxide (ring A synthon) ligand were never dry enough to use because transferring them brings them in contact with air, and the solid can trap water. Instead, they needed to be dissolved in THF and dried overnight in small, oven-dried flasks with molecular sieves. The glassware setup needed to be oven dried overnight and assembled in its entirety while hot (including dropping funnel, molecular sieves in both RBF and funnel, and stir bar), then vacuum and nitrogen purged multiple times as it cooled. Once set, it must remain

under nitrogen and cannot be opened to air; instead, a dropping funnel and syringes were used to transfer/add the reagents.

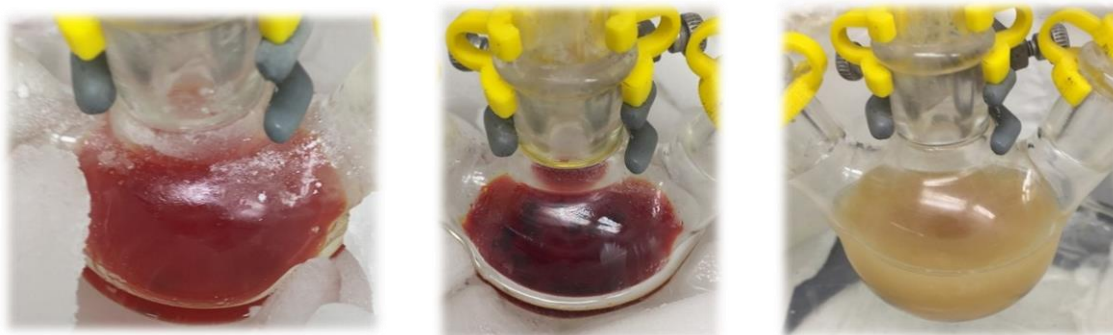
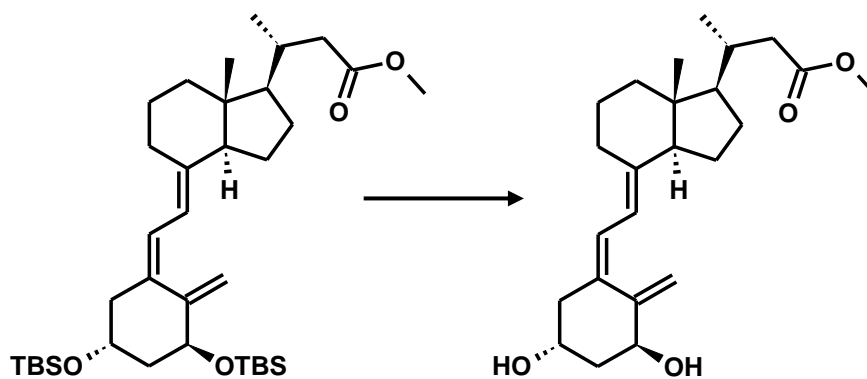


*Figure 15: Wittig-Horner reaction at different stages. From left to right: the deprotonation of organophosphine oxide by *n*-BuLi; reaction color darkened upon brief removal from dry ice bath to ensure full consumption of *n*-BuLi; an unsuccessful reaction turned peach color when quenched by water.*

During the first stage, the phosphine oxide solution was added to the 3-neck RBF from the side neck and the solution was cooled to -78°C . *N*-butyl lithium was added via syringe through the side neck, and a brilliant red color resulted. This color is the main indication of success in the reaction, as its loss indicates that the reaction is exposed to water or that unreacted *n*-BuLi attacked the ketone (1,2 addition) instead of deprotonating the phosphine oxide. While the molar ratio of the *n*-BuLi must be higher than that of the ketone being added, it must be lower than that of the phosphine oxide it is deprotonating (recommended 1:1.5 or greater). After an hour of stirring, the reaction was briefly suspended above the dry ice bath, allowing it to reach a higher temperature and ensure full consumption of the *n*-BuLi. The color darkened to deep blood red (see Figure 15). The reaction was then cooled again to -78°C . In the second phase, the ketone was added from the dropping funnel. This needed to be done very

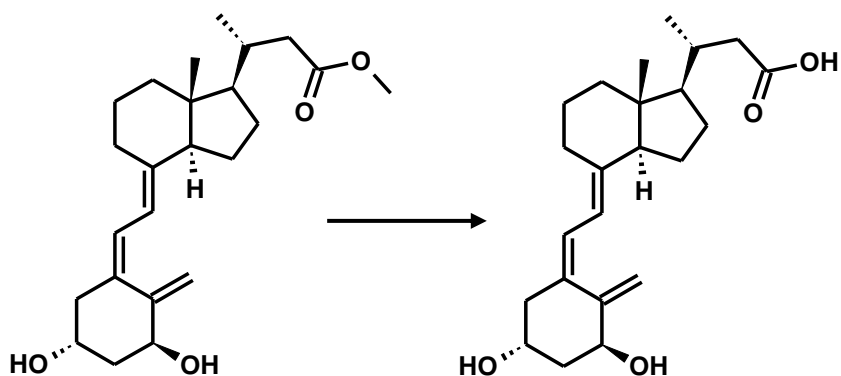
slowly to ensure that the reaction does not warm up significantly. Also, careful monitoring of the color of the solution was necessary. If the reaction started to lose its color, and especially if a quick conversion to yellow was seen, the reaction was aborted immediately and no more ketone was added. Any ketone that had already been added could not be recovered due to 1,2-addition by the *n*-BuLi, so watching this step carefully was imperative. The reaction could then be monitored by TLC, but samples could only be extracted via syringe, as opening the reaction results in noteworthy product loss. The reaction ran for up to 5 hours, then was quenched with water and warmed to room temperature for work-up. The quenched reaction was extracted with TBME, the extract washed with brine, concentrated and purified by column chromatography (78% yield).

Synthesis of calcitric acid methyl ester:



The subsequent TBAF deprotection of the A-ring synthon's silyl ethers needs to be kept very dry and uses ten equivalents of TBAF in order to get excellent yields. This reaction was the highest-yielding option for small reactions. However, for large reactions TBA was difficult to separate from the product. Generally speaking, formation of the TBA-Cl salt using NH_4Cl washes dissolves TBA in the water layer. In practice, even an excessive number of washes does not fully remove TBA from the organic layer. This was okay for small reactions, where the TBA would then be separated via column chromatography, but in larger batches there was far too much leftover TBA even after extraction, and it co-eluted with the product. This problem is bypassed by instead using camphorsulfonic acid (CSA) as a convenient, speedy alternative, requiring only about 15 minutes of reaction and yielding a very clean product after workup. Because of this, the CSA product could be used in the next step without purification, but the yield across the two reactions when we used CSA was never as high as the yield when we used TBAF.

Synthesis of calcitroic acid:



The final reaction of the CTA synthesis is the hydrolysis from the methyl ester to the acid. This synthesis had been previously reported using KOH at 60°C for 1.5 hours. When we struggled to carry out this reaction, we tried several alternate hydrolysis options. We discovered that using room temperature and NaOH resulted in better yields (84% compared to 74%) and avoided the compound degradation that we had been seeing at elevated temperatures.

Discussion

Overall, the Meyer group reported a yield of 12.8% for CTA. This is an impressive improvement over the 0.36% reported earlier. Our improved synthesis starting from the Inhoffen Lythgoe diol had an overall 29% yield. While it was more cost-effective in our lab to

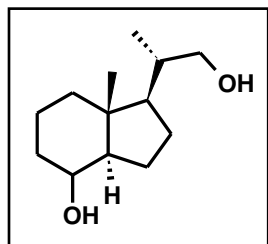
start from ergocalciferol rather than purchasing the diol, the low yield (57%) of the initial ozonolysis and reduction steps decreased the yield for all 13 steps to 16%. Using $K^{13}CN$ to substitute a labeled carbon as outlined by Meyer also afforded the ^{13}C -labeled CTA in the same yield. As an alternate product, the same method was utilized to generate the vitamin D metabolic product calcitric acid: the corresponding A-ring synthon is commercially available and afforded the corresponding O-silylated calcitric acid methyl ester in comparable yields. Using our variation of the Meyer synthetic method, a total of 3.2g of CTA was able to be generated. This material was used to both characterize CTA, provide the substance to various collaborators, and as a scaffold from which to synthesize a variety of secondary metabolic products for CTA.

1. Lacroix, J.-F. Design and Synthesis of A-ring/seco-B-ring vitamin D analogues. McGill University, 2012.
2. Meyer, D.; Rentsch, L.; Marti, R., Efficient and scalable total synthesis of calcitric acid and its ^{13}C -labeled derivative. *RSC Advances* **2014**, 4 (61), 32327-32334.
3. Kürti, L. Czakó, B., Pinnick Oxidation. In *Strategic applications of named reactions in organic synthesis: background and detailed mechanisms*, Elsevier: 2005; pp 354-356.

1.6 Characterization of Calcitroic Acid Synthesis Compounds

Ergocalciferol was purchased from variable commercial sources (Alfa Aesar J62163, AstaTech 44109, Research Products International C20300, Sigma-Aldrich 95220, VWR 101172-472). Both of the phosphine oxides were purchased from ChemScene (CS-M1835, CS-M0003). All moisture or oxygen-sensitive reactions were carried out under a dry nitrogen atmosphere. Reaction temperatures refer to the containing bath temperatures. Reactions were monitored by thin-layer chromatography (TLC) using Merck 60 UV254 silica gel plates (Sigma-Aldrich). Visualization was performed with UV light, cerium molybdate general stain followed by heating, and other methods as noted. Synthesized compounds were purified by normal phase flash chromatography (SPI Biotage, silica gel 230-400 mesh) except where noted. Compound characterization was performed via Shimadzu 2020 LC-MS (single quadrupole) instrument. NMR

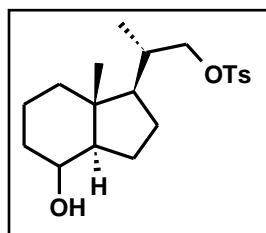
spectra were recorded on a Bruker Avance 500MHz instrument with compounds dissolved in the specified deuterated solvent. Optical rotations were recorded using Jasco DIP-370 Digital Polarimeter instrument in LCMS grade chloroform or methanol.



Inhoffen-Lythgoe diol: Ergocalciferol (3g, 7.5mmol) was dissolved first in dry pyridine (7mL), and then that mixture was diluted in dry methanol (250mL). The 500mL RBF used was single-necked with a diffuse bubbler as the inlet for ozone and a slim outlet for the dissipating gas. The reaction

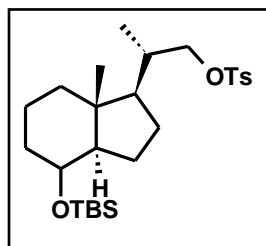
mixture was cooled to -78°C and ozone was bubbled through it for 4-6 hours using an A2Z Ozone A2ZZ-5G 110 V with $38\text{g}/\text{m}^3$ O_3 output. The reaction was monitored by TLC (UV and cerium molybdate). Many spots occur initially, which reduce to three main spots after several hours. One of the two lower spots, partially overlapping with the pyridine spot (R_f 0.10 EtOAc:Hex 1:3) is the product. When no more change was apparent after an additional hour of ozonolysis, the reaction mixture was then brought to 0°C and stirred vigorously. Sodium borohydride (2g, 53mmol) was added carefully. Once fully dissolved, the reaction was quenched with 70mL of water and stirred for 5 minutes before concentrating. The crude reaction mixture was diluted with 100mL of water and extracted with DCM (3x100mL). The organic layers were washed with 5% CuSO_4 solution (100mL), 1M HCl (2x100mL) and saturated NaHCO_3 (100mL), dried over MgSO_4 , concentrated, and purified by column chromatography (EtOAc:Hex 1:3) to yield the Inhoffen Lythgoe diol as a white solid (450mg, 57%). Note that this reaction could not be scaled up, as larger percentages of pyridine were not tolerated and larger reaction vessels could not be

adequately cooled in order to allow ozone saturation. R_f 0.09 (EtOAc: Hex 1:3); $^1\text{H-NMR}$ (500MHz, CDCl_3) δ 0.97 (s, 3H), 1.04 (d, $J = 5.0$, 3H), 1.14-1.23 (m, 2H), 1.31-1.40 (m, 2H), 1.41-1.53 (m, 5H), 1.54-1.62 (m, 2H), 1.78-1.91 (m, 3H), 1.98-2.04 (m, 1H), 3.38 (dd, $J = 5.0$, 3.5 Hz, 1H), 3.65 (dd, $J = 10$, 3.0 Hz, 1H), 4.10 (d, $J = 2.0$, 1H); $^{13}\text{C-NMR}$: (125MHz, CDCl_3) δ 13.6, 16.6, 17.4, 22.6, 26.7, 33.5, 38.2, 40.2, 41.8, 52.4, 53.0, 67.6, 69.2; m/z calculated for $\text{C}_{13}\text{H}_{24}\text{O}_2$ 211 [M – H],⁻ found 211; $[\alpha]_D^{25} = + 24.0$ (c 1.0, CHCl_3)



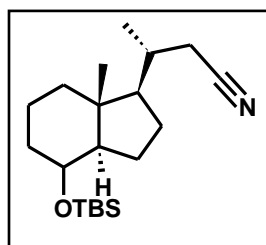
C,D-ring tosylate: To a stirred solution of Inhoffen-Lythgoe diol (0.38g, 1.78mmol) in dry DCM (20mL) was added 4-dimethylaminopyridine (DMAP; 0.44g, 3.58mmol) and p-toluenesulfonyl chloride (0.36g,

1.88mmol). The reaction was stirred overnight at room temperature, then quenched with 1 M HCl (20mL). The reaction mixture was extracted with DCM (3x50mL) and combined organic layers were washed with water (50mL), dried over MgSO_4 , and purified by column chromatography (EtOAc:Hex 3:7) to yield C,D-ring tosylate as a white crystalline solid (410mg, 84%); R_f 0.23 (EtOAc: Hex 1:3); $^1\text{H-NMR}$ (500MHz, CDCl_3) δ 0.92 (s, 3H), 1.00 (d, $J = 5.0$ Hz, 3H), 1.13-1.26 (m, 4H), 1.31-1.38 (m, 1H), 1.42-1.51 (m, 3H), 1.52-1.62 (m, 1H), 1.66-1.75 (m, 2H), 1.77-1.88 (m, 2H), 1.92-1.98 (m, 1H), 2.48 (s, 3H), 3.84 (dd, $J = 6.5$, 3.0 Hz, 1H), 3.98 (dd, $J = 6.2$, 3.0 Hz, 1H), 4.10 (s, 1H), 7.38 (d, $J = 8.4$ Hz, 2H), 7.82 (d, $J = 8.5$ Hz, 2H); $^{13}\text{C-NMR}$: (125MHz, CDCl_3) δ 13.49, 16.75, 17.35, 21.65, 22.46, 26.42, 33.56, 40.06, 41.88, 52.25, 52.26, 69.06, 75.61, 127.92 (2C), 129.79 (2C), 133.10, 144.64; m/z calculated for $\text{C}_{20}\text{H}_{30}\text{O}_4\text{S}$ 430 [M + Na + ACN],⁺ found 430; $[\alpha]_D^{25} = + 19.0$ (c 1.0, CHCl_3)



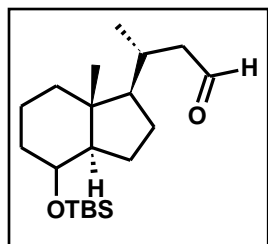
O-silylated C,D-ring tosylate: To a solution of C,D-ring tosylate (0.40g, 1.09mmol) in dry DCM (2mL) at 0°C was added 2,6-lutidine (0.15mL, 1.31mmol) and tert-butyl dimethylsilyl trifluoromethanesulfonate (0.35mL, 1.53mmol). The reaction was monitored by TLC until completion

(2 hours) and quenched with water (2mL). The crude mixture was extracted with DCM (3x15mL), washed with water (15mL), dried over MgSO₄, concentrated, and purified by column chromatography (EtOAc : Hex 1:19) to yield O-silylated C,D-ring tosylate as a clear or slightly pink oil, which solidified during storage (0.32g, 62%); R_f 0.43 (EtOAc: Hex 1:19); ¹H-NMR (500MHz, CDCl₃) δ 0.00 (s, 3H), 0.02 (s, 3H), 0.88 (s, 3H), 0.89 (s, 9H), 0.97 (d, J = 6.5, 3H), 1.08-1.19 (m, 3H), 1.19-1.26 (m, 1H), 1.26-1.42 (m, 3H), 1.49-1.57 (m, 1H), 1.58-1.71 (m, 3H), 1.73-1.84 (m, 1H), 1.86-1.92 (m, 1H), 2.47 (s, 3H), 3.82 (dd, J = 6.5, 2.8 Hz, 1H), 3.95-4.02 (m, 2H), 7.36 (d, J = 8.0 Hz, 2H), 7.80 (d, J = 10.2 Hz, 2H); ¹³C-NMR: (125MHz, CDCl₃) δ -5.2, -4.8, 13.7, 16.8, 17.6, 18.0, 21.6, 23.0, 25.8 (4C), 26.5, 34.3, 35.8, 40.4, 42.2, 52.4, 52.7, 69.2, 75.8, 127.9 (2C), 129.8 (2C), 133.2, 144.6; m/z calculated for C₂₆H₄₈O₄NSSi 499 [M + NH₄]⁺ found 499; m/z calculated for C₂₈H₄₇O₄NSSiNa 544 [M + Na + ACN]⁺ found 544; [α]_D²⁵ = + 34.0 (c 1.0, CHCl₃)



O-silylated C,D-ring nitrile: To a solution of O-silylated C,D-ring tosylate (2.74 g, 5.70 mmol) in dry acetonitrile (75mL) was added NaOH (0.46 g, 11.40mmol), potassium cyanide (0.74g, 11.40mmol), and 18-crown-6 (3.77g, 14.25mmol). The solution was stirred at 75°C for 2.5 hours or until

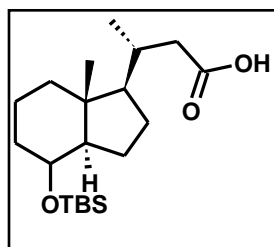
the starting material disappeared by TLC. Acetonitrile was removed under reduced pressure and the residue was dissolved in water (20mL) and extracted with EtOAc (3 x 20mL). The combined organic layers were washed with brine, dried over MgSO₄, concentrated, and purified by column chromatography (EtOAc : Hex 3 : 97) to yield the O-silylated C,D-ring nitrile (1.80g, 94%) as a clear oil; R_f 0.20 (EtOAc: Hex 3:97); ¹H-NMR (500MHz, CDCl₃) δ 0.02 (s, 3H), 0.04 (s, 3H), 0.91 (s, 9H), 0.95 (s, 3H), 1.16 (d, *J* = 6.6Hz, 3H), 1.18-1.29 (m, 3H), 1.30-1.36 (m, 1H), 1.37-1.46 (m, 3H), 1.56-1.66 (m, 1H), 1.67-1.73 (m, 1H), 1.75-1.88 (m, 3H), 1.92-1.97 (m, 1H), 2.25 (dd, *J* = 16.6, 7.0 Hz, 1H), 2.36 (dd, *J* = 16.6, 3.8 Hz, 1H), 4.01-4.04 (m, 1H); ¹³C-NMR: (125MHz, CDCl₃) δ -5.2, -4.8, 13.9, 17.5, 18.0, 19.3, 22.9, 24.7, 25.8 (3C), 27.2, 33.1, 34.2, 40.3, 42.2, 52.9, 55.4, 69.2, 119.1; *m/z* calculated for C₂₀H₄₁N₂OSi 354 [M + NH₄]⁺ found 354; [α]_D²⁵ = + 48.0 (c 1.0, CHCl₃)



O-silylated C,D-ring aldehyde: To a stirred solution of O-silylated C,D-ring nitrile (0.69g, 2.06mmol) in 20mL dry DCM at 0°C was added a solution of DIBAL (1.5 M in toluene, 4.80mL, 7.19mmol) dropwise. The reaction was monitored at 0°C for 45 minutes until complete by TLC. The reaction was

then carefully quenched with 10mL of a saturated solution of NH₄Cl (aq) and stirred for an hour at 0°C. The viscous solution was then broken up by stirring in TBME (60mL), which was kept at 0°C for another two hours and then allowed to warm up overnight. The aqueous layer formed a fluffy white ball, which was dried off directly with MgSO₄ and filtered. The organic filtrate was concentrated under reduced pressure and purified via column chromatography (EtOAc : hexanes 5 : 95) to yield the O-silylated C,D-ring aldehyde (0.66g, 94%) as a clear oil: (R_f 0.41 (EtOAc: Hex

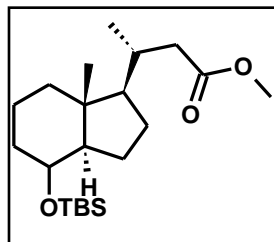
7:93); ¹H-NMR (500MHz, CDCl₃) δ 0.02 (s, 3H), 0.04 (s, 3H), 0.91 (s, 9H), 0.98 (s, 3H), 1.02 (d, *J* = 6.5 Hz, 3H), 1.12-1.19 (m, 2H), 1.23-1.30 (m, 2H), 1.36-1.43 (m, 3H), 1.56-1.65 (m, 1H), 1.67-1.73 (m, 1H), 1.76-1.86 (m, 2H), 1.94-2.00 (m, 1H), 2.02-2.09 (m, 1H), 2.13-2.19 (m, 1H), 2.47 (dd, *J* = 15.7, 2.5 Hz, 1H), 4.01-4.04 (m, 1H), 9.70 (dd, *J* = 3.6, 1.4 Hz, 1H); ¹³C-NMR: (125MHz, CDCl₃) δ – 5.2, –4.8, 13.7, 17.6, 18.0, 20.0, 23.0, 25.8 (3C), 27.6, 31.3, 34.3, 40.6, 42.3, 50.8, 53.0, 56.6, 69.3, 203.7; *m/z* calculated for C₂₀H₄₁N₂OSi 354 [M + NH₄]⁺ found 354; [α]_D²⁵ = + 27.0 (c 1.0, CHCl₃)



O-silylated C,D-ring acid: Sodium phosphate monobasic monohydrate (3.39g, 24.55mmol) was dissolved in 32mL of H₂O. To this was added sodium chlorite (3.41g, 37.65mmol). The aqueous solution was then added to a stirred solution of O-silylated C,D-ring aldehyde (1.39g,

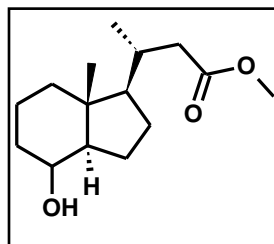
4.09mmol) in *tert*-butanol (77mL) and 2-methyl-2-butene (19mL). The reaction was monitored for 1 hour until completion and then concentrated under reduced pressure. The residue was dissolved in H₂O and extracted with DCM (3x50mL). The organic layers were washed with water (20mL), dried over MgSO₄ and concentrated to the O-silylated C,D-ring acid (3.2g, 99%) as a white powder: R_f 0.19 (EtOAc: Hex 1:4); ¹H-NMR (500MHz, CDCl₃) δ 0.02 (s, 3H), 0.03 (s, 3H), 0.91 (s, 9H), 0.97 (s, 3H), 1.03 (d, *J* = 6.4 Hz, 3H), 1.08-1.19 (m, 2H), 1.25-1.31 (m, 2H), 1.33-1.42 (m, 3H), 1.55-1.65 (m, 1H), 1.66-1.72 (m, 1H), 1.77-1.88 (m, 2H), 1.91-2.08 (m, 3H), 2.49 (d, *J* = 14.8, 3.2 Hz, 1H), 4.01-4.04 (m, 1H), 11.05 (bs, 1H); ¹³C-NMR: (125MHz, CDCl₃) δ –5.2, –4.8, 13.7, 17.6, 18.0, 19.5, 23.0, 25.8 (3C), 27.3, 33.2, 34.4, 40.6, 41.2, 42.3, 53.0, 56.5, 69.4, 179.7; *m/z*

calculated for $C_{20}H_{38}O_3Si$ 356 $[M + H]^+$, found 356; m/z calculated for $C_{20}H_{38}O_3Si$ 353 $[M - H]^-$, found 353; $[\alpha]_D^{25} = +41.0$ (c 1.0, $CHCl_3$)



O-silylated C,D-ring methyl ester: To a stirred solution of O-silylated C,D-ring acid (1.01g, 2.86mmol) in 16.5mL toluene and 11mL MeOH was added trimethylsilyl diazomethane (2.12mL, 2M in diethyl ether, 4.23mmol). The reaction was stirred for 1.5 hours at room temperature

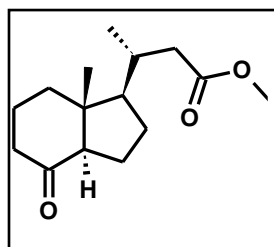
and then quenched with acetic acid. The mixture was concentrated under reduced pressure and purified by column chromatography (EtOAc : hexanes 3 : 97) to yield the O-silylated C,D-ring ester (1.05g, quantitative) as a clear oil: R_f 0.28 (EtOAc: Hex 3:97); 1H -NMR (500MHz, $CDCl_3$) δ 0.01 (s, 3H), 0.02 (s, 3H), 0.90 (s, 9H), 0.95-0.98 (m, 6H), 1.06-1.17 (m, 2H), 1.24-1.30 (m, 2H), 1.33-1.49 (m, 3H), 1.54-1.64 (m, 1H), 1.65-1.71 (m, 1H), 1.74-1.87 (m, 2H), 1.89-2.03 (m, 3H), 2.43 (dd, $J = 14.2, 3.1$ Hz, 1H), 3.67 (s, 3H), 3.99-4.03 (m, 1H); ^{13}C -NMR: (125MHz, $CDCl_3$) δ -5.2, -4.8, 13.8, 17.6, 18.0, 19.5, 23.0, 25.8 (3C), 27.3, 33.4, 34.4, 40.6, 41.3, 42.2, 51.3, 53.0, 56.6, 69.4, 174.0; m/z calculated for $C_{21}H_{39}O_3Si$ 367 $[M - H]^-$, found 367; $[\alpha]_D^{25} = +41.0$ (c 1.0, $CHCl_3$)



Methyl esterified C,D-ring alcohol: To a stirred solution of O-silylated C,D-ring ester (1.48g, 4.01mmol) in dry DCM (45mL) at 0°C was added trifluoroacetic acid (4.5mL, 58.4mmol). The reaction was stirred at 0°C for 1.5 hours until it was complete by TLC. The reaction mixture was

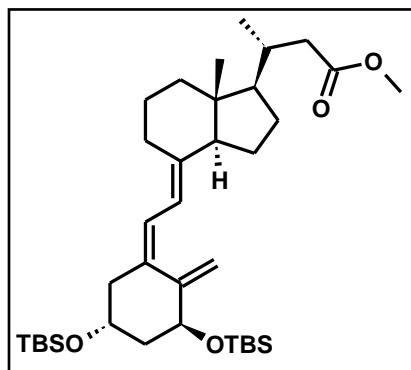
concentrated under reduced pressure and purified by column chromatography (EtOAc : hexanes

1 : 4) to yield the esterified C,D-ring alcohol (0.93g, 91%) as a clear oil: R_f 0.32 (EtOAc: hexanes 1:4); $^1\text{H-NMR}$ (500MHz, CDCl_3) δ 0.96-1.00 (m, 6H), 1.09-1.21 (m, 2H), 1.29-1.40 (m, 3H), 1.40-1.53 (m, 3H), 1.55-1.65 (m, 1H), 1.78-1.89 (m, 3H), 1.89-1.97 (m, 1H), 1.97-2.05 (m, 2H), 2.44 (dd, $J = 14.2, 3.2$ Hz, 1H), 3.68 (s, 3H), 4.08-4.11 (m, 1H); $^{13}\text{C-NMR}$: (125MHz, CDCl_3) δ 13.6, 17.4, 19.4, 22.5, 27.2, 33.4, 33.6, 40.3, 41.3, 42.0, 51.4, 52.6, 56.4, 69.2, 174.0; m/z calculated for $\text{C}_{16}\text{H}_{27}\text{O}_5$ 299 $[\text{M} + \text{FA} - \text{H}]^-$ found 299; $\text{C}_{17}\text{H}_{26}\text{O}_5\text{F}_3$ 367 $[\text{M} + \text{TFA} - \text{H}]^-$ found 367; $[\alpha]_D^{25} = +30.0$ (c 1.0, CHCl_3)



Methyl esterified C,D-ring ketone: To a stirred solution of C,D-ring alcohol (0.653g, 2.57mmol) in dry DCM (50mL) was added freshly ground PDC (1.93g, 5.13mmol). The reaction was monitored for two hours at room temperature, then diluted with TBME (50mL) and filtered over celite. The

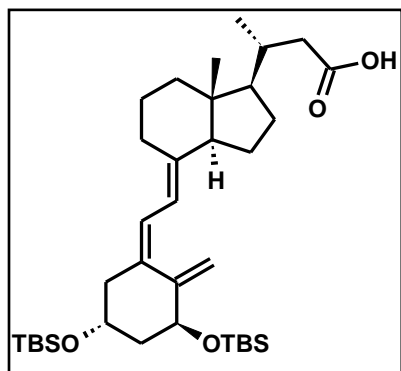
filtered solid was resuspended twice more in fresh DCM (2x25mL) and stirred vigorously for a half hour each before being filtered again. The combined filtrates were concentrated under reduced pressure and purified via column chromatography (EtOAc : hexanes 1 : 4) to yield the C,D-ring ketone (0.565g, 87%) as a white solid: R_f 0.35 (EtOAc: Hex 1:4); $^1\text{H-NMR}$ (500MHz, CDCl_3) δ 0.63 (s, 3H), 0.98 (d, $J = 6.5$, 3H), 1.26-1.36 (m, 1H), 1.42-1.60 (m, 3H), 1.66-1.76 (m, 1H), 1.78-1.93 (m, 3H), 1.94-2.04 (m, 2H), 2.04-2.09 (m, 1H), 2.14-2.27 (m, 2H), 2.36-2.46 (m, 2H), 3.62 (s, 3H); $^{13}\text{C-NMR}$: (125MHz, CDCl_3) δ 12.5, 19.0, 19.5, 23.9, 27.4, 33.3, 38.8, 40.8, 41.0, 49.8, 51.4, 56.2, 61.8, 173.5, 211.5; m/z calculated for $\text{C}_{15}\text{H}_{24}\text{O}_3$ 253.1798 $[\text{M} + \text{H}]^+$, found 253.1766; $[\alpha]_D^{25} = -5.0$ (c 1.0, CHCl_3)



O-Bis-silylated calcitroic acid methyl ester: A solution of n-butyllithium (1.6 M in hexanes, 1.56mL, 2.50mmol) was added dropwise to a solution of the CTA A-ring phosphine oxide (1.84g, 3.16mmol, dried over 3Å molecular sieves in 5 ml THF overnight) at -78°C in the presence of freshly dried 3Å

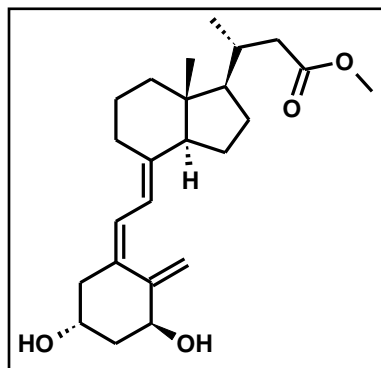
molecular sieves. The solution turned deep red and was stirred for an hour at -78°C . Raising the solution out of the bath briefly deepened the red color and ensured that the deprotonation was complete. The solution was returned to the bath and C,D-ring ketone (0.42g, 1.66mmol, dried over 3Å molecular sieves in 5 ml THF overnight) was added dropwise. The solution was stirred for 5 hours at -78°C and then allowed to come to room temperature. The reaction mixture was then quenched with 10mL water, diluted with TBME, and extracted (TBME, 2x50mL). Combined organic layers were washed with brine, dried over MgSO_4 , and concentrated. The crude product was purified by column chromatography (EtoAc: Hex 5:95) to yield O-Bis-silylated CTA methyl ester (0.66g, 65%) as a viscous white oil; R_f 0.22 (EtOAc:Hex 3:97); $^1\text{H-NMR}$ (500MHz, CDCl_3) δ 0.04-0.10 (m, 12H), 0.58 (s, 3H), 0.89 (s, 18H), 1.00 (d, $J = 6.3$ Hz, 3H), 1.26-1.36 (m, 3H), 1.46-1.61 (m, 3H), 1.61-1.73 (m, 2H), 1.73-1.81 (m, 1H), 1.81-1.96 (m, 3H), 1.96-2.05 (m, 3H), 2.22 (dd, $J = 12.6, 7.6$ Hz, 1H), 2.40-2.48 (m, 2H), 2.80-2.86 (m, 1H), 3.66 (s, 3H), 4.17-4.23 (m, 1H), 4.35-4.40 (m, 1H), 4.84-4.89 (m, 1H), 5.16-5.20 (m, 1H), 6.03 (d, $J = 11.2$ Hz, 1H), 6.24 (d, $J = 11.2$ Hz, 1H); $^{13}\text{C-NMR}$: (125MHz, CDCl_3) δ $-5.1, -4.8, -4.68, -4.67, 12.0, 18.1, 18.2, 19.7, 22.1, 23.4, 25.8, 25.9, 27.7, 28.8, 34.1, 40.5, 41.3, 44.8, 45.8, 46.1, 51.3, 56.3$ (2C), 67.5, 72.1, 111.3, 118.1,

123.1, 135.2, 140.5, 148.3, 173.84; m/z calculated for $C_{38}H_{67}NO_4Si_2Na$ 681 $[M + ACN + H]^+$, found 681; $[\alpha]_D^{25} = +21.0$ (c 1.0, $CHCl_3$)



O-bis-silylated calcitric acid: To a stirred solution of O-Bis-silylated CTA methyl ester (101.0mg, 0.16mmol) in minimal MeOH (5mL) was added a solution of 10% NaOH (%w/v) in MeOH:H₂O 9:1. The reaction stirred overnight at room temperature, then was neutralized with concentrated HCl to

~pH 6. The neutralized reaction mixture was concentrated under reduced pressure to remove MeOH, then diluted with H₂O (20mL). The mixture was extracted once with DCM, then acidified to pH 1 with concentrated HCl, and extracted with DCM again (3x20mL). Combined organic layers were dried over MgSO₄ and concentrated to the O-bis-silylated CTA (70.5mg, 71%) as a white powder. No attempts were made to purify the product further; R_f 0.18 (EtOAc: Hex 1:7); ¹H-NMR (500MHz, CDCl₃) δ 0.07-0.10 (m, 12H), 0.60 (s, 3H), 0.90 (s, 18H), 1.07 (d, $J = 6.4$ Hz, 3H), 1.29-1.39 (m, 3H), 1.49-1.60 (m, 3H), 1.64-1.74 (m, 2H), 1.76-1.82 (m, 1H), 1.86-2.10 (m, 7H), 2.24 (dd, $J = 13.2, 7.5$ Hz, 1H), 2.45-2.54 (m, 2H), 2.82-2.88 (m, 1H), 4.19-4.24 (m, 1H), 4.39 (dd, $J = 6.6, 3.4$ Hz, 1H), 4.89 (d, $J = 2.5$ Hz, 1H), 5.20 (d, $J = 1.75$ Hz, 1H), 6.04 (d, $J = 11.2$ Hz, 1H), 6.26 (d, $J = 11.2$, 1H); ¹³C-NMR: (125MHz, CDCl₃) δ -5.1, -4.8, -4.68, -4.67, 12.0, 18.15, 18.23, 19.7, 22.1, 23.4, 25.8 (3C), 25.9 (3C), 27.7, 28.8, 34.0, 40.5, 41.1, 44.8, 45.8, 46.1, 56.2, 56.3, 67.5, 72.1, 111.3, 118.1, 123.1, 135.3, 140.6, 148.3, 178.9; m/z calculated for $C_{35}H_{62}O_4Si_2$ 603.4259 $[M + H]^+$, found 603.4147; $[\alpha]_D^{25} = +26.0$ (c 1.0, $CHCl_3$)



Calcitroic acid methyl ester: Tetrabutylammonium fluoride (1M in

THF, 23mL, 23.3mmol) was added to a stirred solution of O-bis-silylated CTA methyl ester (0.96g, 1.55mmol) in dry THF (20mL)

at room temperature. The solution was stirred overnight,

quenched with saturated NH_4Cl solution (20mL) and extracted

with EtOAc (3x50mL). The combined organic layers were washed with brine (50mL), dried over

MgSO_4 , concentrated, and separated by column chromatography (EtOAc : Hex 7 : 3) to yield CTA

methyl ester as a slightly yellow oil (0.53g, 88%); R_f 0.26 (EtOAc: Hex 7:3); $^1\text{H-NMR}$ (500MHz,

CDCl_3) δ 0.57 (s, 3H), 0.98 (d, $J = 6.4$ Hz, 3H), 1.27-1.34 (m, 3H), 1.45-1.59 (m, 4H), 1.63-1.72 (m,

2H), 1.81-1.95 (m, 4H), 1.96-2.03 (m, 4H), 2.30 (dd, $J = 14.0, 8.0$ Hz, 1H), 2.43 (dd, $J = 14.5, 3.5$

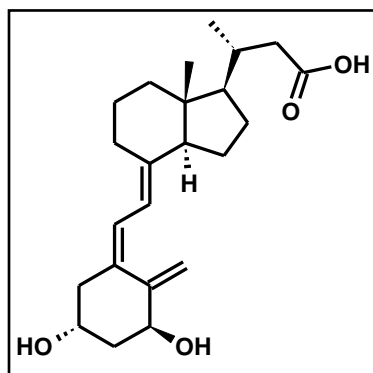
Hz, 1H), 2.57 (dd, $J = 13.7, 3.1$ Hz, 1H), 2.82 (dd, $J = 12.6, 4.3$ Hz, 1H), 3.66 (s, 3H), 4.21 (m, 1H),

4.42 (dd, $J = 7.6, 4.5$ Hz, 1H), 4.98 (s, 1H), 5.32 (s, 1H), 6.02 (d, $J = 11.0$ Hz, 1H), 6.35 (d, $J = 11.0$

Hz, 1H); $^{13}\text{C-NMR}$: (125MHz, CDCl_3) δ 12.0, 19.6, 22.2, 23.5, 27.6, 29.0, 34.1, 40.3, 41.3, 42.8,

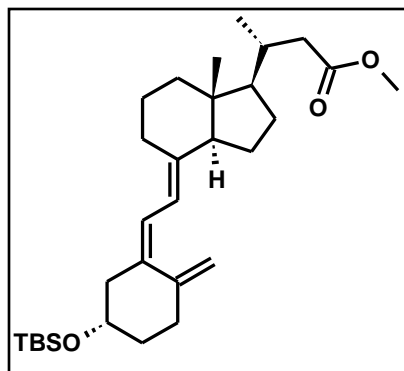
45.2, 45.9, 51.4, 56.3 (2C), 66.7, 70.6, 111.8, 117.3, 124.6, 133.4, 142.5, 147.7, 174.0; m/z

calculated for $\text{C}_{24}\text{H}_{36}\text{O}_4$ 389.2686 $[\text{M} + \text{H}]^+$, found 389.2618; $[\alpha]_D^{25} = -7.0$ (c 1.0, CHCl_3)



Calcitroic acid: CTA methyl ester (0.52g, 1.33mmol) was dissolved in a solution of 10% NaOH in 9:1 MeOH:H₂O (25mL) and stirred at room temperature for two hours. When all starting material had dropped to baseline by TLC, the reaction was neutralized with concentrated HCl to ~pH 7. Excess MeOH was evaporated under

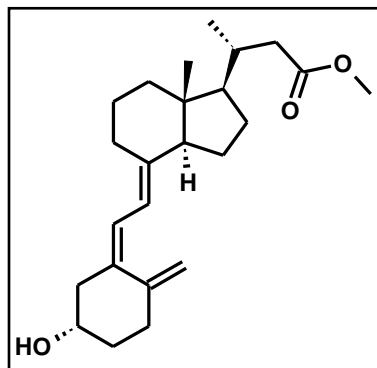
reduced pressure. The reaction was then diluted with H₂O (25mL), acidified with concentrated HCl to pH 1, and extracted with EtOAc (3 x 30mL). The combined organic layers were washed with brine (25mL), dried over MgSO₄, concentrated, and purified by column chromatography (EtOAc) to yield calcitroic acid (CTA) (0.40g, 80%) as a yellow solid; R_f 0.14 (EtOAc); ¹H-NMR (500MHz, CDCl₃) δ 0.60 (s, 3H), 1.06 (d, *J* = 6.5 Hz, 3H), 1.30-1.41 (m, 3H), 1.48-1.61 (m, 3H), 1.67-1.76 (m, 3H), 1.86-1.98 (m, 4H), 1.98-2.12 (m, 4H), 2.34 (dd, *J* = 13.0, 6.5 Hz, 1H), 2.50 (dd, *J* = 15.0, 3.5 Hz, 1H), 2.62 (dd, *J* = 13.5, 3.2 Hz, 1H), 2.85 (dd, *J* = 13.6, 4.6 Hz, 1H), 4.26 (m, 1H), 4.46 (dd, *J* = 4.2, 7.6, 1H), 5.02 (s, 1H), 5.35 (s, 1H), 6.04 (d, *J* = 11.2 Hz, 1H), 6.39 (d, *J* = 11.2 Hz, 1H); ¹³C-NMR: (125MHz, CDCl₃) δ 12.0, 19.7, 22.2, 23.5, 27.6, 29.0, 33.9, 40.3, 41.1, 42.8, 45.2, 45.9, 56.2, 56.3, 66.9, 70.8, 111.9, 117.2, 124.9, 133.1, 142.7, 147.6, 178.4; *m/z* calculated for C₂₃H₃₄O₄ 373.2373 [M + H]⁺, found 373.2335; [α]_D²⁵ = - 6.0 (c 1.0, CHCl₃)



O-silylated calcioic acid methyl ester: A solution of n-

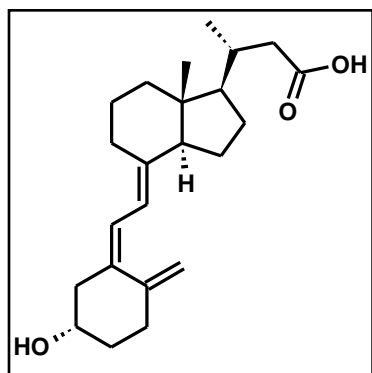
butyllithium (1.6 M in hexanes, 0.55mL, 0.565mmol) was added dropwise to a solution of calcioic acid A-ring phosphine oxide (500mg, 0.715mmol, dried over 3Å molecular sieves in 3 ml THF overnight) at -78°C using freshly dried 3Å molecular sieves.

The solution turned deep red and was stirred for an hour at -78°C. Raising the solution out of the bath briefly deepened the red color and ensured that the deprotonation was complete. The solution was returned to the bath and C,D-ring ketone (147mg, 0.376mmol, dried over 3Å molecular sieves in 2 ml THF overnight) was added dropwise. The solution was stirred for 5 hours at -78°C and allowed to come to room temperature. The reaction mixture was then quenched with 10mL water, diluted with TBME, and extracted (TBME, 2x50mL). Combined organic layers were washed with brine, dried over MgSO₄, and concentrated. The crude product was purified by column chromatography (EtoAc: Hex 5:95) to yield O-silylated calcioic acid methyl ester as a white crystalline solid (117mg, 41%); R_f 0.62 (EtOAc: Hex 1:9); ¹H-NMR (500MHz, CDCl₃) δ 0.06-0.10 (m, 6H), 0.60 (s, 2H), 0.90 (s, 9H), 1.00 (d, *J* = 4.0 Hz, 2H), 1.26-1.37 (m, 3H), 1.48-1.62 (m, 4H), 1.63-1.74 (m, 2H), 1.83-1.79 (m, 3H), 1.98-2.07 (m, 3H), 2.07-2.16 (m, 1H), 2.21-2.29 (m, 1H), 2.35-2.41 (m, 1H), 2.41-2.50 (m, 2H), 2.81-2.88 (m, 1H), 3.68 (s, 3H), 3.79-3.87 (m, 1H), 4.79 (s, 1H), 5.02 (s, 1H), 6.03 (d, *J* = 10.0 Hz, 1H), 6.17 (d, *J* = 10.0, 1H); ¹³C-NMR: (125MHz, CDCl₃) δ -4.6, -4.5, 12.1, 18.2, 19.7, 22.2, 23.4, 25.9 (4C), 27.7, 28.8, 32.8, 34.1, 36.4, 40.4, 41.4, 45.8, 46.9, 51.4, 56.3 (2C), 70.6, 112.2, 118.0, 121.3, 136.6, 141.0, 145.4, 174.0; *m/z* calculated for C₃₀H₅₀O₃Si 487.3602 [M + H]⁺, found 487.3542; [α]_D²⁵ = + 61.0 (c 1.0, CHCl₃)



Calcioic acid methyl ester: To a stirred solution of O-silylated calcioic acid methyl ester (79mg, 0.16mmol) in dry THF (7mL), tetrabutylammonium fluoride (1M in THF, 1.6mL, 1.6mmol) was added. The reaction was stirred at room temperature overnight, then quenched with saturated NH_4Cl solution (10mL). The mixture

was extracted with EtOAc (3x20mL) and the combined organic layers were washed with brine (30mL), dried over MgSO_4 , concentrated, and purified by column chromatography (EtOAc: Hex 3:7) to yield the calcioic acid methyl ester as a clear oil (55mg, 91%); R_f 0.16 (EtOAc: Hex 1:3); $^1\text{H-NMR}$ (500MHz, CDCl_3) δ 0.59 (s, 3H), 1.00 (d, $J = 6.5$ Hz, 3H), 1.28-1.36 (m, 4H), 1.49-1.58 (m, 3H), 1.64-1.71 (m, 3H), 1.84-1.98 (m, 4H), 1.98-2.04 (m, 3H), 2.15-2.22 (m, 1H), 2.26-2.32 (m, 1H), 2.26-2.32 (m, 1H), 2.38-2.48 (m, 2H), 2.56-2.61 (m, 1H), 2.81-2.87 (m, 1H), 3.68 (s, 3H), 3.92-3.98 (m, 1H), 4.82-4.83 (m, 1H), 5.05-5.07 (m, 1H), 6.04 (d, $J = 11.2$, 1H), 6.24 (d, $J = 11.2$, 1H); $^{13}\text{C-NMR}$: (125MHz, CDCl_3) δ 12.0, 19.7, 22.2, 23.5, 27.6, 28.9, 32.0, 34.1, 35.2, 40.4, 41.4, 45.9, 46.0, 51.4, 56.2, 56.3, 69.2, 112.4, 117.8, 122.3, 135.4, 141.7, 145.1, 174.0; m/z calculated for $\text{C}_{24}\text{H}_{36}\text{O}_3$ 373.2737 $[\text{M} + \text{H}]^+$, found 373.2664; $[\alpha]_D^{25} = + 18.0$ (c 1.0, MeOH)



Calcioic acid: To a stirred solution of calcioic acid methyl ester

(44mg, 0.12mmol) in ethanol (1.5mL) was added 1mL of 10%

aqueous NaOH. After disappearance of starting material by TLC

(around 1 hr), the reaction was neutralized with concentrated HCl

to ~pH 7. Excess MeOH was evaporated off under reduced

pressure. The reaction was then diluted with H₂O (25mL), acidified with concentrated HCl to pH

1, and extracted with EtOAc (3x5mL). The organic layers were washed with brine (5mL), dried

over MgSO₄, concentrated, and purified by column chromatography (EtOAc : Hex 4 : 1) to yield

calcioic acid (25mg, 59%) as a white powder; R_f 0.53 (EtOAc); ¹H-NMR (500MHz, CDCl₃) δ 0.61 (s,

3H), 1.06 (d, *J* = 6.5 Hz, 3H), 1.30-1.40 (m, 4H), 1.50-1.61 (m, 3H), 1.65-1.74 (m, 3H), 1.86-1.99

(m, 4H), 1.99-2.10 (m, 3H), 2.17-2.23 (m, 1H), 2.30 (dd, *J* = 12.8, 5.5 Hz, 1H), 2.39-2.46 (m, 1H),

2.51 (dd, *J* = 14.9, 3.0 Hz, 1H), 2.57-2.63 (m, 1H), 2.82-2.88 (m, 1H), 3.94-4.00 (m, 1H), 4.84 (s,

1H), 5.07 (s, 1H), 6.06 (d, *J* = 10 Hz, 1H), 6.25 (d, *J* = 10 Hz, 1H); ¹³C-NMR: (125MHz, CDCl₃) δ

12.02, 19.66, 22.20, 23.46, 27.66, 28.93, 31.95, 33.93, 35.14, 40.37, 41.19, 45.87, 45.88, 56.16,

56.27, 69.28, 112.49, 117.76, 122.32, 135.36, 141.71, 145.06, 178.96; *m/z* calculated for

C₂₃H₃₄O₃ 359.2581 [M + H]⁺, found 359.2524; [α]_D²⁵ = -17.0 (c 1.0, CHCl₃)

1.7 Biological Characterization of Calcitroic Acid

Background

When DeLuca et al. isolated and characterized CTA, they also determined the affinity of CTA for VDR and the vitamin D binding protein, which was 6.8 μ M and 10 μ M, respectively. Applying mouse models in 1981, they observed some calcification of the epiphyseal plate of rats maintained on a low phosphorus diet after a 7 day, 50ng/animal subcutaneous CTA treatment, albeit 3 times less than what occurred with 5ng/animal treatment with calcitriol.⁹² Because of the relative low affinity for CTA towards VDR, further investigations were not conducted.

In vitro investigations conducted a decade later using a luciferase assay under control of a mouse osteopontin vitamin D response element (VDRE) in melanoma epithelial cells found that at 20nM, CTA gene transcription was significantly upregulated in comparison to other 25-hydroxy

vitamin D₃ metabolites.¹⁰⁰ Similar results were observed with a luciferase transcription assay using a *CYP24A1* promoter VDRE.¹⁰¹ However, at 20nM CTA, no induction of the *CYP24A1* gene in HaCaT cells (immortalized keratinocyte) was observed when incubated for 4 hours or 24 hours.

Recently, the Arnold lab showed that while CTA was inactive in promoting the recruitment of SRC2-3 to VDR, it was able to inhibit this interaction with an IC₅₀ of 6.12 ± 2.1 μM in the presence of calcitriol. Using a two-hybrid assay to investigate the interaction between VDR and coregulator SRC-1, we have shown that CTA

promoted this interaction with an EC₅₀ of 0.85 ± 0.33

μM but only 55% efficacy was achieved in

comparison to 20nM calcitriol. Thus, from these

initial results we can conclude that CTA behaves like

a partial VDR agonist. Further transcription assays

using DU145 prostate cancer cells demonstrated that

CTA induced VDR target gene *CYP24A1* 9-fold at

7.5μM (see Figure 16). Also in this case, the

induction was significantly lower than calcitriol at

20nM.

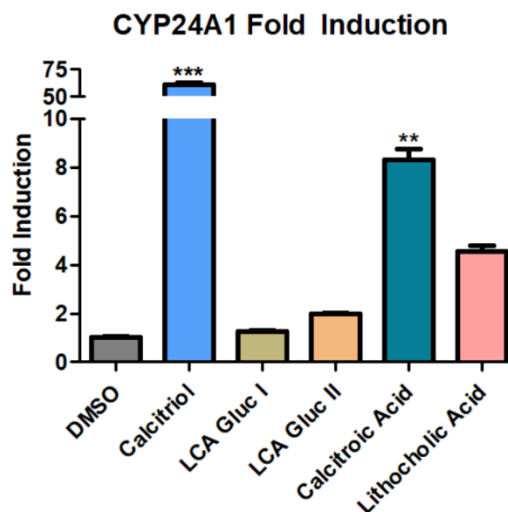


Figure 16: *CYP24A1* upregulation by synthetic phase 2 metabolites of lithocholic acid, LCA, and CTA (7.5μM) in DU145 prostate cancer cells, with 1,25(OH)₂D₃ (20nM) as a positive control and DMSO as a negative control.

It is known that VDR regulates expression of *CYP24A1*¹⁰² in addition to *CYP27B1*¹⁰³ in order to regulate the formation and catabolism of calcitriol. It also regulates *CYP3A4*,¹⁰⁴

CYP19A1,¹⁰⁵ and *CYP1A1*¹⁰⁶ as a xenobiotic sensor similar to the pregnane X receptor (PXR) and

constitutive androstane receptor (CAR).¹⁰⁷ Thus, vitamin D metabolites including CTA might play a role in detoxification by interacting with VDR and taking part in the regulation of several metabolic enzymes.

The synthesis of CTA enabled us to generate large quantities of CTA and to compare its properties to that of previously purchased CTA.

Interaction with VDR using fluorescence polarization

Fluorescence polarization (FP) is a fluorescence-based detection method that enables us to differentiate between the molecular sizes of fluorescent complexes using monochromatic polarized light. Small fluorescent compounds depolarize monochromatic emitted light due to their fast rotation in solution; however, fluorescent compound-protein complexes have a low tendency to depolarize light due to their slow tumbling in solution. For this competition assay we are using a fluorescent peptide that is derived from VDR coactivator SRC2-3 and recombinant expressed VDR-LBD and synthetic agonist LG190178. For this experiment, protein, peptide, and LG190178 are incubated in the presence of different concentrations of CTA and CTA methyl ester (Figure 17).

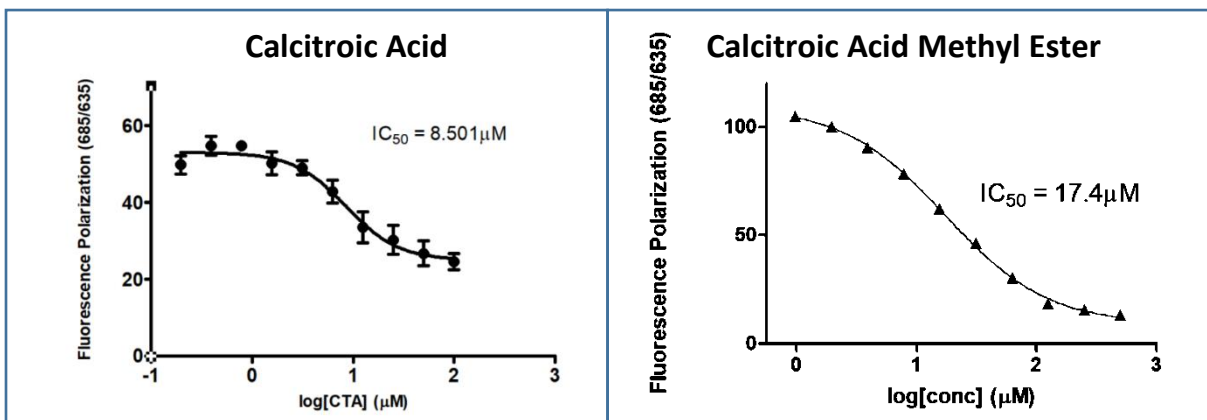


Figure 17: Modulation of binding of SRC2-3 to VDR-LBD in presence of LG190178 as a function of displacement by CTA (A) and CTA methyl ester (B).

Interaction with other nuclear receptors using a fluorescence polarization assay

After confirming that CTA binds to VDR, it is important to verify that this interaction is specific to VDR among other nuclear receptors (NR). To this end, FP data was collected for the binding of CTA to several other nuclear receptors including the androgen receptor, estrogen receptor β , retinoid X receptor α , thyroid hormone receptor α , thyroid hormone receptor β , and peroxisome proliferator-activated receptor γ (Figure 18).

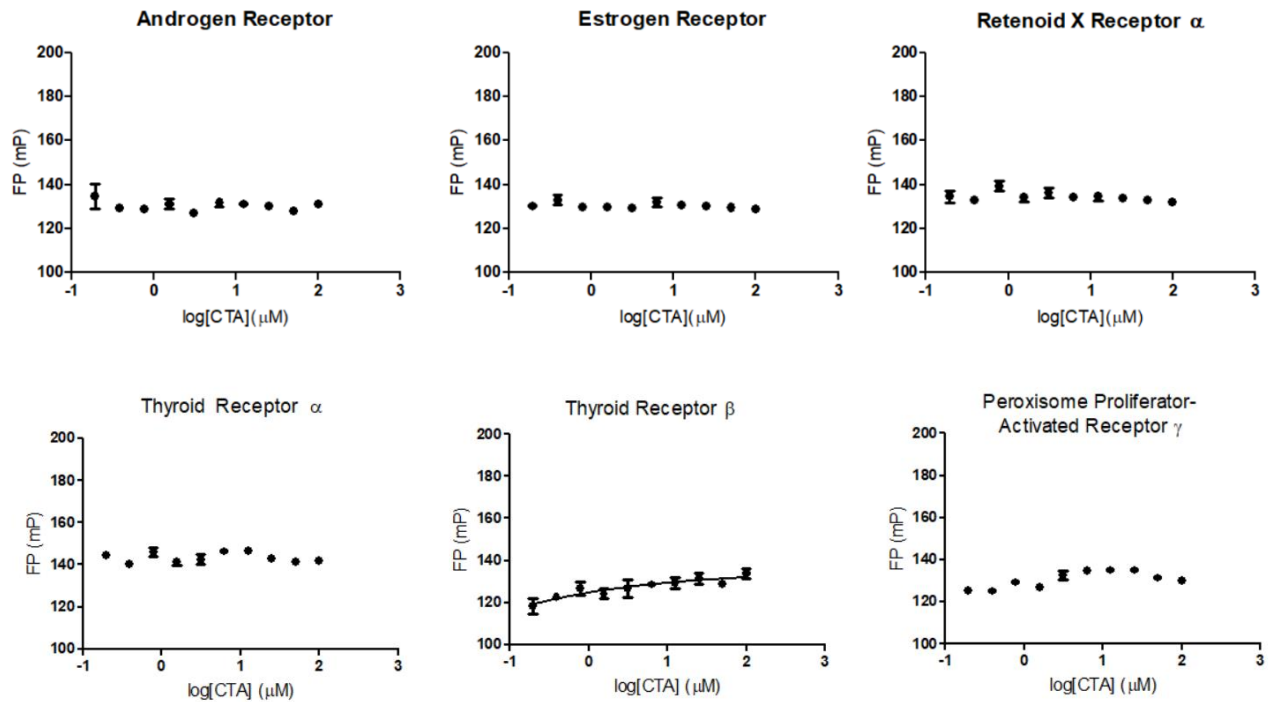


Figure 18: Other nuclear receptors and their fluorescently labeled peptide sequences did not depolarize light in the presence of CTA, providing evidence that CTA's binding to VDR is specific.

For all assays, recombinantly expressed NR-LBDs were incubated with the corresponding labeled coactivator peptide in the presence of different concentrations of CTA. All six nuclear receptor assays did not show any change of FP. Thus, we can conclude that among the nuclear receptors tested, CTA binding to VDR is specific.

Interaction with VDR using x-ray crystallography

CTA was sent to collaborator Natacha Rochel, who generated crystals of CTA bound to both a human and zebrafish recombinant VDR-LBD. The protein was concentrated using Amicon ultra-30 (Millipore) to 3-7mg/mL and incubated with 2x excess of CTA and 3x excess of coactivator peptide. Crystallization experiments occurred at 48°C. Crystals of hVDR complexed with CTA were obtained from a

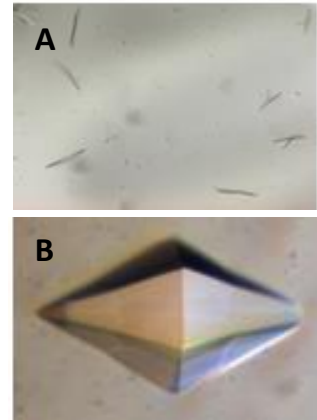


Figure 22: Protein crystals of (A) human LBD-VDR and (B) zebrafish LBD-VDR

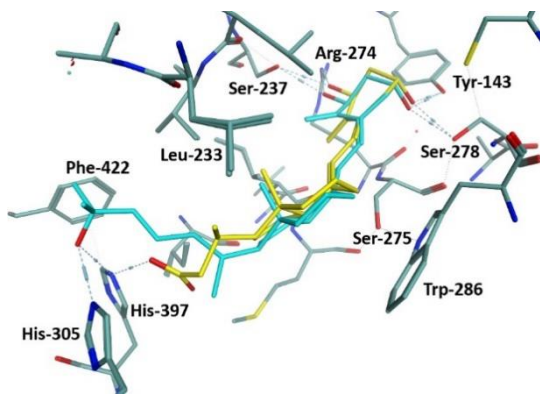


Figure 19: Stick-figure overlays of calcitriol (cyan) and CTA (yellow) within the binding pocket of VDR.

solution containing 0.2M ammonium sulfate, 2.7M sodium formate, and 0.1M PIPES (pH 7.0) (Figure 22A). Crystals of zVDR complexed to CTA were obtained from a solution containing 1.8M LiSO₄ and 0.1M Mes (pH 6.0) (Figure 22B). Protein crystals were mounted in a fiber loop

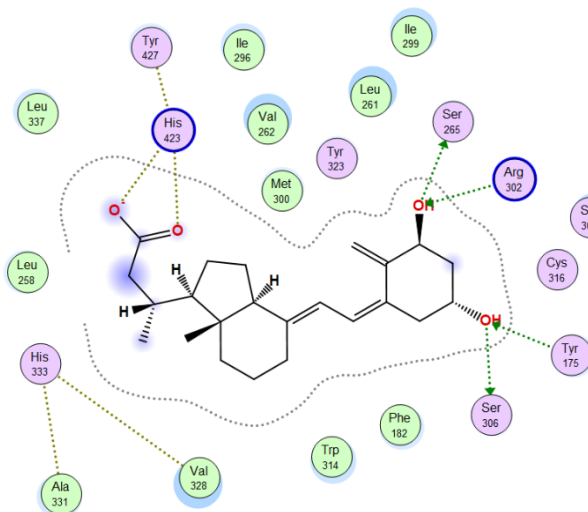


Figure 20: Protein-ligand interactions between CTA and VDR. Green arrows indicate side-chain donation/acceptance.

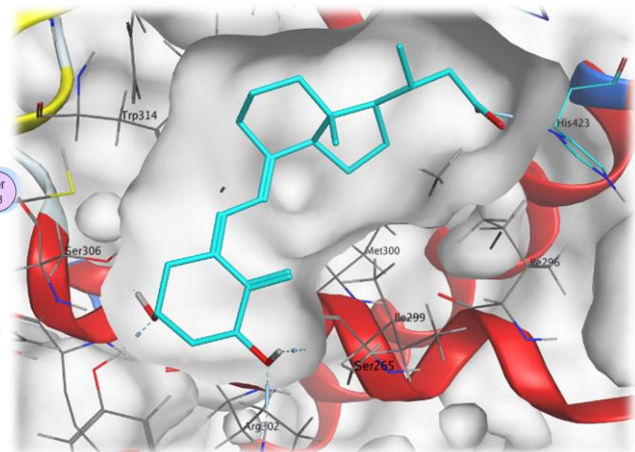


Figure 21: CTA in the binding pocket of zVDR LBD. The two OH residues on the A-ring (lower left, red) are anchored by donor/acceptor interactions with Tyr, Ser, and Arg residues, while the acid function (upper right, red) interacts with histidine.

and flash-cooled under nitrogen flux after cryo-protection with 20% glycerol. X-ray data has been collected from the crystals followed by homology modeling. Overlaying of CTA with calcitriol (Figure 19) visualizes the same binding mode of CTA and calcitriol. CTA forms several donor/acceptor interactions with VDR. Serine 306 and tyrosine 175 interact with the 3-OH of CTA, serine 265 and arginine 302 interact with 1-OH of CTA (Figure 23B), and histidine 423 interacts with the acid functionality of CTA (Figure 23A). The hydrophobic central ring structure of CTA aligns well with the hydrophobic side chains present in the center of the VDR binding pocket (Figure 21).

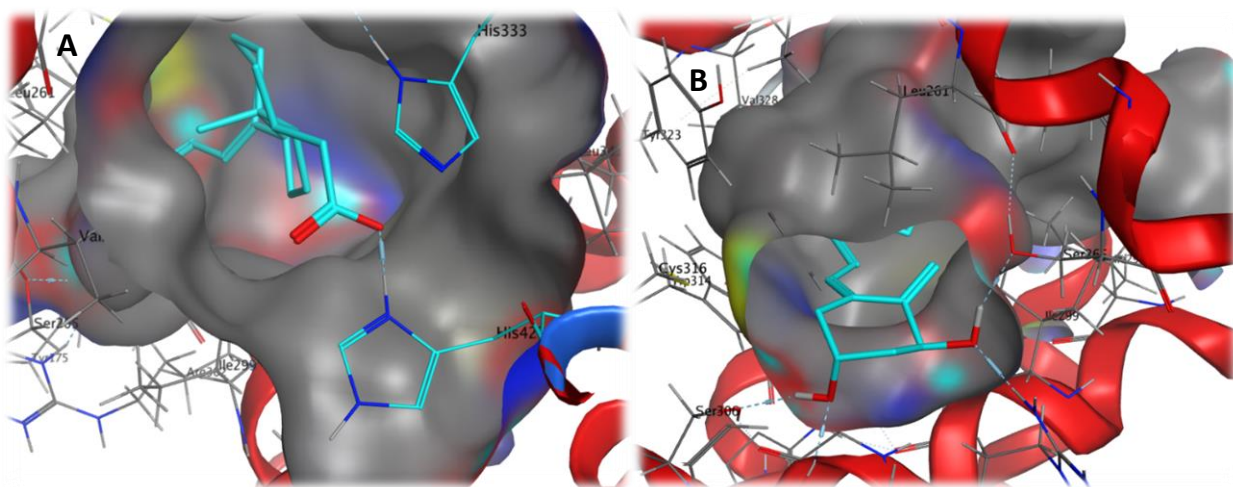


Figure 23: Detailed view of donor/acceptor interactions. (A) The acid functionality on CTA's side chain interacts through solvent contact with His 423. (B) On the other end of the molecule and binding pocket, the two hydroxyl groups make both donor and acceptor contacts with Ser 306, Tyr 175, Ser 265, and Arg 302.

Interaction with other nuclear receptors using a FRET-based assay

Fluorescence resonance energy transfer, or FRET, is a phenomenon where two light-sensitive chromophores situated within a certain distance of each other can transfer energy from an excited state in the donor chromophore to the acceptor chromophore. Because the wavelength used to excite the donor chromophore is different from the emission wavelength of the acceptor chromophore, there is very low background radiation. Because FRET emission only occurs when donor and acceptor chromophores are very close together and is proportional to the sixth power of the distance between them, FRET is extremely sensitive to changes in distance between the two. This makes the use of FRET technology for measuring binding very useful. The recently developed BODIPY FL vindoline¹⁰⁸ is a fluorescent FRET probe specific to PXR. A terbium labeled anti-GST antibody is used to enable time resolved FRET by taking advantage of the persistent fluorescence of lanthanides. Both PXR-LBD and CAR-LBD were generated with a GST tag. The displacement of the probe by compounds that bind to the LBD of PXR reduce the FRET signal, allowing for accurate assessment of PXR–ligand inhibition. A similar principle was used for

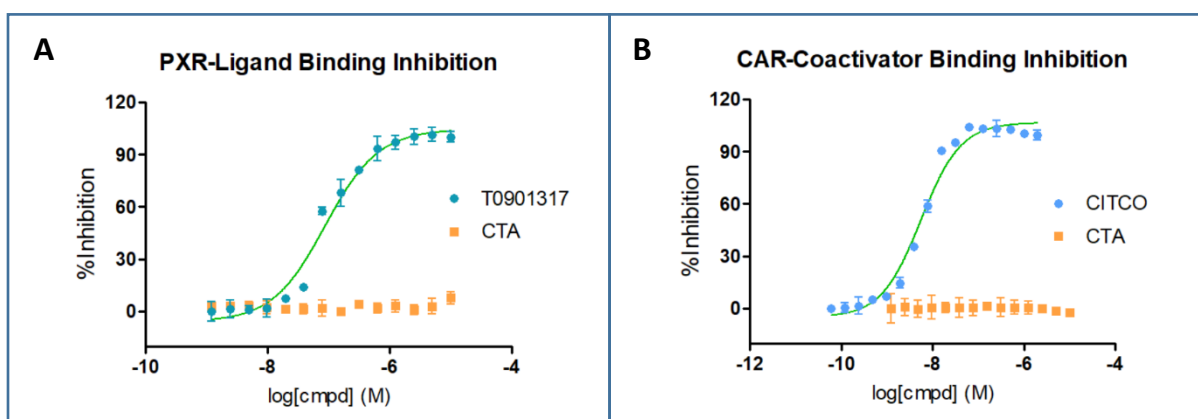


Figure 24: (A) The PXR-BODIPY FL vindoline interaction was not inhibited in the presence of CTA. (B) The CAR-PGC1 α interaction was not inhibited in the presence of CTA.

the FRET assay for the constitutive androstane receptor (CAR). However, in this case CAR-LBD was incubated with a labeled coactivator PGC1 α ,¹⁰⁹ which will bind CAR in the presence of an agonist such as CITCO. When PXR-BODIPY FL vindoline was treated with CTA (Figure 24A) or when CAR-PGC1 α was treated with CTA (Figure 24B), no inhibition of the FRET interaction took place, providing further evidence that CTA does not participate in binding with PXR and CAR.

Interaction with VDR using a transcription assay

With the confirmation from these protein assays that CTA did indeed bind specifically to VDR, we began cell-based assays to determine more about CTA's cell permeability and biological relevance. A transcription assay uses plasmids that are transfected into cells (HEK293T) to enable the generation of promoter-specific luciferase. For our assay, a cytomegalovirus promoter causes overexpression of VDR, and the reporter plasmid's luciferase gene is under control of a CYP24A1 promoter. Thus, in the presence of an agonist, activated overexpressed VDR recognizes the CYP24A1 VDRE and recruits RNA polymerase to transcribe the luciferase reporter gene. The bioluminescence of the generated enzyme in the presence of substrate (Luciferin) is directly proportional to the amount of VDR-mediated transcription.

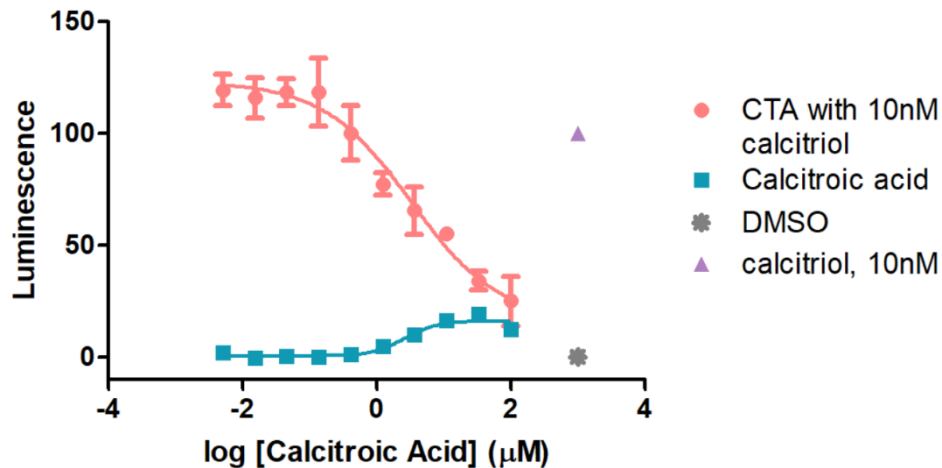


Figure 25: Combined dose response curves showing partial agonistic activity (teal) and competitive inhibition in the presence of calcitriol (pink) of CTA with VDR.

Dr. Teske showed for the first time that CTA behaves like a partial agonist in cells (Figure 25). In the presence of 10nM calcitriol, increasing the concentration of CTA will reduce the level of transcription as low as 20% at concentrations higher than 100µM. The IC_{50} for this inhibition is $3.2 \pm 2.4 \mu\text{M}$. In the absence of calcitriol, CTA is able to activate VDR-mediated transcription to

up to 20% of calcitriol transcriptional activity at 10nM with an EC_{50} of $2.5 \pm 1.0 \mu\text{M}$. Thus, interestingly, CTA inhibits the binding of calcitriol, but it also acts as a partial agonist at nearly the same concentration.

Interaction with other nuclear receptors using transcription assays

The transcriptional activity of other nuclear receptors in the presence of CTA was assessed by Prof. Merk's laboratory (Goethe University Frankfurt). In their assays, plasmids bearing NR-LBDs fused to a GAL4 DNA binding domain and a luciferase reporter with a UAS promoter site are used. Cells were transfected overnight and treated with different concentrations of CTA (Figure 26).

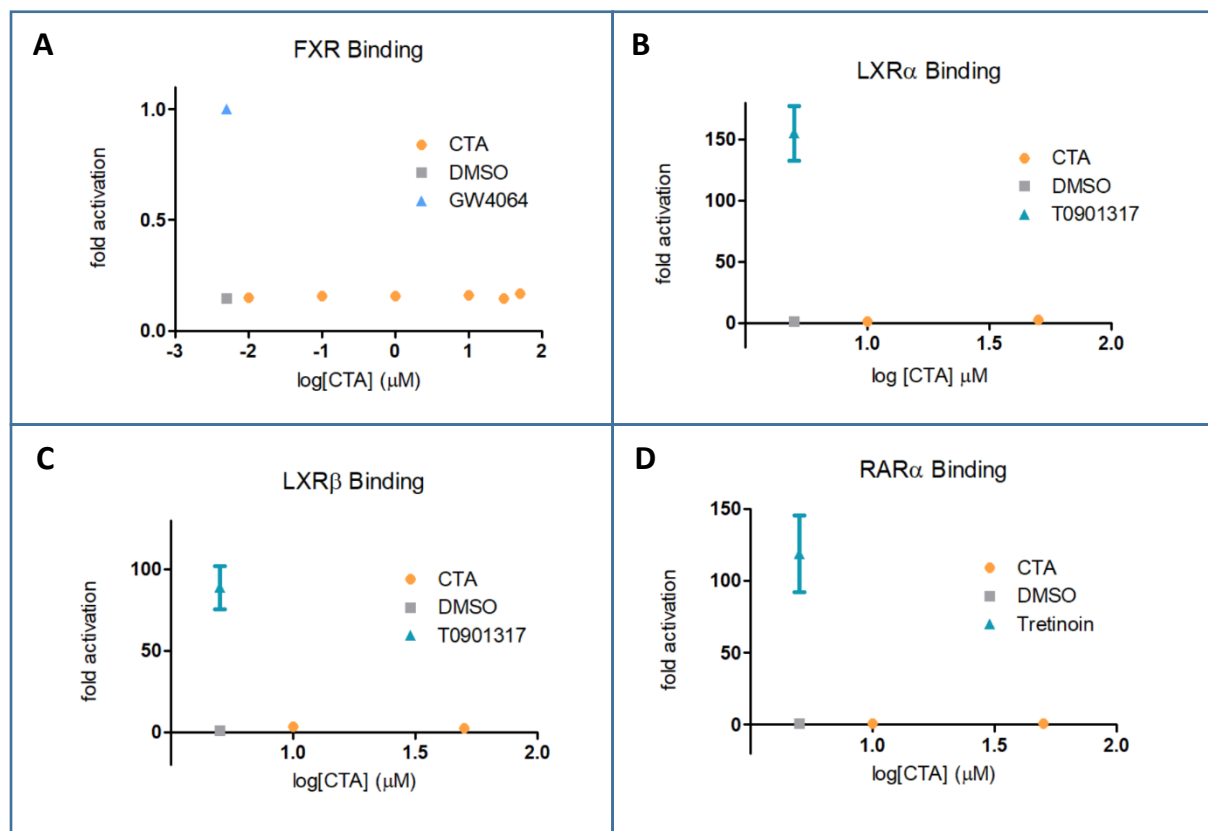


Figure 26: Transcriptional activity was absent in assays of other nuclear receptors treated with CTA.

In all cases tested, positive control compounds upregulated transcription of each nuclear receptor. However, CTA at different concentrations did not influence transcription. This result provides further evidence that the binding of CTA is specific to VDR.

Effect of CTA on macrophages

VDR is expressed in leukocytes, and calcitriol has been shown to modulate the immune system and suppress immune responses.¹¹⁰ Macrophages, a type of phagocytic white blood cell which engulfs and neutralizes foreign substances, are activated by infection and can maintain inflammation.¹¹¹ When stimulated to express an immune response, the activated M1 “killer” macrophages release inflammatory cytokines like IL-1, IL-12, and IL-23 and induce iNOS, the nitric oxide synthase involved in immune response. These transcriptional inflammatory products can be quantified by qRT-PCR (Figure 27B). Nitric oxide (NO) release can be measured by the formation of a brightly colored azo compound using a Griess assay (Figure 27A).¹¹²

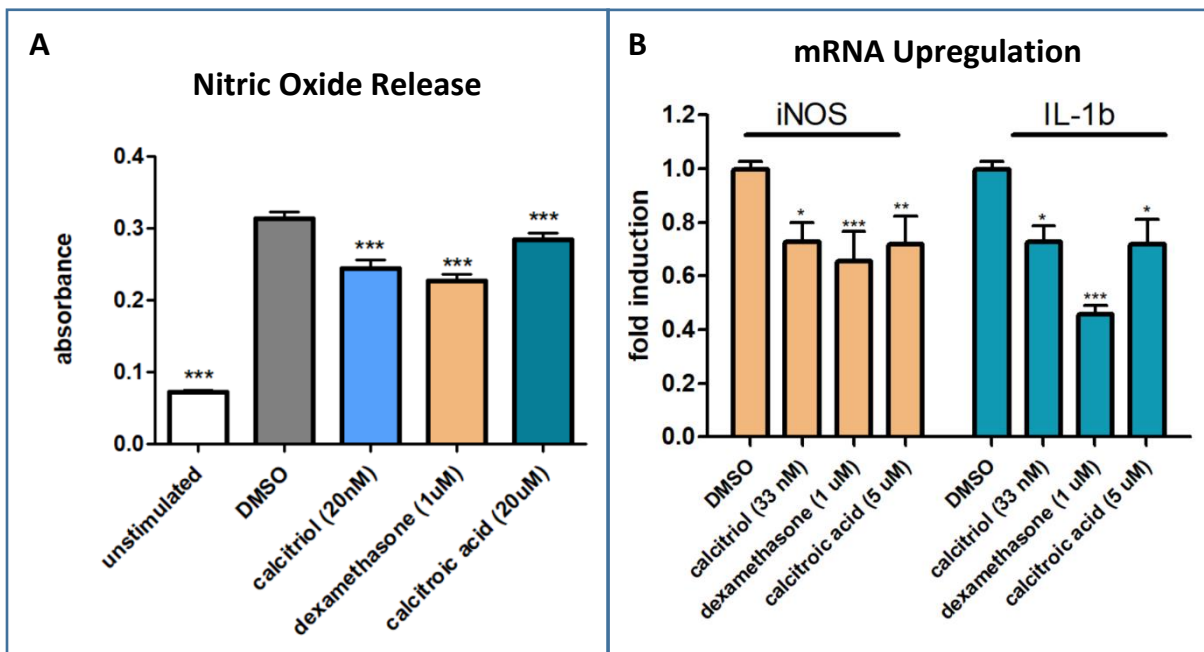


Figure 27: (A) Nitric oxide suppression as measured by Griess assay following stimulation with 150units/mL IFN γ and 50ng/mL LPS in RAW264.7 murine macrophages. 1,25(OH) $_2$ D $_3$ and CTA exhibited a decrease in NO, along with the positive control dexamethasone. (B) Downregulation of mRNA of inflammatory species in the presence of CTA and calcitriol, along with positive control dexamethasone.

To investigate whether CTA in addition to calcitriol can reduce inflammation, rat macrophages (RAW264.7, ATCC TIB-71) were stimulated with 150units/mL IFN γ and 50ng/mL LPS and dosed with calcitriol (20nM) and CTA (20 μ M) using DMSO (vehicle) and dexamethasone as negative and positive controls, respectively. The supernatant media from these cells was used for the Griess assay after 18 hours at 37°C, while the cells were harvested and their mRNA isolated. Figure 27a shows a strong elevation of NO when cells were treated with IFN γ /LPS and vehicle DMSO.

Interestingly, calcitriol, CTA and dexamethasone reduced NO formation, although at different concentrations. Similarly, mRNA of iNOS and IL-1b were downregulated by calcitriol, CTA, and dexamethasone. This is consistent with our hypothesis that CTA interacts with VDR and can regulate transcription.

Effect of CTA on intestinal epithelial cells

Starting with colon cancer (Caco2) cells as a preliminary model of the intestinal barrier, cells were treated with CTA along with LCA (a known weak ligand of VDR that can induce gene expression in the ileum¹¹³) with DMSO and calcitriol as negative and positive controls, respectively. We monitored the upregulation of *CYP3A4* mRNA, along with that of several other CYP genes known to be mediated by VDR (*CYP2B6*, *CYP2C9*).¹¹⁴ We observed specific upregulation of *CYP3A4* mRNA by CTA but not that of other VDR-mediated enzymes *CYP2B6* and *CYP2C9* (Figure 28).

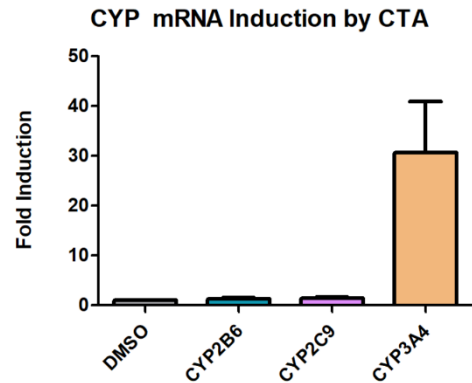


Figure 28: *CYP3A4* upregulation by CTA (6 μ M) in Caco2 cells. DMSO is a negative control. No upregulation of other CYP mRNA was seen under these conditions.

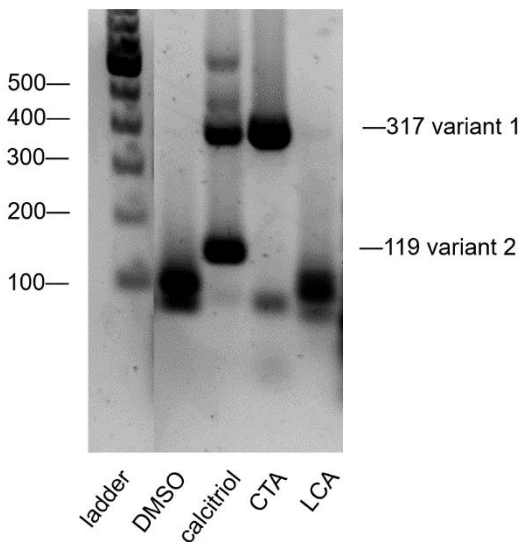


Figure 29: Gel of *CYP3A4* primer, which is differentially upregulated by CTA and calcitriol.

The much slower-growing normal human intestinal epithelial cell line (HIEC-6) derived from crypt cells was then purchased and cultured. In the process of seeking out a better primer for *CYP3A4*, we made an interesting discovery. When running an agarose gel to ensure the selectivity of our *CYP24A1* primers, calcitriol upregulated both the 317 kDa and the 119 kDa splice variants of *CYP24A1*, which was expected. However, CTA preferentially upregulated

the 317 kDa variant, with no 119 kDa splice variant seen (Figure 29). This was repeated several

times with the same result. Investigating this surprising and specific difference may be a target of future studies.

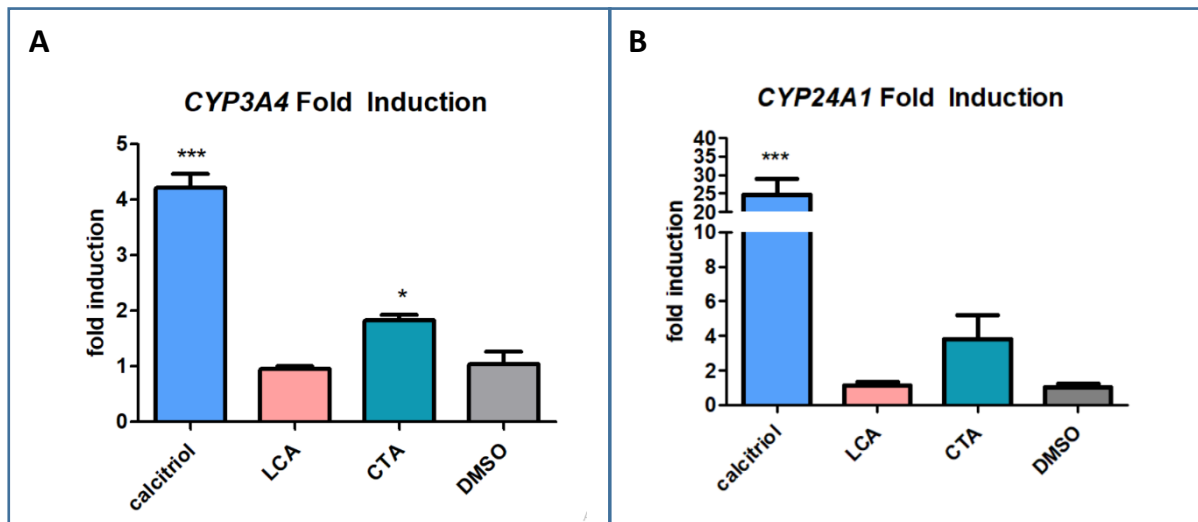


Figure 30: Upregulation by CTA and lithocholic acid (both 10 μ M) in HIEC6 human normal intestinal epithelial cells, with 1,25(OH)₂D₃ (20nM) as a positive control and DMSO at a negative control, against CYP3A4 (A) and CYP24A1 (B).

mRNA quantification was achieved by qRT-PCR (Figure 30). We observed that calcitriol at 20nM highly upregulated both *CYP24A1* and *CYP3A4* in HIEC6 cells. In comparison to 10 μ M LCA, 10 μ M CTA resulted in a more pronounced transcription of both *CYP24A1* and *CYP3A4*, whereas LCA induced no significant transcription. This evidence furthers the hypothesis that CTA may play an integral part in detoxification by elevating CYP3A4 levels, an enzyme which is known to metabolize LCA in the intestines.¹¹⁵

Stability of CTA in the presence of P450 enzymes

It has been established that CYP3A4 plays a role in the hydroxylation of calcitriol as part of its metabolic breakdown in intestines and liver.¹¹⁶ We investigated the stability of both CTA and calcitriol in human liver microsomes (HLM) in order to determine the stability of CTA in the presence of P450 enzymes including CYP3A4. Therefore, HLM were incubated in the presence of CTA and aliquots were taken at specific time intervals. The concentrations of CTA were determined by LCMS-MS and presented as their natural logarithm vs. time (Figure 31).

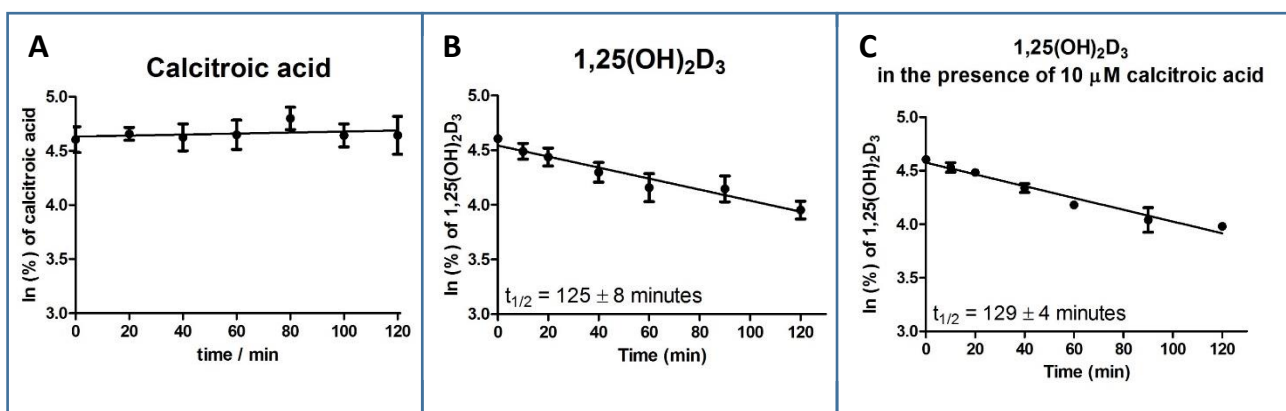


Figure 31: Microsomal digestion of CTA (A), calcitriol (B), and both CTA and calcitriol (C).

While we saw the expected breakdown of calcitriol under these conditions, we did not observe metabolism of CTA during a period of 2 hours. Calcitriol exhibited a half-life of around two hours. This experiment confirms that CTA is not further changed through phase I metabolism. In order to investigate if CTA inhibits P450 enzymes, calcitriol was incubated in the presence of CTA (Figure 31C). Because the half-life of calcitriol is not changing whether CTA is present or not, we can conclude that CTA is not inhibiting P450 enzyme activity.

Discussion

The biological data collected on CTA indicates that CTA is not the inactive metabolic byproduct it had long been assumed to be. Binding data show that CTA binds specifically to VDR among other nuclear receptors. X-ray crystallography confirmed this interaction and shows that CTA adopts the same binding mode as calcitriol.

Cell-based assays demonstrate that CTA is cell membrane-permeable and inhibits the interaction between VDR and calcitriol. However, the inhibition is partial (80%), because CTA is also able to activate VDR-mediated transcription with an efficacy of 20%. Because both equilibria occur at the same concentration, CTA can be described a partial agonist/antagonist.

When metabolism to CTA occurs in the kidney it can lead to urinary excretion; however, phase II metabolism conjugation in the liver could lead to intestinal secretion of conjugated vitamin D metabolites as bile. In the intestines, bacteria and intestinal cells can reverse this process, which would liberate vitamin D metabolites to be reabsorbed and contribute to enterohepatic circulation. Evidence already suggests that bile carries large quantities of vitamin D metabolites, which were isolated and characterized during the last 40 years.⁶⁹ Our work is focused on the physiological activity of CTA in the intestine.

One important cell type mediating the immune response in the intestine are macrophages. It has been reported that macrophages mediate diseases such as inflammatory bowel disease.¹¹⁷ We were able to show for rat macrophages that CTA in addition to calcitriol can significantly decrease inflammation based on the reduction of two inflammation markers, IL-1b

and iNOS, in the presence of IFN γ /LPS. Thus, we believe that CTA is acting as a natural anti-inflammatory molecule.

Another important intestinal cell type are epithelial cells that are part of the gastrointestinal wall. These cells are known to express P450 enzymes to combat xenobiotic toxicity.¹¹⁸ We have shown that CTA and calcitriol were able to upregulate the transcription of these enzymes *in vitro*. Furthermore, we observed that the regulation of *CYP24A1* differs between CTA and calcitriol. Further investigations are necessary to investigate this phenomenon.

In conclusion, we are presenting compelling evidence for the link between the detoxification of the gut and VDR's CTA-mediated activity. We believe that the water-soluble metabolites of vitamin D that are secreted into the intestinal tract protect the colon from inflammation-inducing accumulation of xenobiotics such as lithocholic acid by upregulation of *CYP3A4*.⁸⁵ Vitamin D has been shown to provide a noticeable amount of relief from symptoms in IBD as well.¹¹⁹ The mechanism by which this relief takes place remains unknown, and these results indicate that it could be mediated in part by CTA.

Experimental Procedures:

Fluorescence Polarization Binding Assay Protocol

The FP assay buffer was prepared by adding 25mM PIPES (piperazine-N,N'-bis(ethanesulfonic acid, Sigma-Aldrich), 50mM NaCl (Fisher), and 0.01% NP-40 detergent to 18.2MΩ water. The buffer was filtered and adjusted to pH 6.75. To this was added 7.5nM of the coactivator peptide SRC2-3 (CKKKENALLRYLLDKDDTKD) which had been labeled with cysteine-reactive AlexaFluor647. To this solution was added 250nM of VDR-LBD, which had been expressed and purified as reported previously.¹²⁰ The VDR agonist LG190178, which had been synthesized previously according to a published protocol,¹²¹⁻¹²² was added at a concentration of 600nM. A 10mM stock of CTA in DMSO was serially diluted (1:2) in a 384-well plate (Corning, CLS3702). To a 384-well black polystyrene microplate (Corning, CLS3658), 20μL of the prepared VDR-LBD assay solution was dispensed to test against the CTA serial dilution. Using the Tecan Freedom EVO liquid handler system and a 100nL pin tool (V&P Scientific), a total of 200nL of each CTA concentration was transferred in quadruplicate to the 20μL assay solution for a final maximum concentration of 100μM CTA. Following incubation for 1 hour, fluorescence polarization was detected at an excitation/emission wavelength of 635/685 nm using the Tecan Infinite M1000 plate reader. The result showed CTA binding at an IC₅₀ of 8.5μM. To verify specificity, CTA was investigated with other nuclear receptors and their respective agonists and coactivators (thyroid receptor α LBD (2μM)/Texas Red-labeled SRC2-2 (7nM)/triiodothyronine (1μM); thyroid receptor β LBD (0.8μM)/Texas Red-labeled SRC2-2 (7nM)/triiodothyronine (1μM); peroxisome proliferator-activated receptor γ (5μM)/Texas Red-labeled DRIP2 (7nM)/rosiglitazone (5μM); androgen

receptor LBD (5 μ M)/Alexa Fluor 647-labeled SRC2-3 (7nM)/dihydrotestosterone (10nM);
estrogen receptor β LBD (5 μ M)/Texas Red-labeled SRC2-2 (7nM)/estradiol (20nM)).

Transcription Assay Protocol

Human embryonic kidney (HEK293, ATCC CRL-3249) T cells were cultured in DMEM/High Glucose (Hyclone, #SH3024301) with non-essential amino acids (Hyclone, #SH30238.01), 10 mM HEPES (Hyclone, #SH302237.01), 5 x 10⁶ units of penicillin and streptomycin (Hyclone, #SV30010), and 10% of FBS (Gibco, #10082147). Transfection was carried out with 70-80% confluent cells. For VDR transfection, 2 mL of untreated DMEM/High Glucose media containing 0.7 μ g of VDR-CMV plasmid, 16 μ g of a CYP24A1-luciferase reporter gene, LipofectamineTM LTX (75 μ l, Life Technologies #15338020), and PLUSTM reagent (25 μ l) was added to the flask. After 16 hours of incubation at 37°C with 5% CO₂, the cells were harvested with 3mL of 0.05% Trypsin (Hyclone, #SH3023601), added to 10mL of the assay buffer (DMEM/High Modified buffer without phenol red, Hyclone #SH30284.01) and spun down for 2 minutes at 1000 rpm. The media was removed and cells were resuspended in the DMEM assay media. Prior to adding cells to sterile white, optical bottom 384-well plates, plates were treated with 20 μ L per well of a 0.25% matrigel solution. To each well, 20 μ L of cells were added to yield a final concentration of 15,000 cells per well. The plates were then spun down for 2 minutes at 1000 rpm. After four hours, plated cells were treated with 100 nL of compounds and controls which were added using the EVO liquid handling system with a 100nL pin tool (V&P Scientific). Controls used with VDR were 1,25(OH)₂D₃ (10 nM in DMSO, Endotherm) and DMSO. After 16 hours of incubation at 37°C

with 5% CO₂, 20µL of Bright-Glo™ Luciferase Assay Kit (transcription assay, Promega, Madison, WI) were added and luminescence was read on the Tecan Infinite M1000 reader.

Transcription Assay (provided by Prof. Daniel Merk)

HEK293T cells were cultured in Dulbecco's modified Eagle's medium (DMEM), high glucose with 10% fetal calf serum (FCS), sodium pyruvate (1mM), penicillin (100U/mL), and streptomycin (100µg/mL) at 37°C and 5% CO₂. Twenty-four hours before transfection, HEK293T cells were seeded in 96-well plates (3 × 10⁴ cells/well). Before transfection, medium was changed to OptiMEM without supplements. Transient transfection was carried out using Lipofectamine LTX reagent (Invitrogen) according to the manufacturer's protocol with pFR-Luc (Stratagene), pRL-SV40 (Promega), and the corresponding Gal4-fusion nuclear receptor plasmid. Five hours after transfection, medium was changed to OptiMEM supplemented with penicillin (100 U/mL), streptomycin (100 µg/mL), and additionally containing 0.1% dimethyl sulfoxide (DMSO) and the respective test compound or 0.1% DMSO alone as untreated control. Each concentration was tested in duplicates and each experiment was repeated independently at least three times. After overnight (14–16 h) incubation with the test compounds, the cells were assayed for luciferase activity using the Dual-Glo Luciferase Assay System (Promega) according to the manufacturer's protocol. Luminescence was measured with an Infinite M200 luminometer (Tecan Deutschland GmbH). Normalization of transfection efficiency and cell growth was done by division of firefly luciferase data by Renilla luciferase data and multiplying the value by 1000 resulting in relative light units (RLU). Fold activation was obtained by dividing the mean RLU of a test compound at a

respective concentration by the mean RLU of the untreated control. Relative activation was obtained by dividing the fold activation of a test compound at a respective concentration by the fold activation of a respective reference agonist: RXR α : bexarotene (EC_{50} : 33nM) LXR α/β : T09021317 (EC_{50} ~ 50nM); FXR: GW4064 (EC_{50} = 70nM). All hybrid assays were validated with the above-mentioned reference agonists which yielded EC_{50} values in agreement with the literature.

Griess Assay Immune Modulation Protocol

The murine macrophage cancer cell line RAW264.7 was cultured in DMEM (ATCC 30-2002) with 10% FBS. To initiate an immune response, cells were suspended at a cell density of 1×10^6 cells/mL and a control sample (3mL) was dispensed into a 6-well clear-bottomed sterile plate with a lid (Corning 3516). The remaining suspended cells were then activated with interferon gamma (IFN γ , 150units/mL) and lipopolysaccharide (LPS, 50ng/mL). Activated cells were dispensed into the 6-well plate (3mL/well). Cells were then dosed with compounds of interest to the following final concentrations: calcitriol (20nM), CTA (5 μ M, 20 μ M), with dexamethasone as a positive control (10 μ M), and DMSO as a negative control. The plated cells were then allowed to incubate for 18 hours. Following incubation, aliquots of the supernatant (80 μ L) from each 6-well sample were taken in replicates of 8 and transferred to a 384-well clear-bottomed plate with a lid (CLS3700). To each aliquot was added 10 μ L of sulfanilamide solution (Promega Griess Reagent System, TB229). The covered plate was shaken briefly and incubated in the dark for 10 minutes. Following this, 10 μ L of NED solution (Promega Griess Reagent System, TB229) was added to each

aliquot. The plate was again shaken briefly and incubated in the dark for 10 minutes. The absorbance of the plate was then read on the Tecan Infinite M1000 plate reader (530nm).

Quantitative Real Time Polymerase Chain Reaction Protocol

The human colon cancer cell line Caco2 (ATCC HTB-37) or the human normal intestinal epithelial cell line HIEC-6 (ATCC CRL-3266) were purchased and cultured according to ATCC's listed method. The cells were harvested with 0.25% Trypsin and then were plated (3mL) in a 6-well clear-bottomed sterile plate with lid (Corning 3516) at a concentration of 1×10^6 cells/mL. The plate was incubated overnight at 37°C for the cells to settle and adhere to the plate. Cells were then dosed with compounds of interest to the following final concentrations: calcitriol (20nM), CTA (20μM), lithocholic acid (20μM), and DMSO as a negative control. The plate was incubated for 24 hours at 37°C. The cell media was then removed, the cells rinsed briefly with PBS, and then harvested with 300μL of 0.25% Trypsin. The Trypsin was then diluted when cells were free by addition of 700μL of normal media. The suspended cells were then transferred to Eppendorf 1.5mL tubes. The cells were spun down at 1800rpm for 5 minutes to form a pellet. The media was removed and the cells disrupted by adding 350μL of 1% β-mercaptoethanol in Buffer RLT (from Qiagen RNeasy Mini Kit 74104) to each and vortexing. The lysate was pipetted directly onto QIAshredder spin columns (Qiagen 79654) in a 2mL collection tube and centrifuged for 2 minutes at 1800rpm. To the homogenized lysate 350μL of 70% ethanol was added. The 700μL of solution was transferred to the RNeasy spin column and spun down at 1800rpm for 15 seconds. Flow-throughs were discarded and the column was washed sequentially with 700μL Buffer RW1, 500μL Buffer

RPE x2, and then the RNA eluted into a 1.5mL collection tube with 50µL of The RNA Storage Solution (Ambion, AM7001). The amount of RNA collected and its purity was measured by measuring UV signal at 260nm with the Tecan Infinite M1000. Samples of RNA were then taken and added to a solution containing forward and reverse primers for the sequences of interest along with the calculated amounts of quantifastRT, SYBR Green solution, and RNase-free water. Primers used for various experiments included the *GAPDH* housekeeping gene (forward: 5'-ACCACAGTCCATGCCATCAC-3' reverse: 5'-TCCACCACCCTGTTGCTGTA-3'), *CYP3A4_1* (forward: 5'-CCTACATATACACACCCTTTGGAAG-3' reverse: 5'-GGTTGAAGAAGTCCTCCTAAGCT-3')(Blast see below), *CYP3A4_2*: (forward: 5'-CACAAACCGGAGGCCTTTTG-3' reverse: 5'-ATCCATGCTGTAGGCCCAA-3') (Blast see below) *CYP2B6* (forward: 5'-GGCCATACGGGAGGCCCTTG-3' reverse: 5'-AGGGCCCCTTGATTCC-3'), and *CYP2C9* (forward: 5'-TCCTATCATTGATTACTTCCCG-3' reverse: 5'-AACTGCAGTGTTCCTCAAGC-3'). Replicates were pipetted into a 96-well PCR plate (Eppendorf 951022003). The program used on the thermal cycling machine (Eppendorf AG22331 Hamburg Mastercycler) was 5 minutes at 95°C (initial activation step), and then cycling through 10 seconds at 95° C (denaturation step) and 30 seconds at 60°C (annealing step) for 50 cycles.

Microsomal Stability Assay Protocol

8 μ L of 1mM test compound (at a final concentration of 20 μ M) in DMSO was pre-incubated at 37°C for five minutes on a digital heating shaking dry bath (Fischer scientific, Pittsburgh, PA) in a mixture containing 274 μ L of water, 80 μ L of phosphate buffer (0.5M, pH 7.4), 20 μ L of NADPH Regenerating System Solution A (BD Bioscience, San Jose, CA) and 4 μ L of NADPH Regenerating System Solution B (BD Bioscience, San Jose, CA) in a total volume of 391.2 μ L. Following pre-incubation, the reaction was initiated by addition of 8.8 μ L of either human liver microsomes (BD Gentest, San Jose, CA) or mouse liver microsomes (Life technologies, Rockford, IL), at a protein concentration of 0.5mg/mL. Aliquots of 50 μ L were taken at time intervals of 0 (no microsomes), 10, 20, 40, 60, 90 and 120 minutes (calcitriol) or 0 (no microsomes), 20, 40, 60, 80, 100, and 120 minutes (CTA). Each aliquot was added to 100 μ L of cold methanol solution containing 450nM of 4,5-diphenylimidazole (4,5-DPI) (for a final concentration of 300-nM) as internal standard in a 96 well plate. The quenched samples were transferred to a filter plate and vacuum filtrated. The filtrate was diluted 10-fold and analyzed subsequently by LC-MS/MS with the Shimadzu LCMS 8040 instrument. CTA and calcitriol were monitored under positive mode by Shimadzu 8040 triple quadrupole mass analyzer (Shimadzu, Kyoto, Japan) with electrospray ionization (ESI). The following transitions are monitored in multiple reaction monitoring (MRM) mode. Transitions for calcitriol were m/z 434.30 > 399.35, 434.30 > 381.35, 434.30 > 363.35, and 434.30 > 227.15. Transitions for CTA were m/z 375.35 > m/z 357.25, m/z 375.35 > m/z 339.25, and m/z 375.35 > m/z 121.15. Transition pairs for verapamil are m/z 455.60 > m/z 303.20, m/z 455.60 > m/z

165.20, and m/z 455.60 > m/z 150.00. Collision energy is optimized for each transition to obtain optimal sensitivity. The mass spectrometer was operated with the heat block temperature of 400°C, drying gas flow of 15L/min, desolvation line temperature of 250°C, nebulizing gas flow of 1.5L/min, and both needle and interface voltages of 4.5kV.

1. Esvelt, R. P.; Fivizzani, M. A.; Paaren, H. E.; Schnoes, H. K.; DeLuca, H. F., Synthesis of calcitroic acid, a metabolite of 1.alpha.,25-dihydroxycholecalciferol. *The Journal of Organic Chemistry* **1981**, *46* (2), 456-458.
2. Harant, H.; Andrew, P. J.; Reddy, G. S.; Foglar, E.; Lindley, I. J., 1alpha,25-dihydroxyvitamin D3 and a variety of its natural metabolites transcriptionally repress nuclear-factor-kappaB-mediated interleukin-8 gene expression. *European journal of biochemistry* **1997**, *250* (1), 63-71.
3. Harant, H.; Spinner, D.; Reddy, G. S.; Lindley, I. J., Natural metabolites of 1alpha,25-dihydroxyvitamin D(3) retain biologic activity mediated through the vitamin D receptor. *J Cell Biochem* **2000**, *78* (1), 112-20.
4. Jones, G.; Prosser, D. E.; Kaufmann, M., 25-Hydroxyvitamin D-24-hydroxylase (CYP24A1): its important role in the degradation of vitamin D. *Archives of biochemistry and biophysics* **2012**, *523* (1), 9-18.
5. Jones, G.; Prosser, D. E., Chapter 3: The activating enzymes of vitamin D metabolism (25- and 1alpha-hydroxylase). In *Vitamin D*, third ed.; Feldman, D.; Pike, J. W.; Adams, J. S., Eds. Academic Press: San Diego, CA, USA, 2011; Vol. one.
6. Wang, Z.; Schuetz, E. G.; Xu, Y.; Thummel, K. E., Interplay between vitamin D and the drug metabolizing enzyme CYP3A4. *The Journal of steroid biochemistry and molecular biology* **2013**, *136*, 54-8.
7. Lundqvist, J.; Hansen, S. K.; Lykkesfeldt, A. E., Vitamin D analog EB1089 inhibits aromatase expression by dissociation of comodulator WSTF from the CYP19A1 promoter-a new regulatory pathway for aromatase. *Biochimica et biophysica acta* **2013**, *1833* (1), 40-7.

8. Matsunawa, M.; Akagi, D.; Uno, S.; Endo-Umeda, K.; Yamada, S.; Ikeda, K.; Makishima, M., Vitamin D receptor activation enhances benzo[a]pyrene metabolism via CYP1A1 expression in macrophages. *Drug metabolism and disposition: the biological fate of chemicals* **2012**, *40* (11), 2059-66.
9. Reschly, E. J.; Krasowski, M. D., Evolution and function of the NR1I nuclear hormone receptor subfamily (VDR, PXR, and CAR) with respect to metabolism of xenobiotics and endogenous compounds. *Current drug metabolism* **2006**, *7* (4), 349-65.
10. Lin, W.; Liu, J.; Jeffries, C.; Yang, L.; Lu, Y.; Lee, R. E.; Chen, T., Development of BODIPY FL Vindoline as a Novel and High-Affinity Pregnane X Receptor Fluorescent Probe. *Bioconjugate Chemistry* **2014**, *25* (9), 1664-1677.
11. Carazo, A.; Pávek, P., The Use of the LanthaScreen TR-FRET CAR Coactivator Assay in the Characterization of Constitutive Androstane Receptor (CAR) Inverse Agonists. *Sensors (Basel, Switzerland)* **2015**, *15* (4), 9265-9276.
12. White, J. H., Vitamin D metabolism and signaling in the immune system. *Reviews in endocrine & metabolic disorders* **2012**, *13* (1), 21-9.
13. Eming, S. A.; Krieg, T.; Davidson, J. M., Inflammation in wound repair: molecular and cellular mechanisms. *The Journal of investigative dermatology* **2007**, *127* (3), 514-25.
14. Granger, D. L.; Taintor, R. R.; Boockvar, K. S.; Hibbs, J. B., Jr., Measurement of nitrate and nitrite in biological samples using nitrate reductase and Griess reaction. *Methods in enzymology* **1996**, *268*, 142-51.
15. Ishizawa, M.; Akagi, D.; Makishima, M., Lithocholic Acid Is a Vitamin D Receptor Ligand That Acts Preferentially in the Ileum. *International journal of molecular sciences* **2018**, *19* (7).
16. Drocourt, L.; Ourlin, J. C.; Pascussi, J. M.; Maurel, P.; Vilarem, M. J., Expression of CYP3A4, CYP2B6, and CYP2C9 is regulated by the vitamin D receptor pathway in primary human hepatocytes. *The Journal of biological chemistry* **2002**, *277* (28), 25125-32.
17. Cheng, J.; Fang, Z. Z.; Kim, J. H.; Krausz, K. W.; Tanaka, N.; Chiang, J. Y.; Gonzalez, F. J., Intestinal CYP3A4 protects against lithocholic acid-induced hepatotoxicity in intestine-specific VDR-deficient mice. *Journal of lipid research* **2014**, *55* (3), 455-65.
18. Xu, Y.; Hashizume, T.; Shuhart, M. C.; Davis, C. L.; Nelson, W. L.; Sakaki, T.; Kalthorn, T. F.; Watkins, P. B.; Schuetz, E. G.; Thummel, K. E., Intestinal and hepatic CYP3A4 catalyze hydroxylation of 1 α ,25-dihydroxyvitamin D(3): implications for drug-induced osteomalacia. *Molecular pharmacology* **2006**, *69* (1), 56-65.
19. Esvelt, R. P.; De Luca, H. F., Calcitroic acid: biological activity and tissue distribution studies. *Arch Biochem Biophys* **1981**, *206* (2), 403-13.
20. Bain, C. C.; Mowat, A. M., Macrophages in intestinal homeostasis and inflammation. *Immunological Reviews* **2014**, *260* (1), 102-117.

21. Ding, X.; Kaminsky, L. S., Human extrahepatic cytochromes P450: function in xenobiotic metabolism and tissue-selective chemical toxicity in the respiratory and gastrointestinal tracts. *Annu Rev Pharmacol Toxicol* **2003**, *43*, 149-73.
22. Reddy, G. S.; Omdahl, J. L.; Robinson, M.; Wang, G.; Palmore, G. T.; Vicchio, D.; Yergey, A. L.; Tserng, K. Y.; Uskokovic, M. R., 23-carboxy-24,25,26,27-tetranorvitamin D3 (calcioic acid) and 24-carboxy-25,26,27-trinorvitamin D3 (cholacalcioic acid): end products of 25-hydroxyvitamin D3 metabolism in rat kidney through C-24 oxidation pathway. *Arch Biochem Biophys* **2006**, *455* (1), 18-30.
23. Sprake, E. F.; Grant, V. A.; Corfe, B. M., Vitamin D3 as a novel treatment for irritable bowel syndrome: single case leads to critical analysis of patient-centred data. *BMJ case reports* **2012**, *2012*.
24. Teichert, A.; Arnold, L. A.; Otieno, S.; Oda, Y.; Augustinaite, I.; Geistlinger, T. R.; Kriwacki, R. W.; Guy, R. K.; Bikle, D. D., Quantification of the vitamin D receptor-coregulator interaction. *Biochemistry* **2009**, *48* (7), 1454-61.
25. Hakamata, W.; Sato, Y.; Okuda, H.; Honzawa, S.; Saito, N.; Kishimoto, S.; Yamashita, A.; Sugiura, T.; Kittaka, A.; Kurihara, M., (2S,2'R)-analogue of LG190178 is a major active isomer. *Bioorg Med Chem Lett* **2008**, *18* (1), 120-3.
26. Boehm, M. F.; Fitzgerald, P.; Zou, A.; Elgort, M. G.; Bischoff, E. D.; Mere, L.; Mais, D. E.; Bissonnette, R. P.; Heyman, R. A.; Nadzan, A. M.; Reichman, M.; Allegretto, E. A., Novel nonsecosteroidal vitamin D mimics exert VDR-modulating activities with less calcium mobilization than 1,25-dihydroxyvitamin D3. *Chem Biol* **1999**, *6* (5), 265-75.

1.8 The Phase II Metabolism of Calcitriol Acid

Two principal phases of metabolism exist in living organisms: Phase I (oxidation, reduction and hydrolysis) and Phase II (conjugation). Phase I metabolism has been introduced in Chapter 1.3; it takes place predominately in the kidneys and liver and transforms vitamin D into its metabolites, including both calcitriol and CTA.¹²³ More broadly speaking, Phase I metabolism uses various enzymes to convert xenobiotics in the bloodstream into corresponding metabolites with increased solubility by unmasking polar functional groups or by adding new ones to the existing molecule.¹²⁴ Typically, the xenobiotic metabolite is less toxic and more easily excreted through urine and bile. For pharmaceuticals, metabolism typically reduces their pharmacologic activity.¹²⁵ However, in some cases metabolism increases the physiological activity of certain compounds.¹²⁶ This has long been known to be the case for vitamin D, which does not interact

with the vitamin D receptor; however, upon metabolism, calcitriol and several other metabolites do.¹²⁷

Phase II metabolism refers to the conjugation of compounds to polar molecules which is mediated by enzymes in living organisms. Sometimes, the conjugation occurs at positions that were generated by phase I metabolism through oxidation or unmasking, such as a hydroxyl group.¹²⁸ The addition of water-soluble functional groups increases the overall solubility of the xenobiotic, and as a result it typically reduces toxicity and negates pharmacological activity.¹²⁹ The enzymes involved in these transformations are typically associated with activated coenzymes and transfer the polar compound from the cofactor to the xenobiotic species, although in some cases the opposite occurs and the coenzyme associates with the xenobiotic, transferring it onto the polar group in the presence of the transferase enzyme.¹²⁸ Phase II metabolism occurs in the canonical metabolic sites, the liver and kidneys, but also can occur in other organs, such as the intestines, lungs, and skin.¹³⁰

The phase II metabolites of vitamin D metabolic products have yet to be investigated. It is surprising that despite the wealth of knowledge about vitamin D₂ and D₃ and the recognition that their VDR activity occurs only after metabolism,¹³¹ only the phase I metabolites have been the focus of research. To address this lack of knowledge, our group is investigating phase II conjugates of vitamin D metabolites. Our first focus is on the final metabolite CTA because of its stability, unique carboxylic acid functionality,⁷ and relative abundance in the body.⁵ While conjugation in the kidney often leads to urinary excretion, the liver's conjugation processes can excrete vitamin D metabolites into the intestines as bile by way of the bile duct.¹³² We already

know that the bile is likely the location of the highest concentration of CTA, which nearly 40 years ago was isolated as its corresponding methyl ester.⁸ As such, we expect that conjugates of vitamin D metabolites will likely be found there as well. It is known that bacteria in the gut can reverse conjugations,¹³³ leading to a likely scenario where the intestines are exposed to an elevated concentration of unconjugated vitamin D metabolites, which in turn can be reabsorbed and induce a physiological effect. We have shown that this phenomenon could have important biological ramifications for CTA, which mediates multiple physiological effects, e.g. upregulation of *CYP3A4* in gut epithelia cells.⁴ This pharmacological effect is particularly important with reference to lithocholic acid, the toxic bile acid which is known to be metabolized by P450 enzyme *CYP3A4*.¹³⁴ The *CYP3A4* gene is regulated transcriptionally by the vitamin D receptor.¹³⁵ Interestingly, lithocholic acid interacts weakly with VDR and influences its own catabolism through its induction of *CYP3A4*.¹³⁶ Our hypothesis is thus that CTA, as a ligand interacting with VDR in the gut, is aiding in the intestinal detoxification process and could thus reduce the occurrences of colon cancer, ulcerative colitis, and Crohn's disease.¹³⁷

There are six phase II transformations: sulfation, glucuronidation, acetylation, methylation, glutathione conjugation and amino acid conjugation. Of these, we investigated sulfation, glucuronidation, and amino acid synthetic conjugation to CTA. Acetylation typically forms less polar compounds and does not affect the type of oxygen-containing functional groups found in CTA,¹³⁸ so we excluded it along with methylating transformations.¹³⁹ Glutathione conjugation by contrast is actually the first step in the generation of a set of several conjugated

metabolites.¹⁴⁰ Because this transformation usually occurs with electrophilic groups not present in CTA, we did not investigate this conjugate.

Sulfation, by contrast, is a very common enzymatic transformation that can occur with an alcohol group to form the corresponding sulfate. In humans, four families of sulfotransferases have been identified, nearly all of which use 3'-phosphoadenosine-5'-phosphosulfate (PAPS) as their cofactor.¹⁴¹ Steroids are common substrates for sulfotransferases, producing sulfates such as the estrogen sulfate conjugate.¹²⁸ To investigate the sulfation of CTA *in vivo*, we synthesized both the mono-sulfate and the di-sulfate CTA conjugates as standards for identifying sulfo-CTA conjugates from tissues.

Glucuronidation is one of the most common Phase II metabolic transformations, occurring in many different tissues including the liver, kidneys, and intestine. The transformation produces more water-soluble carbohydrate metabolites.¹³⁰ Glucuronidation involves the conjugation of glucuronic acid, which is widely available as the enzyme cofactor uridine 5'-diphosphate glucuronic acid (UDP-glucuronic acid). The enzymes responsible for this transformation are UDP-glucuronosyltransferases, a large class of cytosolic membrane-bound enzymes.¹⁴² Glucuronidation is arguably one of the most important processes in phase II metabolism, being the major elimination pathway for common xenobiotics, drugs, environmental toxins, and endogenous small molecules, e.g. steroids.¹³⁰ We are currently investigating if glucuronides of CTA are formed *in vitro* and *in vivo*.

We also synthesized the two amino acid conjugates of CTA which reflect the most common phase II amino acid conjugates: glycine and taurine. Both conjugations can be formed

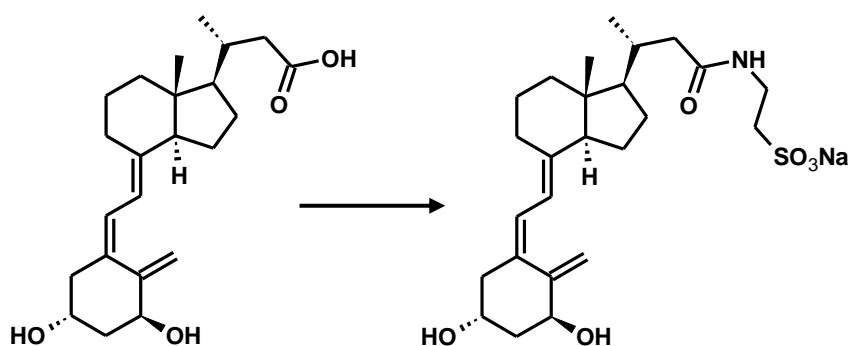
in either liver or kidney. Conjugates generated in the liver are typically secreted as bile.¹⁴³ The process of amino acid conjugation occurs in two steps. First, the ligation of the xenobiotic to acyl-CoA occurs by the corresponding ligase, followed by the formation of an amide bond with glycine by the enzyme glycine N-acyltransferase, or in the case of taurine, by the taurine N-acyltransferase.¹⁴⁴ In the case of CTA, it could be expected that these amino acid conjugates would act as bile acids, secreted into the intestines where they could be de-conjugated by microbes and reabsorbed.¹³⁹

1. Christakos, S.; Ajibade, D. V.; Dhawan, P.; Fechner, A. J.; Mady, L. J., Vitamin D: metabolism. *Endocrinology and metabolism clinics of North America* **2010**, *39* (2), 243-253.
2. Xu, C.; Li, C. Y.-T.; Kong, A.-N. T., Induction of phase I, II and III drug metabolism/transport by xenobiotics. *Archives of Pharmacal Research* **2005**, *28* (3), 249.
3. Bachmann, K., Chapter 8 - Drug Metabolism. In *Pharmacology*, Hacker, M.; Messer, W.; Bachmann, K., Eds. Academic Press: San Diego, 2009; pp 131-173.
4. Guengerich, F. P.; Liebler, D. C., Enzymatic activation of chemicals to toxic metabolites. *Critical reviews in toxicology* **1985**, *14* (3), 259-307.
5. Bikle, D. D., Vitamin D metabolism, mechanism of action, and clinical applications. *Chemistry & biology* **2014**, *21* (3), 319-329.
6. Stanley, L., Drug Metabolism. In *Pharmacognosy: Fundamentals, Applications, and Strategies*, Badal, S., and Delgoda, R, Ed. pp 527-545.
7. A. J. Hutt, J. C. a. R. L. S., The metabolism of aspirin in man: a population study. *Xenobiotica* **1986**, *16* (3), 239-249.
8. Liston, H., Markowitz JS, DeVane CL, Drug glucuronidation in clinical psychopharmacology. *Journal of clinical psychopharmacology* **2001**, *21* (5), 500-515.
9. *Overview of Vitamin D*; Institute of Medicine (US) Committee to Review Dietary Reference Intakes for Vitamin D and Calcium: Washington (DC), 2011.
10. Esvelt, R. P.; Schnoes, H. K.; DeLuca, H. F., Isolation and characterization of 1.alpha.-hydroxy-23-carboxytetranorvitamin D: a major metabolite of 1,25-dihydroxyvitamin D3. *Biochemistry* **1979**, *18* (18), 3977-3983.
11. Yu, O. B.; Arnold, L. A., Calcitroic Acid—A Review. *ACS chemical biology* **2016**, *11* (10), 2665-2672.

12. Boyer, J. L., Bile formation and secretion. *Comprehensive Physiology* **2013**, 3 (3), 1035-1078.
13. Onisko, B. L.; Esvelt, R. P.; Schnoes, H. K.; DeLuca, H. F., Metabolites of 1 alpha, 25-dihydroxyvitamin D3 in rat bile. *Biochemistry* **1980**, 19 (17), 4124-30.
14. Li, H.; He, J.; Jia, W., The influence of gut microbiota on drug metabolism and toxicity. *Expert opinion on drug metabolism & toxicology* **2016**, 12 (1), 31-40.
15. Teske, K. A.; Bogart, J. W.; Sanchez, L. M.; Yu, O. B.; Preston, J. V.; Cook, J. M.; Silvaggi, N. R.; Bikle, D. D.; Arnold, L. A., Synthesis and evaluation of vitamin D receptor-mediated activities of cholesterol and vitamin D metabolites. *Eur J Med Chem* **2016**, 109, 238-46.
16. Pike, J. W.; B. Meyer, M., Chapter 63 - 1,25-Dihydroxyvitamin D3: Synthesis, Actions, and Genome-scale Mechanisms in the Intestine and Colon. In *Physiology of the Gastrointestinal Tract (Fifth Edition)*, Johnson, L. R.; Ghishan, F. K.; Kaunitz, J. D.; Merchant, J. L.; Said, H. M.; Wood, J. D., Eds. Academic Press: Boston, 2012; pp 1681-1709.
17. Wang, Z.; Schuetz, E. G.; Xu, Y.; Thummel, K. E., Interplay between vitamin D and the drug metabolizing enzyme CYP3A4. *The Journal of steroid biochemistry and molecular biology* **2013**, 136, 54-58.
18. Nehring, J. A.; Zierold, C.; DeLuca, H. F., Lithocholic acid can carry out *in vivo* functions of vitamin D. *Proceedings of the National Academy of Sciences* **2007**, 104 (24), 10006.
19. Cantorna MT, Y. S., Bruce D, The paradoxical effects of vitamin D on type 1 mediated immunity. *Mol Asp Med* **2008**, 29, 369-375.
20. Price Evans, D. A., N-acetyltransferase. *Pharmacology & therapeutics* **1989**, 42 (2), 157-234.
21. Hashem, H. Phase II (Conjugation Reactions).
22. Hayes, J. D.; Flanagan, J. U.; Jowsey, I. R., GLUTATHIONE TRANSFERASES. *Annual review of pharmacology and toxicology* **2004**, 45 (1), 51-88.
23. Gamage, N.; Barnett, A.; Hempel, N.; Duggleby, R. G.; Windmill, K. F.; Martin, J. L.; McManus, M. E., Human Sulfotransferases and Their Role in Chemical Metabolism. *Toxicol Sci* **2005**, 90 (1), 5-22.
24. King, C. D.; Rios, G. R.; Green, M. D.; Tephly, T. R., UDP-Glucuronosyltransferases. *Current Drug Metabolism* **2000**, 1 (2), 143-161.
25. Hofmann, A. F., THE FUNCTION OF BILE SALTS IN FAT ABSORPTION. THE SOLVENT PROPERTIES OF DILUTE MICELLAR SOLUTIONS OF CONJUGATED BILE SALTS. *Biochemical Journal* **1963**, 89 (1), 57.
26. Badenhorst, C. P. S.; van der Sluis, R.; Erasmus, E.; van Dijk, A. A., Glycine conjugation: importance in metabolism, the role of glycine N-acyltransferase, and factors that influence interindividual variation. *Expert Opinion on Drug Metabolism & Toxicology* **2013**, 9 (9), 1139-1153.

1.9 Synthetic Strategy for the Production of Calcitroic Acid Conjugates

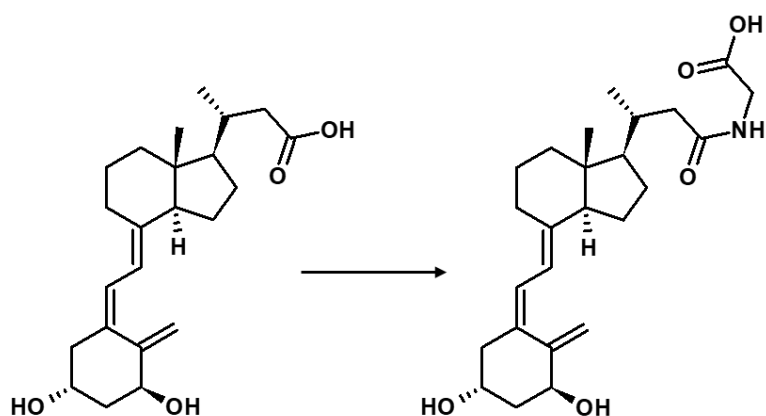
Synthesis of taurine CTA conjugate:



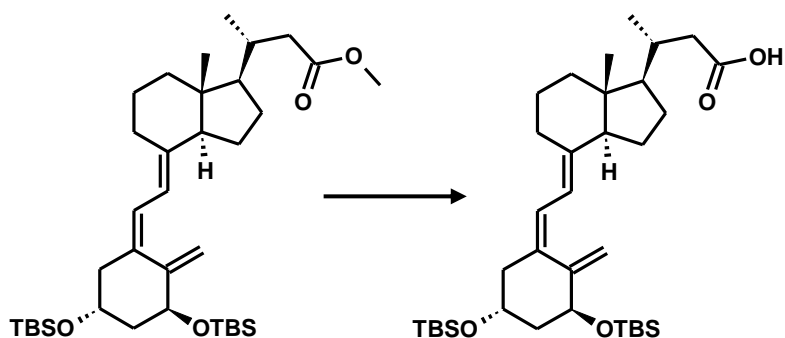
In order to test out reaction conditions with a compound with similar characteristics and reactivity to CTA but less precious and commercially available, I began experimenting with taurine conjugation using the commercially available bile acid lithocholic acid (LCA). Initial

experiments used the Dayal et al. method,¹⁴⁵ which was touted to be quick and effective using a conventional (non-scientific) microwave. If combining LCA, taurine, and EEDQ (coupling reagent) in dry ethanol and triethylamine (base) and microwaving in a water bath sounds unlikely to work to you, you would be right. After testing a few times using different setups, we moved on to a more reasonable synthesis from Tserng involving the same reagents but DMF instead of ethanol to increase solubility. The reaction was stirred at 90°C for 1 hour.¹⁴⁶ The product was formed as determined by TLC, but the suggested isolation procedure, which involves pouring into the solution into a diethyl ether ice bath, would not be effective on the microscale on which we would be synthesizing tauro-CTA. We instead took a page from the Dayal reaction and used ethanol for the solvent, otherwise following the Tserng reaction conditions. This worked perfectly. Switching from LCA to CTA after that successful reaction provided the corresponding product with no further complications. After filtering of the insoluble leftover taurine, we could simply dry off the ethanol. The reaction could then be taken up in a minimum amount of water and the highly nonpolar byproducts extracted away with toluene. What remained was TEA and product. After trying to remove the large amount of remaining TEA by several methods including high vacuum, extraction, and azeotropic distillation to no success, we realized that it was forming a strong ion-pairing with the sulfonate. Therefore, we used solid phase extraction (SPE) to remove TEA by flushing the loaded crude product with a saturated sodium chloride solution (brine) until the TEA eluted. The salt on the cartridge could then be washed away with DI water and the product was eluted in 30% methanol in water. Upon evaporation under reduced pressure, the brown Cl⁻ taurine salt conjugate was isolated in high purity. The detailed procedure can be found in the experimental procedure section.

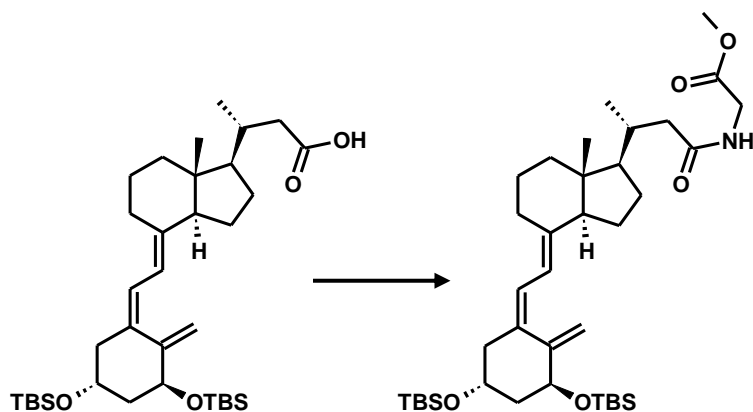
Synthesis of glycine CTA conjugate:



Initially, we attempted the synthesis of the glycine conjugate using LCA to test the method previously established by Incerti et al.,¹⁴⁷ which uses N-(3-dimethylaminopropyl)-N'-ethylcarbodiimide hydrochloride (EDCI) as the coupling reagent and N-methyl morpholine (NMM) as the base to attach O-methylated L-glycine to the LCA acid functionality by stirring in DCM at room temperature overnight. This was followed by deprotection of the ester under basic conditions. The procedure worked as expected for the LCA. However, the reaction failed when we attempted it with CTA. CTA did not dissolve in DCM to the extent that the reaction could proceed, and only trace amounts of product were recovered. We made further attempts in THF and pyridine, which were also unsuccessful, before deciding we needed more than just solvent changes.

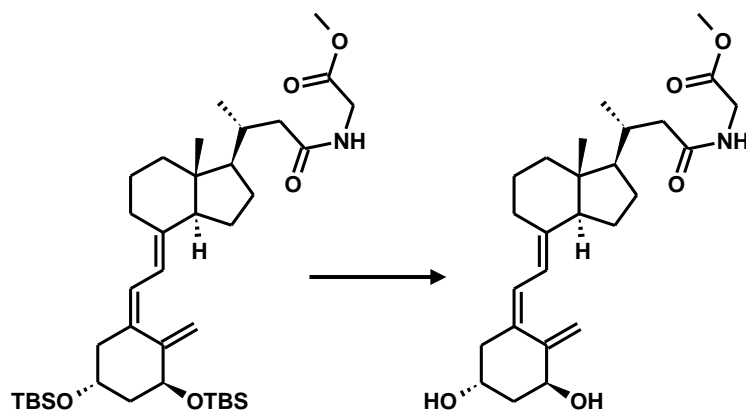


Therefore, we started with the O-Bis-silylated CTA and hydrolyzed it. This reaction was simple and effective in methanol/water that was adjusted to properly dissolve the starting material. NaOH was added up to 10% w/v, and the reaction stirred at room temperature for three hours until it was complete. The mixture was evaporated, redissolved in water followed by extraction with DCM giving the pure acid after evaporation.



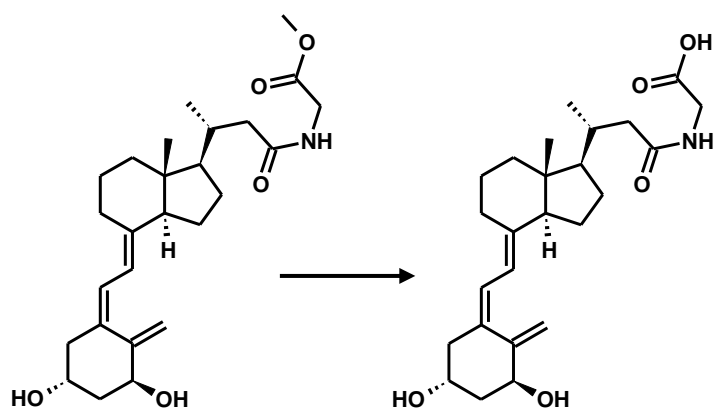
The O-Bis-silylated CTA was able to dissolve completely in DCM; however, very small scale (1-2mg) reactions were not forming the anticipated amide. After experimenting with LCA again, we discovered that the proportions of the reagents were very important: the ratios of NMM, EDCI, and the glycine methyl ester needed to be 9:4:4 respectively. Thus, reactions with

only a milligram or two of CTA and 40-80mg of the other materials would still form the ester after one hour at room temperature as long as the proportions between the other reagents were correct.



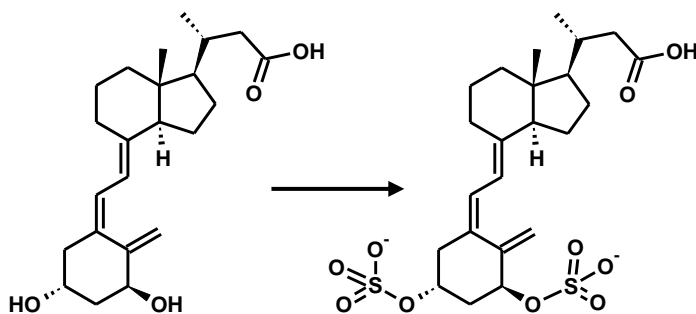
The deprotection of the silyl groups, initially attempted with TBAF, was a clean reaction by TLC, but it was impossible to separate the product from the leftover TBA. After several attempts that included washing with NH_4Cl to dissolve away the salt, extracting using many different solvents, column chromatography, ion-exchange resin,¹⁴⁸ precipitating as a perchlorate,¹⁴⁹ and using KF as an alternative F^- source, we found an alternate TBS deprotection method used by Nakabayashi et al.¹⁵⁰, one of the world's premier laboratories focused on the synthesis of secosteroidal vitamin D analogues. Their group employed the use of camphorsulfonic acid (CSA) to remove TBS groups in a speedy (~15 min) reaction in dry methanol at room temperature. Of note is that running the reaction with stoichiometric amounts of CSA was unsuccessful or at best very slow, and the product as it turns out degrades very quickly in acid. However, with excess (6 eq) of CSA, the reaction was very quickly complete. The

degradation problem was ameliorated by swiftly quenching the completed reaction with enough NaHCO_3 to neutralize the CSA, immediately concentrating it to get rid of the methanol, and then extracting the product with EtOAc. Immediate column chromatography and concentration of purified product gave the best yields.



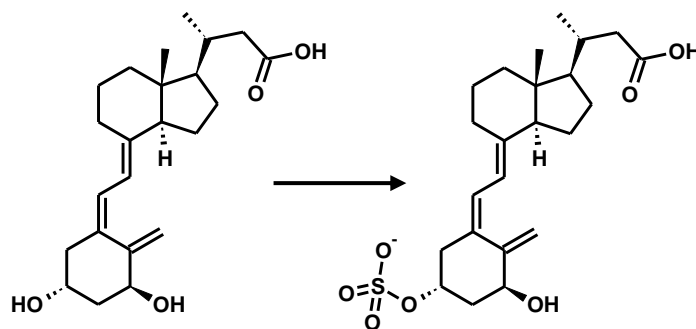
The hydrolysis to the glycine conjugate was a clean reaction, where the final precipitated product was pure provided it was not left long in acid. The reaction in water and methanol with up to 15% NaOH w/v was complete in 10 minutes. After evaporating off all methanol, the residue was dissolved in a minimum amount of water in a small Eppendorf tube, and the pH was adjusted HCl until the solution was just acidic (pH 1). The Eppendorf tube was quickly centrifuged to collect the white, grainy precipitate, which was dried overnight under high vacuum. The precipitate was then loaded on an SPE cartridge to remove salt impurities by washing with water, then eluted in a gradient from water to methanol (product came off between 40-50% methanol). Product was then quickly dried down, and purity was confirmed by NMR. The detailed protocol can be found in the experimental section.

Synthesis of bis-sulfate CTA conjugate:



We used the sulfation method previously established in our lab, which had been used to make the LCA-sulfate conjugate. After testing the reaction conditions with both LCA and ergocalciferol, we tried the same method with CTA. In this reaction, H_2SO_4 and acetic anhydride were lightly heated to dissolve everything in pyridine, and then CTA was added. The reaction was complete after about ten minutes, and it was then cooled to 0°C , quenched with 25% NH_4OH in water, stirred for 15 minutes, filtered, and concentrated. The crude mixture was then loaded on an SPE column, washed with pure water, and then eluted with up to 30% methanol in water. The di-sulfonated CTA conjugate was pure by NMR, and no further purification was necessary.

Synthesis of mono-sulfate CTA conjugate:



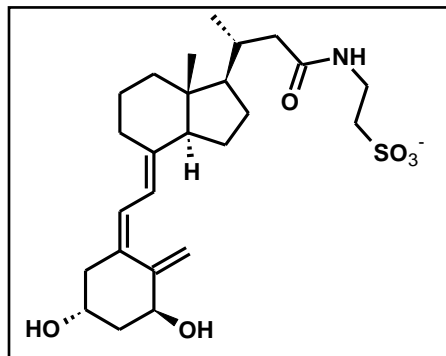
In contrast to the bis-sulfated conjugate, very specific measurements are needed in this reaction to maximize the amount of mono-sulfate produced and minimize the bis-sulfate byproduct, which readily occurs with any sulfuric acid in excess of 1:1 proportions. As such, we prepared a solution of 0.5M H₂SO₄/1.0M acetic anhydride in pyridine and combined it with CTA to make a solution of 1:1:2 CTA:H₂SO₄:acetic anhydride proportions. No heat is necessary in this reaction because the sulfuric acid is dilute enough to stay in solution at room temperature. The reaction is complete within a half hour. Even with a 1:1 stoichiometry both mono and bis-sulfated CTA were formed. The completed reaction was quenched with 25% aqueous NH₄OH, concentrated, loaded onto an SPE cartridge, and eluted using an incremental gradient in order to separate the bis-sulfate from the mono-sulfate. The bis-sulfate eluted up to 25% MeOH in water, with the mono-sulfate eluting up to 35% MeOH in water.

1. Dayal, B.; Rapole, K. R.; Patel, C.; Pramanik, B. N.; Shefer, S.; Tint, G. S.; Salen, G., Microwave-induced rapid synthesis of sarcosine conjugated bile acids. *Bioorganic & Medicinal Chemistry Letters* **1995**, *5* (12), 1301-1306.
2. Tserng, K. Y.; Hachey, D. L.; Klein, P. D., An improved procedure for the synthesis of glycine and taurine conjugates of bile acids. *Journal of lipid research* **1977**, *18* (3), 404-7.
3. Incerti, M.; Tognolini, M.; Russo, S.; Pala, D.; Giorgio, C.; Hassan-Mohamed, I.; Noberini, R.; Pasquale, E. B.; Vicini, P.; Piersanti, S.; Rivara, S.; Barocelli, E.; Mor, M.; Lodola, A., Amino Acid Conjugates of Lithocholic Acid As Antagonists of the EphA2 Receptor. *Journal of Medicinal Chemistry* **2013**, *56* (7), 2936-2947.
4. Kaburagi, Y.; Kishi, Y., Operationally Simple and Efficient Workup Procedure for TBAF-Mediated Desilylation: Application to Halichondrin Synthesis. *Organic Letters* **2007**, *9* (4), 723-726.
5. Everhart, E. T., A Convenient Procedure for Isolation of Alcohols After Cleavage of Protective Groups with Tetra-n-Butylammonium Fluoride AU - Craig, J. Cymerman. *Synthetic Communications* **1990**, *20* (14), 2147-2150.
6. Nakabayashi, M.; Tsukahara, Y.; Iwasaki-Miyamoto, Y.; Mihori-Shimazaki, M.; Yamada, S.; Inaba, S.; Oda, M.; Shimizu, M.; Makishima, M.; Tokiwa, H.; Ikura, T.; Ito, N., Crystal Structures of Hereditary Vitamin D-Resistant Rickets-Associated Vitamin D Receptor Mutants R270L and W282R Bound to 1,25-Dihydroxyvitamin D₃ and Synthetic Ligands. *Journal of Medicinal Chemistry* **2013**, *56* (17), 6745-6760.

1.10 Characterization of Calcitroic Acid Conjugates

The CTA used in these syntheses was generated following the procedures described in Chapter 1.6. All moisture and/or oxygen-sensitive reactions were carried out under a dry nitrogen atmosphere. Reaction temperatures refer to the containing bath temperatures. Reactions were monitored by thin-layer chromatography (TLC) using Merck 60 UV₂₅₄ silica gel plates. Visualization was performed with UV light, cerium molybdate general stain followed by heating, and other methods as noted. Synthesized compounds were purified by normal phase flash chromatography (SPI Biotage, silica gel 230-400 mesh) or solid phase extraction (Waters Sep-Pak C18 6cc Vac cartridge) except where noted. Mass analysis was performed using a Shimadzu 2020 LC-MS (single quadrupole) instrument and exact mass analysis was performed using a Shimadzu LCMS-IT-TOF. NMR spectra were recorded on a Bruker Avance 500MHz

instrument with compounds dissolved in the specified deuterated solvent. Optical rotations were recorded using Jasco DIP-370 Digital Polarimeter instrument in LCMS grade chloroform or methanol.

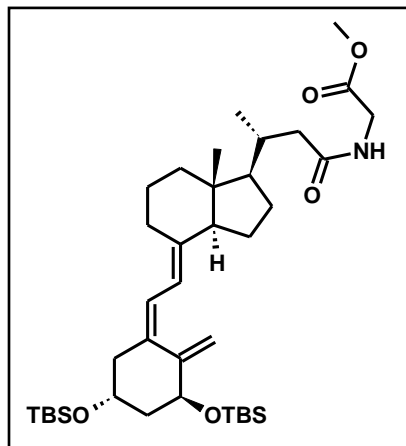


Tauro calcitroic acid: To a stirred solution of CTA (45.6mg, 0.123mmol) in ethanol (1.25mL) was added N-ethoxycarbonyl-2-ethoxy-1,2-dihydroquinoline (75mg, 0.30mmol), taurine (30mg, 0.24mmol), and triethylamine (75 μ L, 0.54mmol). The reaction was refluxed for 1 hour,

then removed from heat and filtered. The filtrate was concentrated and the residue taken up into a minimal amount of water (5mL), then extracted with toluene (2x5mL). The aqueous layer was then loaded onto an 500mg Sep-Pak Vac 6cc C18 cartridge and eluted in a gradient from brine to methanol (brine:MeOH 1:1). Fractions containing product were concentrated, then desalted using a second cartridge (water:methanol 7:3) to yield tauro-calcitroic acid as a yellow solid (20.4mg, 37%); R_f 0.14 (CHCl₃ : MeOH 7 : 3); ¹H-NMR (500MHz, CDCl₃) δ 0.49 (s, 3H), 0.87 (d, J = 6.25 Hz, 3H), 1.21-1.32 (m, 3H), 1.34-1.53 (m, 4H), 1.57-1.68 (m, 2H), 1.72-1.96 (m, 7H), 1.96-2.02 (m, 1H), 2.22 (dd, J = 13.1, 7.6 Hz, 1H), 2.32-2.37 (m, 1H), 2.50-2.55 (m, 1H), 2.76-2.82 (m, 1H), 3.01 (t, J = 6.9 Hz, 2H), 3.50 (t, J = 6.9 Hz, 2H), 4.07-4.13 (m, 1H), 4.33-4.37 (m, 1H), 4.93 (s, 1H), 5.25 (s, 1H), 6.00 (d, J = 11.3 Hz, 1H), 6.40 (d, J = 11.3 Hz, 1H); ¹³C-NMR: (125MHz, CDCl₃) δ 11.2, 18.5, 21.7, 23.1, 27.2, 28.6, 34.4, 35.0, 39.8, 41.1, 43.1, 44.0, 45.9, 49.7, 55.8, 56.1, 66.3,

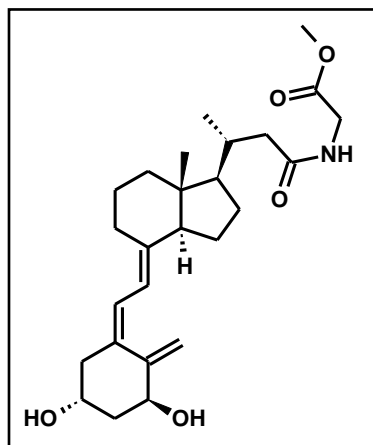
70.5, 112.6, 116.7, 123.9, 134.4, 144.9, 146.5, 176.8; m/z calculated for $C_{25}H_{38}NO_6S$ 480.2340

$[M]^-$, found 480.2333; $[\alpha]_D^{25} = +0.70$ (c 1.0, MeOH)



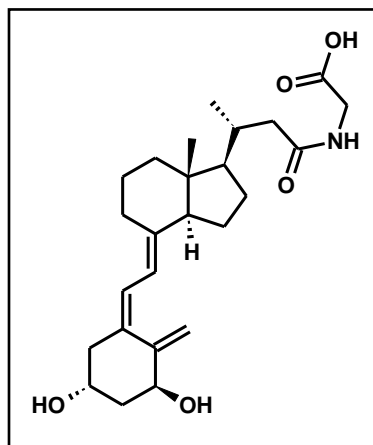
O-bis-silylated glyco calcitroic methyl ester: To a stirred solution of O-bis-silylated CTA (93 mg, 0.15mmol), glycine methyl ester hydrochloride (43mg, 0.35mmol), and N- methyl morpholine (87.5 μ L, 0.88mmol) in dry DCM (10mL) was added 1-ethyl-3-(3-dimethylaminopropyl)carbodiimide (66mg, 0.35mmol). The reaction was allowed to stir for two hours at room

temperature. The reaction mixture was quenched with 10mL of 2M HCl, extracted with DCM (10mLx3), and the combined organic layers were washed with brine. The organic layers were dried over $MgSO_4$ and concentrated to the O-bis-silylated glyco calcitroic methyl ester (93mg, 90%) as a clear oil. No attempts were made to purify the product further: R_f 0.21 (DCM); 1H -NMR (500MHz, $CDCl_3$) δ 0.08 (s, 12H), 0.58 (s, 3H), 0.89 (s, 18H), 1.02 (d, $J = 11.0$ Hz, 3H), 1.30-1.40 (m, 3H), 1.44-1(m, 3H), 1.6-1.71 (m, 2H), 1.75-1.83 (m, 1H), 1.83-2.06 (6H), 2.23 (dd, $J = 24.0, 12.5$ Hz 1H), 2.42-2.52 (m, 2H), 2.79-2.88 (m, 1H), 3.78 (s, 3H), 4.08 (d, $J = 8.5$ Hz, 2H), 4.16-4.26 (m, 1H), 4.38 (dd, $J = 10.5, 5.9$ Hz, 1H), 4.87 (d, $J = 3.7$ Hz, 1H), 5.19 (d, $J = 2.6$ Hz, 1H), 5.94-6.07 (m, 2H), 6.25 (d, $J = 18.8$ Hz, 1H); ^{13}C -NMR: (125MHz, $CDCl_3$) δ -5.1, -4.8, -4.69, -4.67, 12.0, 18.1, 18.2, 19.5, 22.1, 23.4, 25.8 (3C), 25.9 (3C), 27.8, 28.8, 34.5, 40.5, 41.2, 43.7, 44.8, 45.9, 46.1, 52.3, 56.3, 56.5, 67.5, 72.1, 111.3, 118.1, 123.1, 135.2, 140.6, 148.3, 170.6, 173.1; m/z calculated for $C_{38}H_{67}NO_5Si_2$ 674.4631 $[M + H]^+$, found 674.4564



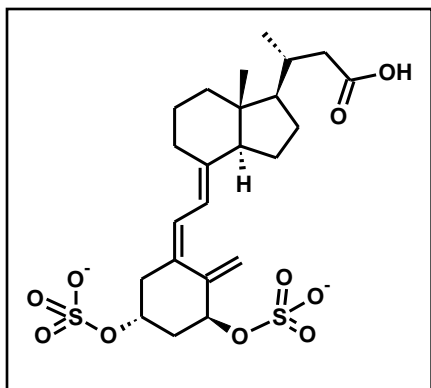
Glyco calcitroic methyl ester: To a solution of O-bis-silylated glyco CTA methyl ester (49mg, 0.073mmol) in dry methanol (3.6mL) was added camphorsulfonic acid (102mg, 0.439mmol). The reaction was monitored closely and quenched with NaHCO_3 (2mL) after 25 minutes. The reaction mixture was concentrated under reduced pressure and the aqueous layer was extracted with DCM

(3x2mL). The combined organic layers were dried with MgSO_4 , concentrated, and purified by column chromatography (MeOH : EtOAc 1:15) to yield glyco calcitroic methyl ester (25mg, 65%) as a fluffy white powder; R_f 0.41 (EtOH: EtOAc 1:7); $^1\text{H-NMR}$ (500MHz, CDCl_3) δ 0.59 (s, 3H), 1.02 (d, $J = 10.0$ Hz, 3H), 1.27-1.41 (m, 3H), 1.43-1.60 (m, 3H), 1.63-1.72 (m, 2H), 1.72-1.83 (m, 3H), 1.83-2.04 (m, 6H), 2.32 (dd, $J = 22.4, 10.8$ Hz, 1H), 2.44 (d, $J = 21.8$ Hz, 1H), 2.60 (d, $J = 22.0$ Hz, 1H), 2.84 (d, $J = 21.1$ Hz, 1H), 3.77 (s, 3H), 4.06 (d, $J = 8.1$ Hz, 2H), 4.24 (s, 1H), 4.44 (s, 1H), 5.01 (s, 1H), 5.34 (s, 1H), 5.97-6.07 (m, 2H), 6.38 (d, $J = 18.7$ Hz, 1H); $^{13}\text{C-NMR}$: (125MHz, CDCl_3) δ 12.1, 19.4, 22.3, 23.5, 27.7, 29.0, 34.4, 40.4, 41.2, 42.9, 43.6, 45.3, 46.0, 52.4, 56.3, 56.6, 66.8, 70.8, 111.8, 117.3, 124.8, 133.2, 142.7, 147.7, 170.6, 173.0; m/z calculated for $\text{C}_{26}\text{H}_{39}\text{NO}_5$ 446.2901 $[\text{M} + \text{H}]^+$, found 446.2851; $[\alpha]_D^{25} = -4.0$ (c 1.0, CHCl_3)



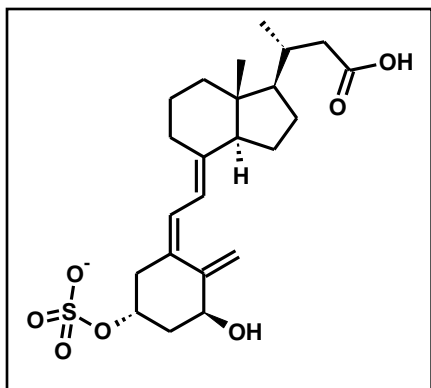
Glyco calcitroic acid: To a stirred solution of glyco CTA methyl ester (20.2mg, 0.045mmol) in a minimum of MeOH (0.9mL) was added 1.8 mL of 15% w/v NaOH in H₂O. The reaction was completed in 10 minutes. Methanol was removed under reduced pressure and the reaction mixture was dissolved in a minimum of water. The reaction mixture was acidified and precipitated with

concentrated HCl to pH 2, then centrifuged and the precipitate collected by decanting the supernatant and drying the remaining solid under reduced pressure. The crude solid was desalted and purified using 500mg Sep-Pak Vac 6cc C18 cartridges (50% methanol/water) to yield an off-white solid (7.3mg, 39%): *R_f* 0.53 (MeOH : EtOAc 3:2); ¹H-NMR (500MHz, D₂O) δ 0.50 (s, 3H), 0.89 (d, *J* = 6.45, 3H), 1.20-1.35 (m, 3H), 1.35-1.55 (m, 4H), 1.58-1.68 (m, 2H), 1.74-1.97 (m, 6H), 1.97-2.03 (m, 1H), 2.23 (dd, *J* = 13.1, 7.5 Hz, 1H), 2.40 (dd, *J* = 13.8, 3.6 Hz, 1H), 2.50-2.55 (m, 1H), 2.76-2.82 (m, 1H), 3.75 (dd, *J* = 27.0, 17.5 Hz, 2H), 4.07-4.12 (m, 1H), 4.34-4.37 (m, 1H), 4.94 (s, 1H), 5.25 (s, 1H), 6.01 (d, *J* = 11.3 Hz, 1H), 6.41 (d, *J* = 11.3 Hz, 1H); ¹³C-NMR: (125MHz, MeOD) δ 11.2, 18.6, 19.3, 22.0, 23.2, 27.4, 28.6, 34.2, 40.5, 42.9, 43.0, 43.6, 45.2, 45.7, 56.3, 65.9, 70.0, 110.4, 118.0, 123.0, 135.5, 140.2, 149.3, 174.2, 175.9; *m/z* calculated for C₂₅H₃₇NO₅ 432.2744 [M + H]⁺, found 432.2680; [α]_D²⁵ = + 24.0 (c 1.0, MeOH)



Bis-sulfo calcitroic acid: A solution of H_2SO_4 (160 μL) and acetic anhydride (280 μL) was stirred in pyridine at 55 $^\circ\text{C}$ for 5 minutes. When everything was solubilized, a solution of CTA (43.1mg, 0.115mmol) was added. The solution was stirred for approximately ten minutes while monitoring by TLC, then

removed from heat and cooled to 0 $^\circ\text{C}$. To the cooled solution was added 25% aqueous NH_4OH (840 μL). The solution was stirred for 5 minutes, filtered over a pad of celite followed by evaporation. The crude residue was then loaded on an SPE cartridge, washed with water, purified in a gradient up to 30% methanol in water, and then concentrated to the bis-sulfated CTA as a white powder (18.4mg, 30.0%); R_f 0.18 (MeOH : EtOAc 3:7); $^1\text{H-NMR}$ (500MHz, CDCl_3) δ 0.63 (s, 3H), 1.04 (d, $J = 6.2$ Hz, 3H), 1.32-1.41 (m, 3H), 1.45-1.52 (m, 1H), 1.54-1.63 (m, 2H), 1.66-1.74 (m, 2H), 1.88-1.96 (m, 3H), 2.01-2.08 (m, 3H), 2.22-2.29 (m, 1H), 2.30-2.36 (m, 1H), 2.42-2.48 (m, 1H), 2.57 (dd, $J = 13.7, 6.7$ Hz, 1H), 2.67-2.72 (m, 1H), 2.85-2.91 (m, 1H), 4.77-4.83 (m, 1H), 5.00-5.06 (m, 2H), 5.47-5.50 (m, 1H), 6.12 (d, $J = 11.1$ Hz, 1H), 6.38 (d, $J = 11.1$ Hz, 1H); $^{13}\text{C-NMR}$: (125MHz, CDCl_3) δ 11.0, 18.7, 21.8, 23.2, 27.2, 28.6, 33.8, 36.6, 40.3, 41.0, 41.9, 45.6, 56.2, 56.3, 73.9, 76.7, 113.2, 117.7, 124.5, 132.8, 141.6, 143.7, 176.0; m/z calculated 533.1532 $[\text{M}]^-$ and 266.0783 $[\text{M}]^{2-}$, found 533.1426 and 266.0674; $[\alpha]_D^{25} = -18.0$ (c 1.0, MeOH)



Mono-sulfo calcitroic acid: A solution of H_2SO_4 (0.5M) and acetic anhydride (1M) in pyridine was prepared. To a stirred solution of CTA (19.8mg, 0.053mmol) in pyridine (0.5mL) at room temperature was added 105.7 μL of the prepared solution (0.053mmol H_2SO_4 ; 0.106mmol acetic anhydride).

The reaction was monitored for a half hour and quenched with 25% aqueous NH_4OH (200 μL).

The solution was stirred for 5 minutes and concentrated. The crude residue was then loaded on an SPE cartridge, washed with water, purified in a gradient up to 60% methanol in water, and concentrated to a clear oil (8.99mg, 37.5%); R_f 0.47 (MeOH : EtOAc 3 : 7); $^1\text{H-NMR}$ (500MHz, CDCl_3) δ 0.64 (s, 3H), 1.04 (d, $J = 6.2$ Hz, 3H), 1.30-1.42 (m, 3H), 1.43-1.64 (m, 4H), 1.66-1.75 (m, 2H), 1.82-2.00 (m, 5H), 2.02-2.09 (m, 2H), 2.29-2.36 (m, 1H), 2.43-2.48 (m, 1H), 2.55-2.66 (m, 2H), 2.86-2.91 (m, 1H), 4.34-4.39 (m, 1H), 4.79-4.84 (m, 1H), 4.92-4.95 (m, 1H), 5.34-5.38 (m, 1H), 6.10 (d, $J = 11.2$ Hz, 1H), 6.34 (d, $J = 11.2$ Hz, 1H); $^{13}\text{C-NMR}$: (125MHz, CDCl_3) δ 10.9, 18.7, 21.9, 23.2, 27.3, 28.5, 33.9, 40.3, 40.4, 41.0, 41.5, 41.9, 45.6, 56.1, 56.2, 68.8, 74.3, 109.6, 117.6, 123.6, 133.9, 141.0, 148.5, 176.1; m/z calculated 453.1958 $[\text{M}]^-$, found 453.1867; $[\alpha]_D^{25} = -18.0$ (c 1.0, MeOH)

1.11 A Brief Biological Characterization of Calcitroic Acid Conjugates

The four conjugates of CTA, which were synthesized using the methods described in Chapter 1.10, were evaluated with different biochemical assays to determine their biological activity. We used fluorescence polarization to determine the binding of these compounds towards VDR and a transcription assay with HEK293 kidney cells to determine if these conjugates modulate the transcription of P450 enzyme CYP24A1. Furthermore, we treated macrophages (RAW264.7) with the CTA conjugated to determine possible anti-inflammatory properties.

Binding to VDR using fluorescence polarization

Using the same method described in Chapter 1.7, recombinant VDR-LBD was incubated in the presence of fluorescently labeled SRC2-3 peptide VDR agonist LG190178 and increasing concentrations of CTA conjugates and calcioic acid. As shown in Figure 32, calcioic acid disrupts the interaction between the agonist and VDR with an IC_{50} of $71\mu\text{M}$. All CTA conjugates were able to compete with LG190178, albeit with IC_{50} values higher than $92\mu\text{M}$.

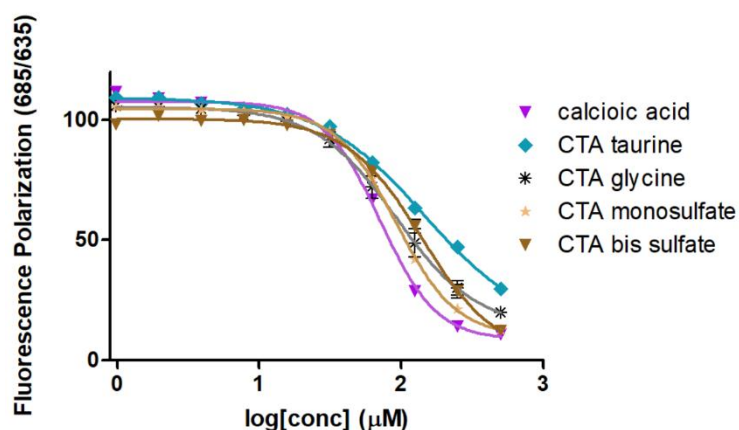


Figure 32: Binding curves for conjugates by FP analysis. EC_{50} values: calcioic acid ($71 \pm 4 \mu\text{M}$), CTA taurine ($145 \pm 25 \mu\text{M}$), CTA glycine ($92 \pm 17 \mu\text{M}$), CTA mono sulfate ($92 \pm 5 \mu\text{M}$), CTA bis sulfate ($139 \pm 20 \mu\text{M}$).

Interaction with VDR using a transcription assay

Using the same method described in Chapter 1.7, HEK293T cells were transfected with CMV-VDR plasmid for overexpression of VDR and the reporter plasmid of a luciferase gene under the control of a *CYP24A1* promoter. In the presence of VDR agonists, induction of the luciferase gene occurs. This produces luciferase, which in the presence of luciferin substrate generates a proportional bioluminescence signal. As shown in Figure 33, CTA glycine was the only CTA

conjugate that exhibited an agonist behavior with an EC_{50} of $49\mu\text{M}$ for the measured concentration range. Calcioic acid was not able to induce VDR-mediated transcription but rather showed some antagonistic behavior.

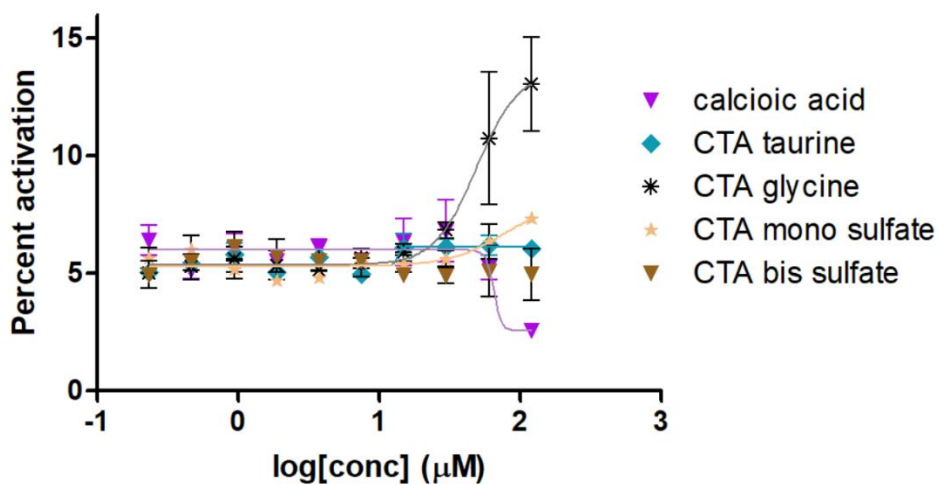


Figure 33: Transcription activation of CTA and its conjugates and related compounds, shown as percentages of full calcitriol activation at 60nM . EC_{50} of CTA taurine is $49 \pm 21 \mu\text{M}$.

Effect of CTA conjugates on macrophages

Using a Griess assay, the released NO concentration from activated RAW264.7 cells was measured in the presence of CTA conjugates. This assay was introduced in Chapter 1.7 and the results are summarized in Figure 34. Interestingly, all of the CTA conjugates and calcioic acid showed a significant reduction of nitric oxide production at $12.5\mu\text{M}$ (Figure 34A). Positive control compound dexamethasone at 100nM showed a similar effect. The reduction of NO in the

presence of 25 μ M and 50 μ M CTA glycine was the most pronounced among all other CTA conjugates (Figure 34B&C).

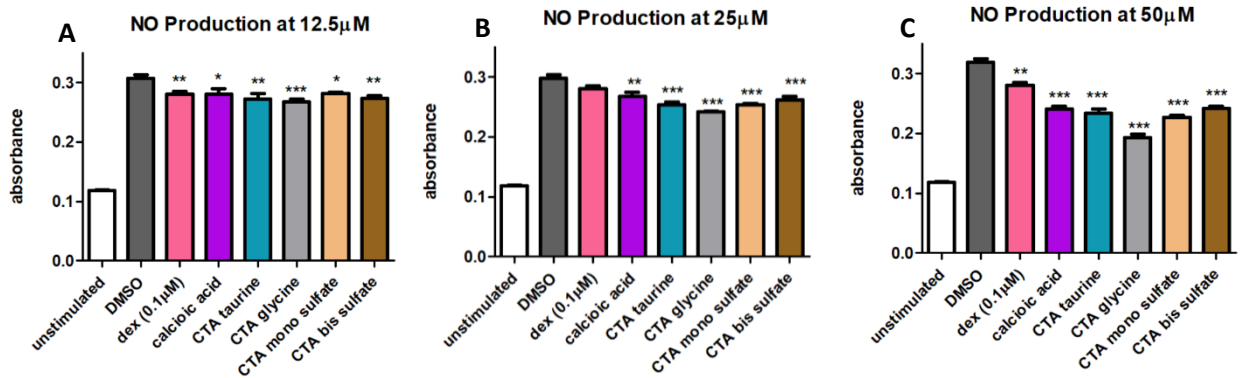


Figure 34: Significant deviation from stimulated macrophage (DMSO-treated) NO production seen at 12.5 μ M, with trends increasing in significance at higher concentrations

In parallel, we investigated a possible toxic effect that could lead to a reduction of NO production. Therefore, we determined the viability of these macrophages under the same condition using Cell-Titer Glo. The results are summarized in Figure 35. For CTA conjugate concentrations of up to a 100 μ M, no reduction of cell viability was observed.

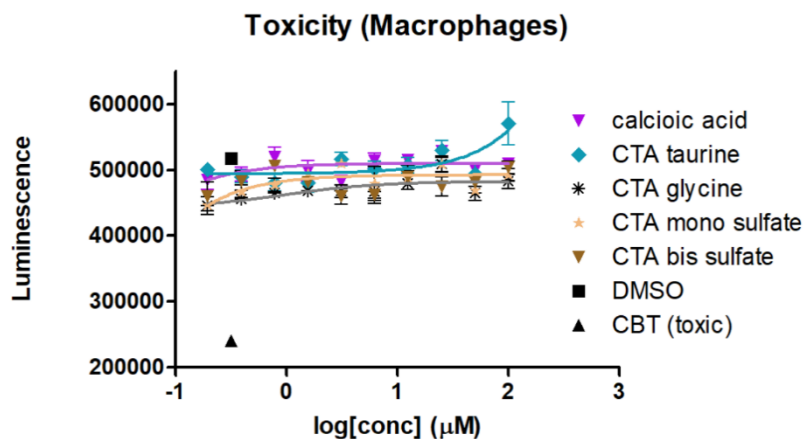


Figure 35: Toxicity assay for macrophages. No toxicity was seen up to 100 μ M for any of the compounds

Discussion

Based on the defined VDR binding pocket for VDR agonists that was elucidated by X-ray crystallography, it was not anticipated that any of the CTA conjugates would interact with VDR or induce a VDR-mediated effects even at very high concentrations. Our results however confirmed that these compounds at concentrations of 60 μ M and higher can interact with VDR. CTA glycine was the only CTA conjugate showing an agonistic VDR-mediated effect at concentrations of 15 μ M and higher. Furthermore, we confirmed with the agonistic effect of CTA glycine that this compound is cell-membrane permeable.

The CTA-related compound calcioic acid, however, was expected to bind to VDR, albeit at higher concentrations than CTA because of its missing 1 α -hydroxyl group. We were able to confirm this hypothesis. However, the interaction between calcioic acid and VDR did not result in any appreciable induction of transcription at a concentration of 100 μ M.

When macrophages were treated with CTA conjugates, a decrease in nitric oxide production at 12.5 μ M and greater concentrations was observed. While no cell death was apparent by our Cell-Titer Glow viability assay at any concentration, the possibility exists that general protein production was compromised at these high concentrations of CTA conjugates that in turn reduced the formation of NO. The only evidence that the reduction of NO formation is linked to VDR in this study is the behavior of CTA glycine that showed activation of VDR-mediated transcription and a very pronounced reduction of NO production. Similar effects were described for CTA before. Assessing the toxicity of these conjugates using other metrics than ATP

quantification (Cell-Titer Glo) will be carried out in the future to further investigate the anti-inflammatory effect of vitamin D metabolites.

Experimental Procedures:

Fluorescence Polarization Binding Assay Protocol

The FP assay buffer was prepared by adding 25mM PIPES (piperazine-N,N'-bis(ethanesulfonic acid, Sigma-Aldrich), 50mM NaCl (Fisher), and 0.01% NP-40 detergent to 18.2MΩ water. The buffer was filtered and adjusted to pH 6.75. To this was added 7.5nM of the coactivator peptide SRC2-3 (CKKKENALLRYLLDKDDTKD) which had been labeled with cysteine-reactive AlexaFluor647. To this solution was added 500nM of VDR-LBD, which had been expressed and purified as reported previously.¹²⁰ The VDR agonist LG190178, which had been synthesized previously according to a published protocol,¹²¹⁻¹²² was added at a concentration of 600nM. A 20mM stock of each CTA conjugate in DMSO was serially diluted (1:2) in a 384-well plate (Corning, CLS3702). To a 384-well black polystyrene microplate (Corning, CLS3658), 20μL of the prepared VDR-LBD assay solution was dispensed to test against the CTA conjugates' serial dilution. Using the Tecan Freedom EVO liquid handler system and a 100nL pin tool (V&P Scientific), a total of 100nL of each CTA conjugate concentration was transferred in quadruplicate to the 20μL assay solution for a final maximum concentration of 100μM of each conjugate. Following incubation for 1 hour, fluorescence polarization was detected at an excitation/emission wavelength of 635/685 nm using the Tecan Infinite M1000 plate reader.

Transcription Assay Protocol

Human embryonic kidney (HEK293, ATCC CRL-3249) T cells were cultured in DMEM/High Glucose (Hyclone, #SH3024301) with non-essential amino acids (Hyclone, #SH30238.01), 10 mM HEPES (Hyclone, #SH302237.01), 5×10^6 units of penicillin and streptomycin (Hyclone, #SV30010), and 10% of FBS (Gibco, #10082147). Transfection was carried out with 70-80% confluent cells. For VDR transfection, 2 mL of untreated DMEM/High Glucose media containing 0.7 μg of VDR-CMV plasmid, 16 μg of a CYP24A1-luciferase reporter gene, Lipofectamine™ LTX (75 μl , Life Technologies #15338020), and PLUS™ reagent (25 μl) was added to the flask. After 16 hours of incubation at 37°C with 5% CO₂, the cells were harvested with 3mL of 0.05% Trypsin (Hyclone, #SH3023601), added to 10mL of the assay buffer (DMEM/High Modified buffer without phenol red, Hyclone #SH30284.01) and spun down for 2 minutes at 1000 rpm. The media was removed and cells were resuspended in the DMEM assay media. Prior to adding cells to sterile white, optical bottom 384-well plates, plates were treated with 20 μL per well of a 0.25% matrigel solution. To each well, 20 μL of cells were added to yield a final concentration of 15,000 cells per well. The plates were then spun down for 2 minutes at 1000 rpm. After four hours, plated cells were treated with 100 nL of compounds and controls which were added using the EVO liquid handling system with a 100nL pin tool (V&P Scientific). Controls used with VDR were 1,25(OH)₂D₃ (10 nM in DMSO, Endotherm) and DMSO. After 16 hours of incubation at 37°C with 5% CO₂, 20 μL of Bright-Glo™ Luciferase Assay Kit (transcription assay, Promega, Madison, WI) were added and luminescence was read on the Tecan Infinite M1000 reader.

Griess Assay Immune Modulation Protocol

The murine macrophage cancer cell line RAW264.7 was cultured in DMEM (ATCC 30-2002) with 10% FBS. To initiate an immune response, cells were suspended at a cell density of 1×10^6 cells/mL and a control sample ($80 \mu\text{L} \times 8$) was dispensed into a 384-well clear-bottomed sterile plate with a lid (Nunc 142762). The remaining suspended cells were then activated with interferon gamma ($\text{IFN}\gamma$, 150units/mL) and lipopolysaccharide (LPS, 50ng/mL). Activated cells were dispensed into a 384-well plate ($80 \mu\text{L}/\text{well}$). A dose-response 384-well plate (highest concentration each: 100mM) of the compounds of interest was then used to dose the activated cell plate with 100 nL using the EVO liquid handling system with a 100nL pin tool (V&P Scientific) for a final highest concentration in the assay plate of $100 \mu\text{M}$. Each concentration was tested in quadruplicate. The following controls were also dosed in octuplicate: activated cells with only DMSO, dexamethasone ($1 \mu\text{M}$), and the toxic compound CBT ($10 \mu\text{M}$). The dosed cells were then allowed to incubate for 24 hours.

Following incubation, aliquots of supernatant ($40 \mu\text{L}$) from each well were moved to a separate 384-well clear-bottomed plate with a lid (CLS3700). To each aliquot was added $40 \mu\text{L}$ of sulfanilamide solution (Promega Griess Reagent System, TB229). The covered plate was shaken briefly and incubated in the dark for 10 minutes. Following this, $40 \mu\text{L}$ of NED solution (Promega Griess Reagent System, TB229) was added to each aliquot. The plate was incubated in the dark for 10 minutes. The absorbance of the plate was then read on the Tecan Infinite M1000 plate reader (530nm).

To the remaining 40 μ L of dosed cells and media was added 40 μ L of Cell Titer Glow luminescent cell viability assay (Promega, G7572). The plate was shaken for 20 minutes and the luminescence then read on the Tecan Infiniate M1000 plate reader.

PART II: TOWARD THE DEVELOPMENT OF A NOVEL ORALLY-AVAILABLE ASTHMA
TREATMENT TARGETING GABA_A RECEPTORS IN THE LUNGS

2.1 A Brief Introduction to Asthma

The treatment and control of asthma remains a persistent modern clinical problem, despite being recognized for decades and occurring all across the globe.¹⁰ An estimated 300 million people have asthma worldwide, including nearly 40 million in the United States.¹⁴ Its prevalence is expected to continue to rise. The central hallmarks of asthma are chronically inflamed airways, hypersensitivity to certain external stimuli, and obstruction of the airways.¹¹ These characteristics lead to clinical features that include persistent cough, shortness of breath, wheezing, coughing, and chest tightness.¹²

As a long-term disease affecting both children and adults, solutions for effective treatment remain limited. The first line of chronic therapy is based on long-acting β_2 adrenergic receptor agonists with or without anti-inflammatory corticosteroids delivered with an inhaler.¹⁴

Some cases of chronic asthma are able to be controlled using this method, and it does have the advantage of providing a targeted delivery to the bronchial submucosa, thus avoiding the systemic effects of corticosteroids delivered orally.¹⁵¹ However, the expected disadvantages due to imprecise dosing and poor compliance are ubiquitous, and sometimes lead to loss of control over the asthmatic symptoms.¹⁵¹ In more severe cases, asthmatic symptoms are treated systemically with corticosteroids. These treatments can cause adverse side effects that include growth suppression, thinning of the skin or excessive bruising, formation of cataracts, adrenal suppression, and increased mortality.¹⁵⁻¹⁹ An alternative oral treatment exists in the form of a leukotriene receptor antagonist (Montelukast) for those who do not respond well to other methods;¹⁵² however, this treatment has a low success rate (somewhere between 35% and 78% of patients do not respond to it).¹⁵³ It is believed that genetic variations in leukotriene signaling are responsible for this alternative therapy being inefficacious.¹⁵³ A final treatment option is injectable biological treatments such as the mIgE-expressing B lymphocyte-specific monoclonal antibody omalizumab,¹⁵⁴ or the interleukin-5-specific monoclonal antibody mepolizumab for eosinophilic asthma.¹⁵⁵ However, with patient costs for such treatments up to \$30,000 a year and the risk for anaphylaxis up to 0.2% with omalizumab,¹⁵⁴ the widespread use of these treatments is limited to only the most severe cases.

Our laboratory, in collaboration with the Cook laboratory at UWM, is seeking an alternate therapy to combat multiple symptoms associated with living with acute asthma.^{1, 13} There are several factors upon which current treatments could be improved: (1) A better asthma drug alternative should be orally administered to improve patient compliance and eliminate dosage

irregularity. (2) Furthermore, unwanted central nervous system effects should be avoided at all cost. (3) Finally, the alternative drug should alleviate a full range of asthma symptoms, such as relaxing the smooth muscle constriction and decreasing inflammation in the airways, rendering combination treatments obsolete.²⁰

Central to achieving those goals is a new therapeutic target for asthma, which is the family of gamma-aminobutyric acid A receptors (GABA_AR). GABA_ARs are ligand-gated chloride ion channels, whose primary function is to regulate intracellular chloride concentrations, especially in neurons. The GABA_AR consists of five subunits combined into a heteropentamer. A typical GABA_AR on neurons consists of two alpha, two beta, and one “other” subunit out of the 19 known subunits (α 1-6, β 1-3, γ 1-3, δ , ϵ , π , θ , ρ 1–3).²¹ Recently, GABA_ARs have been identified on airway smooth muscle cells, airway epithelia cells, and inflammatory cells.^{1, 24, 156-160} These cell types contain α 4 and α 5 subunits.²⁴ In recent decades, the Cook group has introduced subtype-selective GABA_AR ligands based on the benzodiazepine scaffold.²² Further investigations have shown that these ligands mediate distinct pharmacological properties including relaxation of airway smooth muscle and anti-inflammation. Proof of concept that GABA_AR ligands can alleviate asthma symptoms was first shown with plant-based positive allosteric modulator honokiol by Munroe et al.²³ Our group has since developed imidazobenzodiazepine-based compounds that target relevant GABA_AR subtypes expressed in the lung with pronounced efficacy in several asthmatic mouse models.^{1, 13, 20, 24} Achieving targeted asthmatic relief with oral medication and thus eliminating the use of corticosteroids is seen as a huge step forward in asthma treatment.

1. Trends in Asthma Morbidity and Mortality. . Services., A. L. A. E. S. U. R. a. P., Ed.
2. *Guidelines for the Diagnosis and Management of Asthma*; National Heart, Lung, and Blood Institute: August 2007.
3. Pascual, R. M.; Peters, S. P., Airway remodeling contributes to the progressive loss of lung function in asthma: an overview. *The Journal of allergy and clinical immunology* **2005**, *116* (3), 477-86; quiz 487.
4. Moorman, J. E.; Rudd, R. A.; Johnson, C. A.; King, M.; Minor, P.; Bailey, C.; Scalia, M. R.; Akinbami, L. J., National surveillance for asthma--United States, 1980-2004. *Morbidity and mortality weekly report. Surveillance summaries (Washington, D.C. : 2002)* **2007**, *56* (8), 1-54.
5. Everard, M. L., Aerosol therapy past, present, and future: a clinician's perspective. *Respir Care* **2000**, *45*, 769-776.
6. Cates, C. J.; Cates, M. J., Regular treatment with salmeterol for chronic asthma: serious adverse events. *The Cochrane database of systematic reviews* **2008**, (3), Cd006363.
7. Cates, C. J.; Cates, M. J., Regular treatment with formoterol for chronic asthma: serious adverse events. *The Cochrane database of systematic reviews* **2012**, (4), Cd006923.
8. Dahl, R., Systemic side effects of inhaled corticosteroids in patients with asthma. *Respiratory medicine* **2006**, *100* (8), 1307-17.
9. Kelly, H. W.; Sternberg, A. L.; Lescher, R.; Fuhlbrigge, A. L.; Williams, P.; Zeiger, R. S.; Raissy, H. H.; Van Natta, M. L.; Tonascia, J.; Strunk, R. C., Effect of inhaled glucocorticoids in childhood on adult height. *The New England journal of medicine* **2012**, *367* (10), 904-12.
10. Lipworth, B. J., Systemic adverse effects of inhaled corticosteroid therapy: A systematic review and meta-analysis. *Archives of internal medicine* **1999**, *159* (9), 941-55.
11. Montuschi, P.; Peters-Golden, M. L., Leukotriene modifiers for asthma treatment. *Clinical and experimental allergy : journal of the British Society for Allergy and Clinical Immunology* **2010**, *40* (12), 1732-41.
12. Lima, J. J.; Zhang, S.; Grant, A.; Shao, L.; Tantisira, K. G.; Allayee, H.; Wang, J.; Sylvester, J.; Holbrook, J.; Wise, R.; Weiss, S. T.; Barnes, K., Influence of leukotriene pathway polymorphisms on response to montelukast in asthma. *American journal of respiratory and critical care medicine* **2006**, *173* (4), 379-85.
13. Schumann, C.; Kropf, C.; Wibmer, T.; Rüdiger, S.; Stoiber, K. M.; Thielen, A.; Rottbauer, W.; Kroegel, C., Omalizumab in patients with severe asthma: the XCLUSIVE study. *The Clinical Respiratory Journal* **2012**, *6* (4), 215-227.
14. Abonia, J. P.; Putnam, P. E., Mepolizumab in eosinophilic disorders. *Expert review of clinical immunology* **2011**, *7* (4), 411-7.
15. Forkuo, G. S.; Nieman, A. N.; Yuan, N. Y.; Kodali, R.; Yu, O. B.; Zahn, N. M.; Jahan, R.; Li, G.; Stephen, M. R.; Guthrie, M. L.; Poe, M. M.; Hartzler, B. D.; Harris, T. W.; Yocum, G. T.; Emala, C. W.; Steeber, D. A.; Stafford, D. C.; Cook, J. M.; Arnold, L. A., Alleviation of Multiple Asthmatic

Pathologic Features with Orally Available and Subtype Selective GABAA Receptor Modulators. *Molecular pharmaceutics* **2017**, *14* (6), 2088-2098.

16. Jahan, R.; Stephen, M. R.; Forkuo, G. S.; Kodali, R.; Guthrie, M. L.; Nieman, A. N.; Yuan, N. Y.; Zahn, N. M.; Poe, M. M.; Li, G.; Yu, O. B.; Yocum, G. T.; Emala, C. W.; Stafford, D. C.; Cook, J. M.; Arnold, L. A., Optimization of substituted imidazobenzodiazepines as novel asthma treatments. *European journal of medicinal chemistry* **2017**, *126*, 550-560.

17. Forkuo, G. S.; Nieman, A. N.; Kodali, R.; Zahn, N. M.; Li, G.; Rashid Roni, M. S.; Stephen, M. R.; Harris, T. W.; Jahan, R.; Guthrie, M. L.; Yu, O. B.; Fisher, J. L.; Yocum, G. T.; Emala, C. W.; Steeber, D. A.; Stafford, D. C.; Cook, J. M.; Arnold, L. A., A Novel Orally Available Asthma Drug Candidate That Reduces Smooth Muscle Constriction and Inflammation by Targeting GABAA Receptors in the Lung. *Molecular pharmaceutics* **2018**, *15* (5), 1766-1777.

18. Olsen, R. W.; Sieghart, W., International Union of Pharmacology. LXX. Subtypes of gamma-aminobutyric acid(A) receptors: classification on the basis of subunit composition, pharmacology, and function. Update. *Pharmacological reviews* **2008**, *60* (3), 243-60.

19. Mizuta, K.; Xu, D.; Pan, Y.; Comas, G.; Sonett, J. R.; Zhang, Y.; Panettieri, R. A., Jr.; Yang, J.; Emala, C. W., Sr., GABAA receptors are expressed and facilitate relaxation in airway smooth muscle. *American journal of physiology. Lung cellular and molecular physiology* **2008**, *294* (6), L1206-16.

20. Xiang, Y. Y.; Wang, S.; Liu, M.; Hirota, J. A.; Li, J.; Ju, W.; Fan, Y.; Kelly, M. M.; Ye, B.; Orser, B.; O'Byrne, P. M.; Inman, M. D.; Yang, X.; Lu, W. Y., A GABAergic system in airway epithelium is essential for mucus overproduction in asthma. *Nature medicine* **2007**, *13* (7), 862-7.

21. Gallos, G.; Yim, P.; Chang, S.; Zhang, Y.; Xu, D.; Cook, J. M.; Gerthoffer, W. T.; Emala, C. W., Sr., Targeting the restricted alpha-subunit repertoire of airway smooth muscle GABAA receptors augments airway smooth muscle relaxation. *American journal of physiology. Lung cellular and molecular physiology* **2012**, *302* (2), L248-56.

22. Clayton, T.; Poe, M. M.; Rallapalli, S.; Biawat, P.; Savic, M. M.; Rowlett, J. K.; Gallos, G.; Emala, C. W.; Kaczorowski, C. C.; Stafford, D. C.; Arnold, L. A.; Cook, J. M., A Review of the Updated Pharmacophore for the Alpha 5 GABA(A) Benzodiazepine Receptor Model. *International journal of medicinal chemistry* **2015**, *2015*, 430248.

23. Gallos, G.; Yocum, G. T.; Siviski, M. E.; Yim, P. D.; Fu, X. W.; Poe, M. M.; Cook, J. M.; Harrison, N.; Perez-Zoghbi, J.; Emala, C. W., Sr., Selective targeting of the alpha5-subunit of GABAA receptors relaxes airway smooth muscle and inhibits cellular calcium handling. *American journal of physiology. Lung cellular and molecular physiology* **2015**, *308* (9), L931-42.

24. Forkuo, G. S.; Guthrie, M. L.; Yuan, N. Y.; Nieman, A. N.; Kodali, R.; Jahan, R.; Stephen, M. R.; Yocum, G. T.; Treven, M.; Poe, M. M.; Li, G.; Yu, O. B.; Hartzler, B. D.; Zahn, N. M.; Ernst, M.; Emala, C. W.; Stafford, D. C.; Cook, J. M.; Arnold, L. A., Development of GABAA Receptor

Subtype-Selective Imidazobenzodiazepines as Novel Asthma Treatments. *Molecular pharmacology* **2016**, *13* (6), 2026-38.

25. Sieghart, W.; Savic, M. M., International Union of Basic and Clinical Pharmacology. CVI: GABAA Receptor Subtype- and Function-selective Ligands: Key Issues in Translation to Humans. *Pharmacological reviews* **2018**, *70* (4), 836-878.

26. Munroe, M. E.; Businga, T. R.; Kline, J. N.; Bishop, G. A., Anti-Inflammatory Effects of the Neurotransmitter Agonist Honokiol in a Mouse Model of Allergic Asthma. *The Journal of Immunology* **2010**, *185* (9), 5586-5597.

2.2 Mucin Volume Density as a Marker of Asthmatic Disease State

Embedded within the epithelial layer of the bronchi, larger bronchioles, and trachea are goblet cells.¹⁶¹ Their role is to maintain the protective mucus membrane, which they do by secreting mucins: large glycoproteins consisting mainly of carbohydrates (Figure 36).¹⁶¹ The bound

carbohydrates attract appreciable amounts of water, giving

the mucin layer a jelly-like consistency and allowing surfaces to stay well-lubricated. The

essential protective role that mucins play keeps the surfaces of the lungs clean, as it immobilizes stimulants like dust particles and bacteria. The cilia of the epithelial cells covered by the mucins

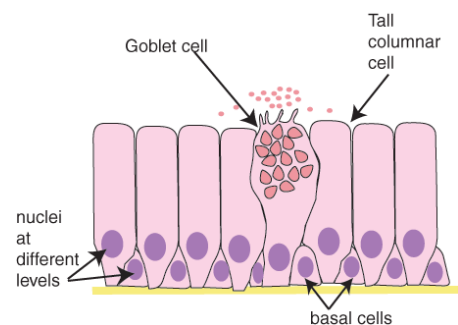


Figure 36: Goblet cells adopted from <https://www.histology.leeds.ac.uk>

beat the secretions and direct contaminants up out of the lungs, while the goblet cells continue to produce more mucins as needed to replenish the mucous membrane.¹⁶¹

In the asthmatic disease state, goblet cells are overrepresented.¹⁶² This can be due to the caused by the goblet cells dividing too often, known as goblet cell hyperplasia, or by too many epithelial cells differentiating into goblet cells, known as mucus metaplasia.¹⁶³ Both processes create too many mucins, and both are known to occur in asthma. This excess of secretions causes a dense, thick mucus layer that cannot be thinned out or removed in the usual manner by cilia movement or even by coughing. Combined with the other classical asthma symptoms such as constriction of the airways, the danger of clogging airways increases leading to asthma exacerbations.

The purpose of this study was therefore to observe mucus overproduction in the epithelial layer of an asthmatic mouse model and monitor the effect of new asthma drug candidates.

Experimental section

Male BALB/c mice were injected i.p. with 50 µg ovalbumin adsorbed with 2 mg aluminum hydroxide (alum) in saline (0.9% NaCl) to sensitize them on day 0, 7, and 14 of a study. On days 23-27, the asthmatic model was induced by challenging those mice intranasally with 25 µl of a 0.4 mg/ml ovalbumin solution. Concurrently, mice in testing groups received an assigned dosage of small molecule, positive control compounds (β -agonists or Montelukast) or vehicle only as

negative control. The mice were then given a final administration of these compounds before euthanasia on day 28 followed by collections of tissues and fluids.

For evaluating lung mucin volume density, a cannula was inserted into the trachea of the deceased mouse. The lungs were inflated with phosphate buffered saline to keep the airways from collapsing. The larger left lung was collected and put in 10% buffered formalin over night at 4°C, followed by washes with 70% ethanol and storage in 70% ethanol. The samples were send to Wisconsin Children’s Hospital for embedding and sectioning in paraffin. The lungs were sectioned as follows: held vertically, the lung was cut through the middle, side to side, so that the main axial airway was exposed as a circular disk. The primary concern during this process was that lungs could be mishandled or crushed so that the mucus layer dislocates. However, the presence of mucus secreted by goblet cell hyperplasia was consistent within every population surveyed. Two slides were made for every mouse lung that was collected (one utilized and one as a “backup” in case the first had problems, detailed below).

The returned slides with lung sections were handled as follows:

Preparation of solutions:

- Fluorescent Schiff reagent solution: 0.75 g acriflavin HCl, 150 mL distilled water, 1.5 g sodium metabisulphite, and 1.5 mL of a 10M solution of HCl. The solution must be kept in the dark for 48 hrs 4°C before use. It will still decompose and stain much less brightly within a week, so small batches are recommended.

- 1% periodic acid solution: 1 g periodic acid and 100 mL distilled water. This solution must be made fresh every time slides are stained.
- Acid alcohol solution: 70mL ethanol, 29mL distilled water, and 1mL 10M HCl
- Canada balsam mounting media: 50:50 Canada balsam and methyl salicylate

Dewaxing and rehydration of slides:

- Immersed in histoclear, 2x for 30 minutes;
- Immersed in 100% ethanol, 2x for 5 minutes;
- Immersed in 95% ethanol in water, 2x for 5 minutes;
- Immersed in 80% and then 70% ethanol in water for 5 minutes;
- Immersed in PBS, 2x for 5 minutes.

Staining and preservation of slides:

- Slides were oxidized in 1% periodic acid for 10 minutes;
- Slides were rinsed with DI water, 3x for 5 minutes;
- Slides were stained with fluorescent Schiff's reagent for 20 minutes;
- Slides were rinsed with DI water, 3x for 5 minutes;
- Slides were rinsed with acid alcohol, 2x for 5 minutes;
- Slides were air-dried in the dark.

- A few microliters of Canada balsam mounting media was placed on the section and the coverslip was tilted carefully over it in order to avoid trapping air bubbles and protect from disturbing the tissue. After leaving overnight, fixing is complete. The slides were then evaluated the following day to avoid loss of fluorescence.

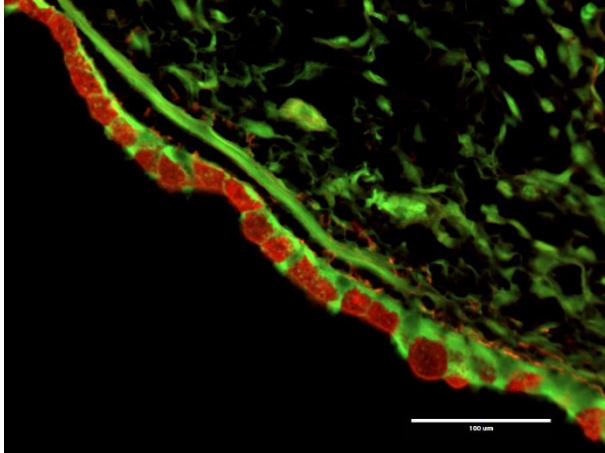


Figure 37: Overlay of GFP and RFP filtered images of ovalbumin sensitized and challenged mouse airway

Image collection: Using an EVOS inverted digital fluorescence microscope (Thermo Fisher), the slides were carefully observed. The main axial airway forms a large unstained hole through the center of each lung section. Using the green fluorescent protein (GFP) filter, the epithelia of the axial airway was zoomed to 40X. The

circumference was inspected to find areas that exhibited cells that were cut cleanly (ex: without many layers of epithelial cells apparent in the background, making the “surface” of the epithelium appear thicker than it really is) and a basement membrane free of “wrinkles.” The scale bar of 100 μm was displayed on each image for scaling purposes later. Images of these smooth, clean areas were taken, at a rate of exactly 4 per slide, spaced as much as was allowable around the axial airway. If four acceptable non-overlapping images were unable to be captured in a single sample, the “backup” slide was used instead. There were no cases wherein both slides failed to have four acceptable images taken.

Images were taken using the GFP and the RFP (red fluorescent protein) filters on the same image, and the two were overlaid to form a single image that exhibits green epithelium

and basement tissue and red mucus in goblet cells (Figure 37). These raw images were saved as JPG files and carefully numbered and categorized for later processing.

Processing procedure: Following the instructions of V. Kim et al,¹⁶³ the images were opened with the ImageJ software. Images were resized (image→adjust→size) to 680w x 512h pixels. Next, the “straight line tool” was used to draw a line equal to the distance between the two points on the ends of the scale bar. This line then was used to scale the picture (analyze → set scale). The distance in pixels is displayed, and the length and units (100 um respectively) were entered. Note that once this scale is known, it can be entered directly into the “set scale” selection for future images.

Next, the length of the basement membrane was measured. The ROI manager was opened (analyze→tools→ROI manager). The “straight line tool” was used to draw lines along the basement membrane, hitting CTRL+D each time to make the line permanent (alternatively: edit→draw). After each segment is drawn, hitting “T” adds it to the ROI manager (alternatively, clicking Add(t) in the ROI Manager window) (see Figure 38). When the basement membrane had been fully outlined, “measure” was clicked in the ROI Manager window. A new window pops up containing multiple fields with quantities concerning those lines. The “length” measurement

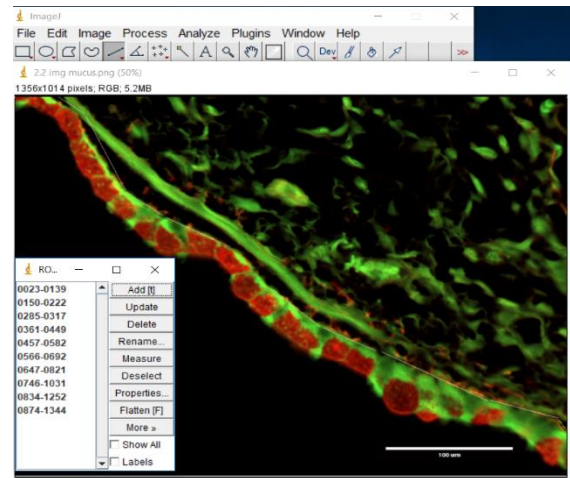


Figure 38: Using ROI manager to quantify data concerning drawn line segments in airway epithelium image opened in ImageJ

is all that is needed, but it is easier to save the whole set than select just that piece of data. The whole set was saved, again carefully naming each one to reflect the image it came from.

Next, the area of mucus was measured. Whatever measurements are in the ROI Manager were deleted. Then using the “freehand selection tool,” the circumference of an area of mucus was outlined. The tool automatically closes the area off if the beginning and ending of an area are not perfectly overlapped. As with the length measurements, after each area was finished, CTRL+D and “T” are hit to make the lines permanent and add them to the ROI Manager. Once all mucus areas were outlined, “measure” was clicked in the ROI Manager and the window that pops up with quantities concerning those areas was saved.

This process was repeated for every image, which is why saving and naming them carefully is an essential part of this data collection. Once all quantities were acquired, they were consolidated. For each lung section, an Excel file was made. In that Excel file, the four images and their quantities were first separately considered. Columns for “Length,” “Total Length,” “Area,” “Total Area,” and “Mucin Volume Density” were made. For each of the four images, the measured “Lengths” from the saved length file were added to the “Length” column, and the measured “Areas” from the saved area file were added to the “Area” column. The “Total Length” and “Total Area” columns displayed the sum of those values (=SUM(x)). The “Mucin Volume Density” column uses the following equation:

$$\frac{\text{total area}}{\text{total length}} \cdot \frac{4}{\pi} = \text{mucin volume density} \quad \text{Equation 1}$$

which converts the measured values (area density and length, effectively) into volume density. These quantities need to be separately evaluated for each image in each lung. The four Mucin Volume Densities were then averaged into a separate column for Mucin Volume Density Average (=AVERAGE(Mucin Volume Densities)). Secondary values of Mucin Volume Density Standard Deviation (=STDEV(Mucin Volume Densities)) and Standard Error (Standard Deviation/(3^{0.5})) were also calculated.

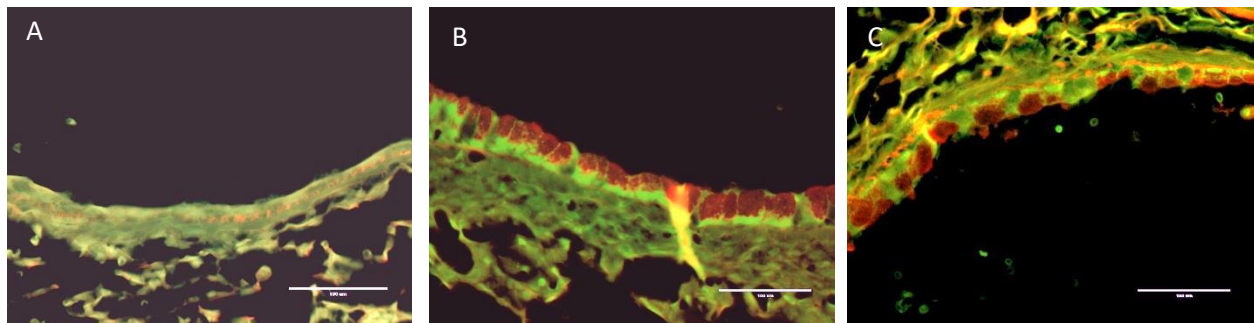


Figure 39: (a) Representative control: vehicle-only mouse airway epithelium; (b) Representative positive control/treatments: ovalbumin sensitized and challenged mouse airway epithelium. Note that all mice tested with small molecules also had the same appearance; (c) Representative negative control: the corticosteroid dexamethasone decreased mucin quantities.

Results

We have investigated the pharmacological effects of α 4-selective GABA_AR positive modulator (XHE-III-74EE)¹⁶⁴ in an ovalbumin sensitized and challenged (Ova S/C) murine model of asthma that represents an acute allergic pulmonary inflammation model. The results were published in 2016 and are summarized in Figure 40.²⁴

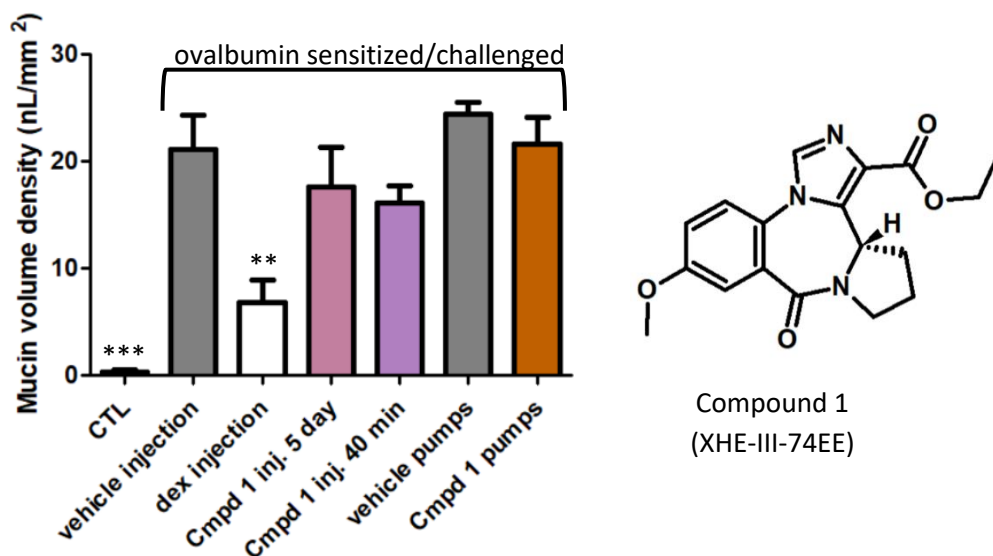


Figure 40: Mucin volume densities of mouse lungs treated with compound 1. CTL: Non-challenged; vehicle (3 % DMSO, 20% propylene glycol and 77% water) given i.p. twice a day for 5 days; Dexamethasone (Dex) 4 mg/kg/day i.p. (5 days); Cmpd1: 20 mg/kg b.i.d., i.p. for 5 days or 40 minutes before euthanasia; osmotic mini-pumps that release 20 mg/kg/day for 7 days. Data is represented as mean \pm SEM, n = 7. ANOVA repeated measured was used for statistical analysis; *, **, *** indicates $p < 0.05$ with reference to the vehicle injection/pumps mice.

Non-challenged mice treated with i.p. injection of vehicle twice a day for five days were used to determine the baseline levels of mucus produced by the mouse lung. Sensitization and challenge with ovalbumin, however, significantly increase in mucin volume density levels to almost 20 nL/mm². When Ova S/C mice were injected for five days with 4 mg/kg/day of glucocorticoid dexamethasone, a significant reduction of the lung mucin volume density was observed. By comparison, XHE-III-74EE, when administered i.p. twice a day for five days at 20 mg/kg neither increased nor decreased the mucin volume density. A single i.p. injection of XHE-III-74EE 40 minutes before euthanasia showed that acute dosage also had no effect on mucin volume density. To study a continuous release model of XHE-III-74EE, mini-pumps were deposited under the skin on the back of the animals. The continuous application of vehicle resulted in a mucin volume density similar to that of the vehicle i.p. injection. The continuous

release of XHE-III-74EE at 20 mg/kg/day similarly did not significantly increase or decrease the mucin volume over a period of seven days.

In the same paper, Compound 2, an $\alpha 5$ -selective GABA_AR positive modulator (SH-053-2F'-R-CH₃) was also tested in the same Ova S/C murine asthmatic inflammation model. The results are summarized in Figure 41.²⁴

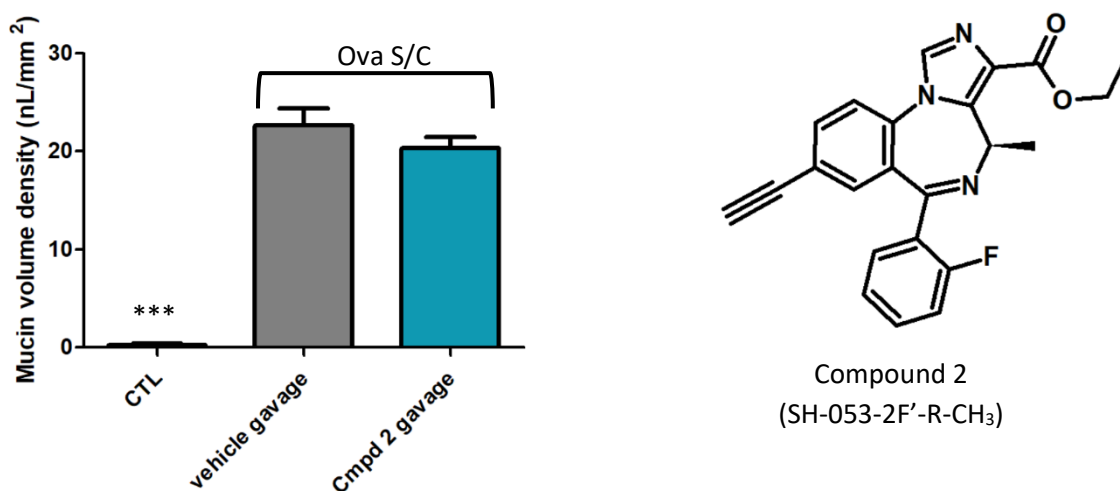


Figure 41: Mucin volume densities for Compound 2.¹ CTL: non-challenged; vehicle gavage: vehicle (3 % DMSO, 20% propylene glycol and 77% water) administered twice daily for 5 days by oral gavage; Cmpd 2 gavage: 100 mg/kg administered twice daily for 5 days by oral gavage. Data is represented as mean \pm SEM, n = 7. ANOVA repeated measured was used for statistical analysis; *, **, *** indicates $p < 0.05$ with reference to the vehicle gavage mice.

Non-challenged mice in this study were challenged with i.n. saline twice a day for five days to determine the baseline levels of mucus produced by the mouse lung. Sensitization and challenge with ovalbumin again produced a comparable increase in mucin volume density levels to around 20 nL/mm². SH-053-2F'-R-CH₃, when administered twice a day for five days at 100mg/kg neither increased nor decreased the mucin volume density.

In the same publication, Compound 3, an $\alpha 4$ -selective GABA_AR positive modulator (XHE-III-74A) was also tested in the same Ova S/S murine asthmatic inflammation model. The results are summarized in Figure 42.²⁴



Figure 42: Mucin volume densities for Compound 3.¹ CTL: non-challenged; vehicle injection: vehicle (3 % DMSO, 20% propylene glycol and 77% water) administered i.p. twice daily for 5 days.; Cmpd 3 inj.: 20 mg/kg b.i.d., i.p. for 5 days or 40 minutes before euthanasia. Data is represented as mean \pm SEM, n = 7. ANOVA repeated measured was used for statistical analysis; *, **, *** indicates $p < 0.05$ with reference to the vehicle injection mice.

Non-challenged mice treated with i.p. injection of vehicle twice a day for five days were used to determine the baseline levels of mucus produced by the mouse lung. Sensitization and challenge again produced the expected mucin volume density levels. Again, XHE-III-74A when administered i.p. twice a day for five days at 20 mg/kg or when given as a single i.p. injection 40 minutes before euthanasia neither increased nor decreased the mucin volume density.

Discussion

None of the asthma drug candidates produced a result that deviated significantly from their respective ovalbumin sensitized and challenged positive control group. This was apparent both by visual inspection of the images and by quantitation. However, dexamethasone was effective at significantly reducing the mucus volume density.

References

1. Forkuo, G. S.; Nieman, A. N.; Yuan, N. Y.; Kodali, R.; Yu, O. B.; Zahn, N. M.; Jahan, R.; Li, G.; Stephen, M. R.; Guthrie, M. L.; Poe, M. M.; Hartzler, B. D.; Harris, T. W.; Yocum, G. T.; Emala, C. W.; Steeber, D. A.; Stafford, D. C.; Cook, J. M.; Arnold, L. A., Alleviation of Multiple Asthmatic Pathologic Features with Orally Available and Subtype Selective GABAA Receptor Modulators. *Molecular pharmaceuticals* **2017**, *14* (6), 2088-2098.
2. Orlov, I.; Rochel, N.; Moras, D.; Klaholz, B. P., Structure of the full human RXR/VDR nuclear receptor heterodimer complex with its DR3 target DNA. *The EMBO journal* **2012**, *31* (2), 291-300.
3. Brzozowski, A. M.; Pike, A. C.; Dauter, Z.; Hubbard, R. E.; Bonn, T.; Engstrom, O.; Ohman, L.; Greene, G. L.; Gustafsson, J. A.; Carlquist, M., Molecular basis of agonism and antagonism in the oestrogen receptor. *Nature* **1997**, *389* (6652), 753-8.
4. Teske, K. A.; Bogart, J. W.; Sanchez, L. M.; Yu, O. B.; Preston, J. V.; Cook, J. M.; Silvaggi, N. R.; Bikle, D. D.; Arnold, L. A., Synthesis and evaluation of vitamin D receptor-mediated activities of cholesterol and vitamin D metabolites. *European journal of medicinal chemistry* **2016**, *109*, 238-46.
5. Yu, O. B.; Arnold, L. A., Calcitroic Acid—A Review. *ACS Chemical Biology* **2016**, *11* (10), 2665-2672.
6. Shaffer, P. L.; Gewirth, D. T., Structural analysis of RXR-VDR interactions on DR3 DNA. *The Journal of steroid biochemistry and molecular biology* **2004**, *89-90* (1-5), 215-9.
7. Esvelt, R. P.; Schnoes, H. K.; DeLuca, H. F., Isolation and characterization of 1.alpha.-hydroxy-23-carboxytetranorvitamin D: a major metabolite of 1,25-dihydroxyvitamin D3. *Biochemistry* **1979**, *18* (18), 3977-3983.
8. Onisko, B. L.; Esvelt, R. P.; Schnoes, H. K.; DeLuca, H. F., Metabolites of 1 alpha, 25-dihydroxyvitamin D3 in rat bile. *Biochemistry* **1980**, *19* (17), 4124-30.
9. Pike, W. S., N. K., In *Vitamin D*, 2005; Vol. 2nd Ed.
10. Trends in Asthma Morbidity and Mortality. . Services., A. L. A. E. S. U. R. a. P., Ed.
11. Pascual, R. M.; Peters, S. P., Airway remodeling contributes to the progressive loss of lung function in asthma: an overview. *The Journal of allergy and clinical immunology* **2005**, *116* (3), 477-86; quiz 487.
12. Moorman, J. E.; Rudd, R. A.; Johnson, C. A.; King, M.; Minor, P.; Bailey, C.; Scalia, M. R.; Akinbami, L. J.; Centers for Disease, C.; Prevention, National surveillance for asthma--United States, 1980-2004. *MMWR Surveill Summ* **2007**, *56* (8), 1-54.
13. Jahan, R.; Stephen, M. R.; Forkuo, G. S.; Kodali, R.; Guthrie, M. L.; Nieman, A. N.; Yuan, N. Y.; Zahn, N. M.; Poe, M. M.; Li, G.; Yu, O. B.; Yocum, G. T.; Emala, C. W.; Stafford, D. C.; Cook, J. M.; Arnold, L. A., Optimization of substituted imidazobenzodiazepines as novel asthma treatments. *European journal of medicinal chemistry* **2017**, *126*, 550-560.
14. *Guidelines for the Diagnosis and Management of Asthma*; National Heart, Lung, and Blood Institute: August 2007.
15. Cates, C. J.; Cates, M. J., Regular treatment with formoterol for chronic asthma: serious adverse events. *The Cochrane database of systematic reviews* **2012**, (4), Cd006923.
16. Cates, C. J.; Cates, M. J., Regular treatment with salmeterol for chronic asthma: serious adverse events. *The Cochrane database of systematic reviews* **2008**, (3), Cd006363.
17. Dahl, R., Systemic side effects of inhaled corticosteroids in patients with asthma. *Respiratory medicine* **2006**, *100* (8), 1307-17.
18. Kelly, H. W.; Sternberg, A. L.; Lescher, R.; Fuhlbrigge, A. L.; Williams, P.; Zeiger, R. S.; Raissy, H. H.; Van Natta, M. L.; Tonascia, J.; Strunk, R. C., Effect of inhaled glucocorticoids in childhood on adult height. *The New England journal of medicine* **2012**, *367* (10), 904-12.

19. Lipworth, B. J., Systemic adverse effects of inhaled corticosteroid therapy: A systematic review and meta-analysis. *Archives of internal medicine* **1999**, *159* (9), 941-55.
20. Forkuo, G. S.; Nieman, A. N.; Kodali, R.; Zahn, N. M.; Li, G.; Rashid Roni, M. S.; Stephen, M. R.; Harris, T. W.; Jahan, R.; Guthrie, M. L.; Yu, O. B.; Fisher, J. L.; Yocum, G. T.; Emala, C. W.; Steeber, D. A.; Stafford, D. C.; Cook, J. M.; Arnold, L. A., A Novel Orally Available Asthma Drug Candidate That Reduces Smooth Muscle Constriction and Inflammation by Targeting GABAA Receptors in the Lung. *Molecular pharmaceutics* **2018**, *15* (5), 1766-1777.
21. Olsen, R. W.; Sieghart, W., International Union of Pharmacology. LXX. Subtypes of gamma-aminobutyric acid(A) receptors: classification on the basis of subunit composition, pharmacology, and function. Update. *Pharmacological reviews* **2008**, *60* (3), 243-60.
22. Sieghart, W.; Savic, M. M., International Union of Basic and Clinical Pharmacology. CVI: GABAA Receptor Subtype- and Function-selective Ligands: Key Issues in Translation to Humans. *Pharmacological reviews* **2018**, *70* (4), 836-878.
23. Munroe, M. E.; Businga, T. R.; Kline, J. N.; Bishop, G. A., Anti-Inflammatory Effects of the Neurotransmitter Agonist Honokiol in a Mouse Model of Allergic Asthma. *The Journal of Immunology* **2010**, *185* (9), 5586-5597.
24. Forkuo, G. S.; Guthrie, M. L.; Yuan, N. Y.; Nieman, A. N.; Kodali, R.; Jahan, R.; Stephen, M. R.; Yocum, G. T.; Treven, M.; Poe, M. M.; Li, G.; Yu, O. B.; Hartzler, B. D.; Zahn, N. M.; Ernst, M.; Emala, C. W.; Stafford, D. C.; Cook, J. M.; Arnold, L. A., Development of GABAA Receptor Subtype-Selective Imidazobenzodiazepines as Novel Asthma Treatments. *Molecular pharmaceutics* **2016**, *13* (6), 2026-38.
25. Rosenfeld, L., Vitamine--vitamin. The early years of discovery. *Clinical chemistry* **1997**, *43* (4), 680-5.
26. Hopkins, F. G., Feeding Experiments Illustrating the Importance of Accessory Food Factors in Normal Diets. *J. Physiol* **1912**, *44*, 425-460.
27. Funk, C., On the Chemical Nature of the Substance Which Cures Polyneuritis in Birds Induced by a Diet of Polished Rice. *J. Physiol* **1911**, *43*, 395-402.
28. McCollum, E. V.; Davis, M., The Necessity of Certain Lipins in the Diet During Growth. *J. Biol. Chem* **1913**, *15*, 167-175.
29. T. B. Osborne, L. B. M., The role of vitamins in the diet. *J. Biol. Chem.* **1917**, *31*, 149-163.
30. McCollum, E. V.; Simmonds, N.; Pitz, W., The Relation of the Unidentified Dietary Factors, the Fat-Soluble A, and Water-Soluble B, of the Diet to the Growth-Promoting Properties of Milk. *J. Biol. Chem* **1916**, *27*, 33-38.
31. Hess, A., *The history of rickets*. Lea & Febiger: Philadelphia, Pennsylvania, 1929.
32. McCollum, E. V.; Simmonds, N.; Becker, J. E., An Experimental Demonstration of the Existence of a Vitamin Which Promotes Calcium Deposition. *J Biol. Chem* **1922**, *53*, 293-298.
33. Deluca, H. F., Historical Overview of Vitamin D. In *Vitamin D, 3rd Edition*, Feldman, D.; Pike, J. W.; Adams, J. S., Eds. 2011; Vol. 1.
34. Huldshinsky, K., Heilung von rachitis durch kunstlich hohen-sonne. *Deut. Med. Wochenschr* **1919**, *45*, 712-713.
35. Chick, D. H., Study of Rickets in Vienna 1919-1922. *Medical Research Council, Special Report* **1923**.
36. Vieth, R., Why "Vitamin D" is not a hormone, and not a synonym for 1,25-dihydroxy-vitamin D, its analogs or diltanoids. *The Journal of steroid biochemistry and molecular biology* **2004**, *89-90* (1-5), 571-3.
37. A. Windaus, O. L., Vitamin D1. *Ann. Chem.* **1928**, *465*, 148.
38. Askew, F. A.; Bourdillon, R. B.; Bruce, H. M.; Jenkins, R. G. C.; Webster, T. A., The Distillation of Vitamin D. *Proc. R. Soc.* **1930**, *B107*, 76-90.

39. Windaus, A.; Linsert, O.; Lüttringhaus, A.; Weidlich, G., Über das kristallisierte Vitamin D₂. *Justus Liebigs Annalen der Chemie* **1932**, 492 (1), 226-241.
40. Windaus, A.; Bock, F., Über das Provitamin aus dem Sterin der Schweineschwarte. In *Hoppe-Seyler's Zeitschrift für physiologische Chemie*, 1936; Vol. 245, p 168.
41. Windaus, A.; Schenck, F., Über das antirachitisch wirksame bestrahlungs-produkt aus 7-dehydrocholesterin. *Hoppe.-Seylers. Z. Physiol. Chem* **1936**, 241, 100-103.
42. Morii, H.; Lund, J.; Neville, P. F.; DeLuca, H. F., Biological activity of a vitamin D metabolite. *Archives of Biochemistry and Biophysics* **1967**, 120 (3), 508-512.
43. Blunt, J. W.; DeLuca, H. F.; Schnoes, H. K., 25-Hydroxycholecalciferol. A biologically active metabolite of vitamin D₃. *Biochemistry* **1968**, 7 (10), 3317-3322.
44. Holick, M. F.; Schnoes, H. K.; DeLuca, H. F.; Suda, T.; Cousins, R. J., Isolation and Identification of 1,25-Dihydroxycholecalciferol A Metabolite of Vitamin D Acite in Instestine. *Biochemistry* **1971**, 10, 2799-2804.
45. Pike, J. W.; Meyer, M. B.; Lee, S.-M.; Onal, M.; Benkusky, N. A., The vitamin D receptor: contemporary genomic approaches reveal new basic and translational insights. *The Journal of Clinical Investigation* **2017**, 127 (4), 1146-1154.
46. Askew, F. A.; Bourdillon, R. B.; Bruce, H. M.; Jenkins, R. G. C.; Webster, T. A., The Distillation of Vitamin D. *Proceedings of the Royal Society. Series B.* **1930**, 107, 76-90.
47. Brumbaugh, P. F.; Haussler, M. R., α ,25-dihydroxyvitamin D₃ receptor: competitive binding of vitamin D analogs. *Life Sciences* **1973**, 13 (12), 1737-1746.
48. McDonnell, D. P.; Mangelsdorf, D. J.; Pike, J. W.; Haussler, M. R.; O'Malley, B. W., Molecular cloning of complementary DNA encoding the avian receptor for vitamin D. *Science (New York, N.Y.)* **1987**, 235 (4793), 1214-7.
49. Rochel, N.; Wurtz, J. M.; Mitschler, A.; Klaholz, B.; Moras, D., The crystal structure of the nuclear receptor for vitamin D bound to its natural ligand. *Molecular cell* **2000**, 5 (1), 173-9.
50. Wärnmark, A.; Treuter, E.; Wright, A. P. H.; Gustafsson, J.-A. k., Activation Functions 1 and 2 of Nuclear Receptors: Molecular Strategies for Transcriptional Activation. *Molecular Endocrinology* **2003**, 17 (10), 1901-1909.
51. Kumar, R.; Thompson, E. B., The structure of the nuclear hormone receptors. *Steroids* **1999**, 64 (5), 310-319.
52. Pike, W.; Shevde, N. K., The Vitamin D Receptor. In *Vitamin D, 2nd Edition*, Feldman, D.; Pike, J. W.; Glorieux, F. H., Eds. Elsevier Academic Press: 2005; Vol. 1, pp 167-191.
53. Whitfield, G. K.; Jurutka, P. W.; Haussler, C. A.; Hsieh, J.-C.; Barthel, T. K.; Jacobs, E. T.; Dominguez, C. E.; Thatcher, M. L.; Haussler, M. R., Nuclear Vitamin D Receptor: Structure-Function, Molecular Control of Gene Transcription, and Novel Bioactions. In *Vitamin D Receptor, 2nd Edition*, Feldman, D.; Pike, J. W.; Glorieux, F. H., Eds. Elsevier Academic Press: Burlington, MA, 2005; Vol. 1, pp 219-261.
54. Kurokawa, R.; Yu, V. C.; N α α p, A.; Kyakumoto, S.; Han, Z.; Silverman, S.; Rosenfeld, M. G.; Glass, C. K., Differential orientations of the DNA-binding domain and carboxy-terminal dimerization interface regulate binding site selection by nuclear receptor heterodimers. *Genes Dev.* **1993**, 7, 1423-1435.
55. Pike, W. M., M; Lee, S.M., The Vitamin D Receptor: Biochemical, Molecular, Biological, and Genomic Era Investigations. In *Vitamin D*, Pike, W. S., N. K., Ed. 2011; Vol. 3rd Ed, pp 97-135.
56. Blanco, J. C.; Wang, I. M.; Tsai, S. Y.; Tsai, M. J.; O'Malley, B. W.; Jurutka, P. W.; Haussler, M. R.; Ozato, K., Transcription factor TFIIB and the vitamin D receptor cooperatively activate ligand-dependent transcription. *Proceedings of the National Academy of Sciences of the United States of America* **1995**, 92 (5), 1535-1539.

57. Rochel, N.; Moras, D., Structural Basis for Ligand Activity in VDR. In *Vitamin D, 3rd Edition*, Feldman, D.; Pike, J. W.; Adams, J. S., Eds. Elsevier Inc: 2011; Vol. II, pp 171-191.
58. Moras, D.; Gronemeyer, H., The Nuclear Receptor Ligand-binding Domain: Structure and Function. *Current Opinion in Cell Biology* **1998**, *10* (3), 384-91.
59. Umesono, K.; Murakami, K. K.; Thompson, C. C.; Evans, R. M., Direct repeats as selective response elements for the thyroid hormone, retinoic acid, and vitamin D3 receptors. *Cell* **1991**, *65* (7), 1255-1266.
60. Bikle, D., Vitamin D: Production, Metabolism, and Mechanisms of Action. . Vitamin D: Production, M., and Mechanisms of Action. , Ed. Endotext: South Dartmouth (MA), 2000.
61. Mangelsdorf, D. J.; Thummel, C.; Beato, M.; Herrlich, P.; Schutz, G.; Umesono, K.; Blumberg, B.; Kastner, P.; Mark, M.; Chambon, P.; Evans, R. M., The Nuclear Receptor Superfamily: The Second Decade. *Cell* **1995**, *83*, 835-839.
62. Pike, J. W.; Meyer, M. B.; Lee, S. M., The Vitamin D Receptor. In *The Vitamin D Receptor, 3rd Edition*, Feldman, D.; Pike, J. W.; Adams, J. S., Eds. Elsevier: 2011; Vol. 1.
63. Chalk, K. J.; Kodicek, E., The association of ¹⁴C-labelled vitamin D2 with rat serum proteins. *The Biochemical journal* **1961**, *79* (1), 1-7.
64. DeLuca, H. F.; Holick, M. F.; Schnoes, H. K.; Suda, T.; Cousins, R. J., Isolation and identification of 1,25-dihydroxycholecalciferol. A metabolite of vitamin D active in intestine. *Biochemistry* **1971**, *10* (14), 2799-2804.
65. Brumbaugh, P. F.; Haussler, M. R., 1 α ,25-dihydroxyvitamin D3 receptor: competitive binding of vitamin D analogs. *Life Sci* **1973**, *13* (12), 1737-46.
66. Callow Robert, K.; Kodicek, E.; Thompson, G. A., Metabolism of tritiated vitamin D. *Proceedings of the Royal Society of London. Series B. Biological Sciences* **1966**, *164* (994), 1-20.
67. Bell, P. A.; Kodicek, E., Investigations on metabolites of vitamin D in rat bile. Separation and partial identification of a major metabolite. *The Biochemical journal* **1969**, *115* (4), 663-669.
68. Tsai, H. C.; Wong, R. G.; Norman, A. W., Studies on Calciferol Metabolism: IV. SUBCELLULAR LOCALIZATION OF 1,25-DIHYDROXY-VITAMIN D3 IN INTESTINAL MUCOSA AND CORRELATION WITH INCREASED CALCIUM TRANSPORT. *Journal of Biological Chemistry* **1972**, *247* (17), 5511-5519.
69. Esvelt, R. P.; De Luca, H. F., Calcitric acid: biological activity and tissue distribution studies. *Arch Biochem Biophys* **1981**, *206* (2), 403-13.
70. Suda, T.; DeLuca, H. F.; Schnoes, H. K.; Ponchon, G.; Tanaka, Y.; Holick, M. F., 21,25-Dihydroxycholecalciferol. A metabolite of vitamin D3 preferentially active on bone. *Biochemistry* **1970**, *9* (14), 2917-2922.
71. Holick, M. F.; Schnoes, H. K.; DeLuca, H. F.; Gray, R. W.; Boyle, I. T.; Suda, T., Isolation and identification of 24,25-dihydroxycholecalciferol, a metabolite of vitamin D3 made in the kidney. *Biochemistry* **1972**, *11* (23), 4251-4255.
72. Tanaka, Y.; DeLuca, H. F., Stimulation of 24,25-Dihydroxyvitamin D₃ Production by 1,25-Dihydroxyvitamin D₃. *Science (New York, N.Y.)* **1974**, *183* (4130), 1198-1200.
73. Knutson, J. C.; DeLuca, H. F., 25-Hydroxyvitamin D3-24-hydroxylase. Subcellular location and properties. *Biochemistry* **1974**, *13* (7), 1543-1548.
74. Burgos-Trinidad, M.; Brown, A. J.; DeLuca, H. F., Solubilization and reconstitution of chick renal mitochondrial 25-hydroxyvitamin D3 24-hydroxylase. *Biochemistry* **1986**, *25* (9), 2692-2696.
75. Ohyama, Y.; Okuda, K., Isolation and characterization of a cytochrome P-450 from rat kidney mitochondria that catalyzes the 24-hydroxylation of 25-hydroxyvitamin D3. *Journal of Biological Chemistry* **1991**, *266* (14), 8690-8695.
76. Ohyama, Y.; Noshiro, M.; Okuda, K., Cloning and expression of cDNA encoding 25-hydroxyvitamin D3 24-hydroxylase. *FEBS Letters* **1991**, *278* (2), 195-198.

77. Jones, G.; Kung, M.; Kano, K., The isolation and identification of two new metabolites of 25-hydroxyvitamin D₃ produced in the kidney. *The Journal of biological chemistry* **1983**, *258* (21), 12920-8.
78. Reddy, G. S.; Tserng, K. Y.; Thomas, B. R.; Dayal, R.; Norman, A. W., Isolation and identification of 1,23-dihydroxy-24,25,26,27-tetranorvitamin D₃, a new metabolite of 1,25-dihydroxyvitamin D₃ produced in rat kidney. *Biochemistry* **1987**, *26* (1), 324-31.
79. Reddy, G. S.; Tserng, K. Y., Calcitric acid, end product of renal metabolism of 1,25-dihydroxyvitamin D₃ through C-24 oxidation pathway. *Biochemistry* **1989**, *28* (4), 1763-9.
80. Makin, G.; Lohnes, D.; Byford, V.; Ray, R.; Jones, G., Target cell metabolism of 1,25-dihydroxyvitamin D₃ to calcitric acid. Evidence for a pathway in kidney and bone involving 24-oxidation. *Biochem J* **1989**, *262* (1), 173-80.
81. Turner, R. T.; Puzas, J. E.; Forte, M. D.; Lester, G. E.; Gray, T. K.; Howard, G. A.; Baylink, D. J., In vitro synthesis of 1 alpha,25-dihydroxycholecalciferol and 24,25-dihydroxycholecalciferol by isolated calvarial cells. *Proceedings of the National Academy of Sciences of the United States of America* **1980**, *77* (10), 5720-5724.
82. Sakaki, T.; Sawada, N.; Komai, K.; Shiozawa, S.; Yamada, S.; Yamamoto, K.; Ohyama, Y.; Inouye, K., Dual metabolic pathway of 25-hydroxyvitamin D₃ catalyzed by human CYP24. *European journal of biochemistry* **2000**, *267* (20), 6158-65.
83. Sakaki, T.; Sawada, N.; Nonaka, Y.; Ohyama, Y.; Inouye, K., Metabolic studies using recombinant escherichia coli cells producing rat mitochondrial CYP24 CYP24 can convert 1alpha,25-dihydroxyvitamin D₃ to calcitric acid. *European journal of biochemistry* **1999**, *262* (1), 43-8.
84. Inouye, K.; Sakaki, T., Enzymatic studies on the key enzymes of vitamin D metabolism; 1 alpha-hydroxylase (CYP27B1) and 24-hydroxylase (CYP24). *Biotechnology annual review* **2001**, *7*, 179-94.
85. Reddy, G. S.; Omdahl, J. L.; Robinson, M.; Wang, G.; Palmore, G. T.; Vicchio, D.; Yergey, A. L.; Tserng, K. Y.; Uskokovic, M. R., 23-carboxy-24,25,26,27-tetranorvitamin D₃ (calcioic acid) and 24-carboxy-25,26,27-trinorvitamin D₃ (cholocalcioic acid): end products of 25-hydroxyvitamin D₃ metabolism in rat kidney through C-24 oxidation pathway. *Arch Biochem Biophys* **2006**, *455* (1), 18-30.
86. Zimmerman, D. R.; Reinhardt, T. A.; Kremer, R.; Beitz, D. C.; Reddy, G. S.; Horst, R. L., Calcitric acid is a major catabolic metabolite in the metabolism of 1 alpha-dihydroxyvitamin D(2). *Arch Biochem Biophys* **2001**, *392* (1), 14-22.
87. Horst, R. L.; Omdahl, J. A.; Reddy, S., Rat cytochrome P450C24 (CYP24) does not metabolize 1,25-dihydroxyvitamin D₂ to calcitric acid. *Journal of cellular biochemistry* **2003**, *88* (2), 282-5.
88. Tachibana, Y.; Tsuji, M., Study on the metabolites of 1alpha,25-dihydroxyvitamin D₄. *Steroids* **2001**, *66* (2), 93-97.
89. Sakaki, T.; Kagawa, N.; Yamamoto, K.; Inouye, K., Metabolism of vitamin D₃ by cytochromes P450. *Frontiers in bioscience : a journal and virtual library* **2005**, *10*, 119-34.
90. Tang, E. K. Y.; Tieu, E. W.; Tuckey, R. C., Expression of human CYP27B1 in Escherichia coli and characterization in phospholipid vesicles. *The FEBS journal* **2012**, *279* (19), 3749-3761.
91. Hector F. DeLuca, H. K. S., Robert P. Esvelt Processes for preparing calcitric acid and esters thereof. 1981.
92. Esvelt, R. P.; Fivizzani, M. A.; Paaren, H. E.; Schnoes, H. K.; DeLuca, H. F., Synthesis of calcitric acid, a metabolite of 1.alpha.,25-dihydroxycholecalciferol. *The Journal of Organic Chemistry* **1981**, *46* (2), 456-458.
93. de Costa, B. R.; Makk, N.; Midgley, J. M.; Modi, N. T.; Watt, R. A.; Whalley, W. B., Unsaturated steroids. Part 12. Synthesis of 1 α ,3 β -dihydroxy-24-nor-9,10-secochola-5,7,10(19)trien-23-oic (calcitric acid) and of the cholic-and 25-homocholic acid analogues. *Journal of the Chemical Society, Perkin Transactions 1* **1985**, (0), 1331-1336.

94. Zhu, G.-D.; Okamura, W. H., Synthesis of Vitamin D (Calciferol). *Chemical Reviews* **1995**, *95* (6), 1877-1952.
95. Calverley, M. J., The Seleno-Acetal Route to Side-Chain Modified 1-Alpha-Hydroxy-Vitamin-D Analogs - Stereoselective Synthesis of the New 22z Isomer of Mc903 (Calcipotriol). *Synlett* **1990**, *1990*, 157-159.
96. Meyer, D.; Rentsch, L.; Marti, R., Efficient and scalable total synthesis of calcitroic acid and its ¹³C-labeled derivative. *RSC Advances* **2014**, *4* (61), 32327-32334.
97. Posner, G. H.; Lee, J. K.; White, M. C.; Hutchings, R. H.; Dai, H.; Kachinski, J. L.; Dolan, P.; Kensler, T. W., Antiproliferative Hybrid Analogs of the Hormone 1alpha,25-Dihydroxyvitamin D(3): Design, Synthesis, and Preliminary Biological Evaluation. *J Org Chem* **1997**, *62* (10), 3299-3314.
98. Lacroix, J.-F. Design and Synthesis of A-ring/seco-B-ring vitamin D analogues. McGill University, 2012.
99. Kürti, L. B. C., Pinnick Oxidation. In *Strategic applications of named reactions in organic synthesis: background and detailed mechanisms*, Elsevier: 2005; pp 354-356.
100. Harant, H.; Andrew, P. J.; Reddy, G. S.; Foglar, E.; Lindley, I. J., 1alpha,25-dihydroxyvitamin D3 and a variety of its natural metabolites transcriptionally repress nuclear-factor-kappaB-mediated interleukin-8 gene expression. *European journal of biochemistry* **1997**, *250* (1), 63-71.
101. Harant, H.; Spinner, D.; Reddy, G. S.; Lindley, I. J., Natural metabolites of 1alpha,25-dihydroxyvitamin D(3) retain biologic activity mediated through the vitamin D receptor. *J Cell Biochem* **2000**, *78* (1), 112-20.
102. Jones, G.; Prosser, D. E.; Kaufmann, M., 25-Hydroxyvitamin D-24-hydroxylase (CYP24A1): its important role in the degradation of vitamin D. *Archives of biochemistry and biophysics* **2012**, *523* (1), 9-18.
103. Jones, G.; Prosser, D. E., Chapter 3: The activating enzymes of vitamin D metabolism (25- and 1alpha-hydroxylase). In *Vitamin D*, third ed.; Feldman, D.; Pike, J. W.; Adams, J. S., Eds. Academic Press: San Diego, CA, USA, 2011; Vol. one.
104. Wang, Z.; Schuetz, E. G.; Xu, Y.; Thummel, K. E., Interplay between vitamin D and the drug metabolizing enzyme CYP3A4. *The Journal of steroid biochemistry and molecular biology* **2013**, *136*, 54-8.
105. Lundqvist, J.; Hansen, S. K.; Lykkesfeldt, A. E., Vitamin D analog EB1089 inhibits aromatase expression by dissociation of comodulator WSTF from the CYP19A1 promoter-a new regulatory pathway for aromatase. *Biochimica et biophysica acta* **2013**, *1833* (1), 40-7.
106. Matsunawa, M.; Akagi, D.; Uno, S.; Endo-Umeda, K.; Yamada, S.; Ikeda, K.; Makishima, M., Vitamin D receptor activation enhances benzo[a]pyrene metabolism via CYP1A1 expression in macrophages. *Drug metabolism and disposition: the biological fate of chemicals* **2012**, *40* (11), 2059-66.
107. Reschly, E. J.; Krasowski, M. D., Evolution and function of the NR1I nuclear hormone receptor subfamily (VDR, PXR, and CAR) with respect to metabolism of xenobiotics and endogenous compounds. *Current drug metabolism* **2006**, *7* (4), 349-65.
108. Lin, W.; Liu, J.; Jeffries, C.; Yang, L.; Lu, Y.; Lee, R. E.; Chen, T., Development of BODIPY FL Vindoline as a Novel and High-Affinity Pregnane X Receptor Fluorescent Probe. *Bioconjugate Chemistry* **2014**, *25* (9), 1664-1677.
109. Carazo, A.; Pávek, P., The Use of the LanthaScreen TR-FRET CAR Coactivator Assay in the Characterization of Constitutive Androstane Receptor (CAR) Inverse Agonists. *Sensors (Basel, Switzerland)* **2015**, *15* (4), 9265-9276.
110. White, J. H., Vitamin D metabolism and signaling in the immune system. *Reviews in endocrine & metabolic disorders* **2012**, *13* (1), 21-9.

111. Eming, S. A.; Krieg, T.; Davidson, J. M., Inflammation in wound repair: molecular and cellular mechanisms. *The Journal of investigative dermatology* **2007**, *127* (3), 514-25.
112. Granger, D. L.; Taintor, R. R.; Boockvar, K. S.; Hibbs, J. B., Jr., Measurement of nitrate and nitrite in biological samples using nitrate reductase and Griess reaction. *Methods in enzymology* **1996**, *268*, 142-51.
113. Ishizawa, M.; Akagi, D.; Makishima, M., Lithocholic Acid Is a Vitamin D Receptor Ligand That Acts Preferentially in the Ileum. *International journal of molecular sciences* **2018**, *19* (7).
114. Drocourt, L.; Ourlin, J. C.; Pascussi, J. M.; Maurel, P.; Vilarem, M. J., Expression of CYP3A4, CYP2B6, and CYP2C9 is regulated by the vitamin D receptor pathway in primary human hepatocytes. *The Journal of biological chemistry* **2002**, *277* (28), 25125-32.
115. Cheng, J.; Fang, Z. Z.; Kim, J. H.; Krausz, K. W.; Tanaka, N.; Chiang, J. Y.; Gonzalez, F. J., Intestinal CYP3A4 protects against lithocholic acid-induced hepatotoxicity in intestine-specific VDR-deficient mice. *Journal of lipid research* **2014**, *55* (3), 455-65.
116. Xu, Y.; Hashizume, T.; Shuhart, M. C.; Davis, C. L.; Nelson, W. L.; Sakaki, T.; Kalhorn, T. F.; Watkins, P. B.; Schuetz, E. G.; Thummel, K. E., Intestinal and hepatic CYP3A4 catalyze hydroxylation of 1 α ,25-dihydroxyvitamin D(3): implications for drug-induced osteomalacia. *Molecular pharmacology* **2006**, *69* (1), 56-65.
117. Bain, C. C.; Mowat, A. M., Macrophages in intestinal homeostasis and inflammation. *Immunological Reviews* **2014**, *260* (1), 102-117.
118. Ding, X.; Kaminsky, L. S., Human extrahepatic cytochromes P450: function in xenobiotic metabolism and tissue-selective chemical toxicity in the respiratory and gastrointestinal tracts. *Annu Rev Pharmacol Toxicol* **2003**, *43*, 149-73.
119. Sprake, E. F.; Grant, V. A.; Corfe, B. M., Vitamin D3 as a novel treatment for irritable bowel syndrome: single case leads to critical analysis of patient-centred data. *BMJ case reports* **2012**, *2012*.
120. Teichert, A.; Arnold, L. A.; Otieno, S.; Oda, Y.; Augustinaite, I.; Geistlinger, T. R.; Kriwacki, R. W.; Guy, R. K.; Bikle, D. D., Quantification of the vitamin D receptor-coregulator interaction. *Biochemistry* **2009**, *48* (7), 1454-61.
121. Hakamata, W.; Sato, Y.; Okuda, H.; Honzawa, S.; Saito, N.; Kishimoto, S.; Yamashita, A.; Sugiura, T.; Kittaka, A.; Kurihara, M., (2S,2'R)-analogue of LG190178 is a major active isomer. *Bioorg Med Chem Lett* **2008**, *18* (1), 120-3.
122. Boehm, M. F.; Fitzgerald, P.; Zou, A.; Elgort, M. G.; Bischoff, E. D.; Mere, L.; Mais, D. E.; Bissonnette, R. P.; Heyman, R. A.; Nadzan, A. M.; Reichman, M.; Allegretto, E. A., Novel nonsecosteroidal vitamin D mimics exert VDR-modulating activities with less calcium mobilization than 1,25-dihydroxyvitamin D3. *Chem Biol* **1999**, *6* (5), 265-75.
123. Christakos, S.; Ajibade, D. V.; Dhawan, P.; Fechner, A. J.; Mady, L. J., Vitamin D: metabolism. *Endocrinology and metabolism clinics of North America* **2010**, *39* (2), 243-253.
124. Xu, C.; Li, C. Y.-T.; Kong, A.-N. T., Induction of phase I, II and III drug metabolism/transport by xenobiotics. *Archives of Pharmacol Research* **2005**, *28* (3), 249.
125. Bachmann, K., Chapter 8 - Drug Metabolism. In *Pharmacology*, Hacker, M.; Messer, W.; Bachmann, K., Eds. Academic Press: San Diego, 2009; pp 131-173.
126. Guengerich, F. P.; Liebler, D. C., Enzymatic activation of chemicals to toxic metabolites. *Critical reviews in toxicology* **1985**, *14* (3), 259-307.
127. Bikle, D. D., Vitamin D metabolism, mechanism of action, and clinical applications. *Chemistry & biology* **2014**, *21* (3), 319-329.
128. Stanley, L., Drug Metabolism. In *Pharmacognosy: Fundamentals, Applications, and Strategies*, Badal, S., and Delgoda, R, Ed. pp 527-545.
129. A. J. Hutt, J. C. a. R. L. S., The metabolism of aspirin in man: a population

- study. *Xenobiotica* **1986**, *16* (3), 239-249.
130. Liston, H., Markowitz JS, DeVane CL, Drug glucuronidation in clinical psychopharmacology. *J Clin Psychopharmacol* **2001**, *21* (5), 500-515.
131. *Overview of Vitamin D*; Institute of Medicine (US) Committee to Review Dietary Reference Intakes for Vitamin D and Calcium: Washington (DC), 2011.
132. Boyer, J. L., Bile formation and secretion. *Comprehensive Physiology* **2013**, *3* (3), 1035-1078.
133. Li, H.; He, J.; Jia, W., The influence of gut microbiota on drug metabolism and toxicity. *Expert opinion on drug metabolism & toxicology* **2016**, *12* (1), 31-40.
134. Pike, J. W.; B. Meyer, M., Chapter 63 - 1,25-Dihydroxyvitamin D3: Synthesis, Actions, and Genome-scale Mechanisms in the Intestine and Colon. In *Physiology of the Gastrointestinal Tract (Fifth Edition)*, Johnson, L. R.; Ghishan, F. K.; Kaunitz, J. D.; Merchant, J. L.; Said, H. M.; Wood, J. D., Eds. Academic Press: Boston, 2012; pp 1681-1709.
135. Wang, Z.; Schuetz, E. G.; Xu, Y.; Thummel, K. E., Interplay between vitamin D and the drug metabolizing enzyme CYP3A4. *The Journal of steroid biochemistry and molecular biology* **2013**, *136*, 54-58.
136. Nehring, J. A.; Zierold, C.; DeLuca, H. F., Lithocholic acid can carry out &em>in vivo functions of vitamin D. *Proceedings of the National Academy of Sciences* **2007**, *104* (24), 10006.
137. Cantorna MT, Y. S., Bruce D, The paradoxical effects of vitamin D on type 1 mediated immunity. *Mol Asp Med* **2008**, *29*, 369-375.
138. Price Evans, D. A., N-acetyltransferase. *Pharmacology & Therapeutics* **1989**, *42* (2), 157-234.
139. Hashem, H. Phase II (Conjugation Reactions).
140. Hayes, J. D.; Flanagan, J. U.; Jowsey, I. R., GLUTATHIONE TRANSFERASES. *Annual Review of Pharmacology and Toxicology* **2004**, *45* (1), 51-88.
141. Gamage, N.; Barnett, A.; Hempel, N.; Duggleby, R. G.; Windmill, K. F.; Martin, J. L.; McManus, M. E., Human Sulfotransferases and Their Role in Chemical Metabolism. *Toxicological Sciences* **2005**, *90* (1), 5-22.
142. King, C. D.; Rios, G. R.; Green, M. D.; Tephly, T. R., UDP-Glucuronosyltransferases. *Current Drug Metabolism* **2000**, *1* (2), 143-161.
143. Hofmann, A. F., THE FUNCTION OF BILE SALTS IN FAT ABSORPTION. THE SOLVENT PROPERTIES OF DILUTE MICELLAR SOLUTIONS OF CONJUGATED BILE SALTS. *Biochemical Journal* **1963**, *89* (1), 57.
144. Badenhorst, C. P. S.; van der Sluis, R.; Erasmus, E.; van Dijk, A. A., Glycine conjugation: importance in metabolism, the role of glycine N-acyltransferase, and factors that influence interindividual variation. *Expert Opinion on Drug Metabolism & Toxicology* **2013**, *9* (9), 1139-1153.
145. Dayal, B.; Rapole, K. R.; Patel, C.; Pramanik, B. N.; Shefer, S.; Tint, G. S.; Salen, G., Microwave-induced rapid synthesis of sarcosine conjugated bile acids. *Bioorganic & Medicinal Chemistry Letters* **1995**, *5* (12), 1301-1306.
146. Tserng, K. Y.; Hachey, D. L.; Klein, P. D., An improved procedure for the synthesis of glycine and taurine conjugates of bile acids. *Journal of lipid research* **1977**, *18* (3), 404-7.
147. Incerti, M.; Tognolini, M.; Russo, S.; Pala, D.; Giorgio, C.; Hassan-Mohamed, I.; Noberini, R.; Pasquale, E. B.; Vicini, P.; Piersanti, S.; Rivara, S.; Barocelli, E.; Mor, M.; Lodola, A., Amino Acid Conjugates of Lithocholic Acid As Antagonists of the EphA2 Receptor. *Journal of Medicinal Chemistry* **2013**, *56* (7), 2936-2947.
148. Kaburagi, Y.; Kishi, Y., Operationally Simple and Efficient Workup Procedure for TBAF-Mediated Desilylation: Application to Halichondrin Synthesis. *Organic Letters* **2007**, *9* (4), 723-726.

149. Everhart, E. T., A Convenient Procedure for Isolation of Alcohols After Cleavage of Protective Groups with Tetra-n-Butylammonium Fluoride AU - Craig, J. Cymerman. *Synthetic Communications* **1990**, *20* (14), 2147-2150.
150. Nakabayashi, M.; Tsukahara, Y.; Iwasaki-Miyamoto, Y.; Mihori-Shimazaki, M.; Yamada, S.; Inaba, S.; Oda, M.; Shimizu, M.; Makishima, M.; Tokiwa, H.; Ikura, T.; Ito, N., Crystal Structures of Hereditary Vitamin D-Resistant Rickets-Associated Vitamin D Receptor Mutants R270L and W282R Bound to 1,25-Dihydroxyvitamin D3 and Synthetic Ligands. *Journal of Medicinal Chemistry* **2013**, *56* (17), 6745-6760.
151. Everard, M. L., Aerosol therapy past, present, and future: a clinician's perspective. *Respir Care* **2000**, *45*, 769-776.
152. Montuschi, P.; Peters-Golden, M. L., Leukotriene modifiers for asthma treatment. *Clinical and experimental allergy : journal of the British Society for Allergy and Clinical Immunology* **2010**, *40* (12), 1732-41.
153. Lima, J. J.; Zhang, S.; Grant, A.; Shao, L.; Tantisira, K. G.; Allayee, H.; Wang, J.; Sylvester, J.; Holbrook, J.; Wise, R.; Weiss, S. T.; Barnes, K., Influence of leukotriene pathway polymorphisms on response to montelukast in asthma. *American journal of respiratory and critical care medicine* **2006**, *173* (4), 379-85.
154. Schumann, C.; Kropf, C.; Wibmer, T.; Rüdiger, S.; Stoiber, K. M.; Thielen, A.; Rottbauer, W.; Kroegel, C., Omalizumab in patients with severe asthma: the XCLUSIVE study. *The Clinical Respiratory Journal* **2012**, *6* (4), 215-227.
155. Abonia, J. P.; Putnam, P. E., Mepolizumab in eosinophilic disorders. *Expert review of clinical immunology* **2011**, *7* (4), 411-7.
156. Mizuta, K.; Xu, D.; Pan, Y.; Comas, G.; Sonett, J. R.; Zhang, Y.; Panettieri, R. A., Jr.; Yang, J.; Emala, C. W., Sr., GABAA receptors are expressed and facilitate relaxation in airway smooth muscle. *American journal of physiology. Lung cellular and molecular physiology* **2008**, *294* (6), L1206-16.
157. Xiang, Y. Y.; Wang, S.; Liu, M.; Hirota, J. A.; Li, J.; Ju, W.; Fan, Y.; Kelly, M. M.; Ye, B.; Orser, B.; O'Byrne, P. M.; Inman, M. D.; Yang, X.; Lu, W. Y., A GABAergic system in airway epithelium is essential for mucus overproduction in asthma. *Nature medicine* **2007**, *13* (7), 862-7.
158. Gallos, G.; Yim, P.; Chang, S.; Zhang, Y.; Xu, D.; Cook, J. M.; Gerthoffer, W. T.; Emala, C. W., Sr., Targeting the restricted alpha-subunit repertoire of airway smooth muscle GABAA receptors augments airway smooth muscle relaxation. *American journal of physiology. Lung cellular and molecular physiology* **2012**, *302* (2), L248-56.
159. Clayton, T.; Poe, M. M.; Rallapalli, S.; Biawat, P.; Savic, M. M.; Rowlett, J. K.; Gallos, G.; Emala, C. W.; Kaczorowski, C. C.; Stafford, D. C.; Arnold, L. A.; Cook, J. M., A Review of the Updated Pharmacophore for the Alpha 5 GABA(A) Benzodiazepine Receptor Model. *International journal of medicinal chemistry* **2015**, *2015*, 430248.
160. Gallos, G.; Yocum, G. T.; Siviski, M. E.; Yim, P. D.; Fu, X. W.; Poe, M. M.; Cook, J. M.; Harrison, N.; Perez-Zoghbi, J.; Emala, C. W., Sr., Selective targeting of the alpha5-subunit of GABAA receptors relaxes airway smooth muscle and inhibits cellular calcium handling. *American journal of physiology. Lung cellular and molecular physiology* **2015**, *308* (9), L931-42.
161. Hodges, R. R.; Dartt, D. A., Conjunctival Goblet Cells. In *Encyclopedia of the Eye*, Dartt, D. A., Ed. Academic Press: Oxford, 2010; pp 369-376.
162. Tanabe, T.; Kanoh, S.; Tsushima, K.; Yamazaki, Y.; Kubo, K., & Rubin, B., Clarithromycin inhibits interleukin-13-induced goblet cell hyperplasia in human airway cells. *American Journal of Respiratory Cell and Molecular Biology* **2011**, *45* (5), 1075-83.
163. Kim, V.; Kelemen, S. E.; Abuel-Haija, M.; Gaughan, J. P.; Sharafkaneh, A.; Evans, C. M.; Dickey, B. F.; Solomides, C. C.; Rogers, T. J.; Criner, G. J., Small airway mucous metaplasia and inflammation in chronic obstructive pulmonary disease. *Copd* **2008**, *5* (6), 329-38.

164. Ramerstorfer, J.; Furtmuller, R.; Vogel, E.; Huck, S.; Sieghart, W., The point mutation gamma 2F77I changes the potency and efficacy of benzodiazepine site ligands in different GABA(A) receptor subtypes. *European journal of pharmacology* **2010**, *636* (1-3), 18-27.

Curriculum Vitae

Olivia Brooke Yu

Education: **University of Wisconsin—Milwaukee** **Milwaukee, Wisconsin**
Ph.D. in Chemistry, May 2019 GPA: 4.0
Dissertation: “An Investigation of Calcitroic Acid and Its Phase II Conjugates”

The University of Chicago **Chicago, Illinois**
Master’s Degree in Chemistry, June 2014 GPA: 3.0

Grand Valley State University **Allendale, Michigan**
Bachelor of Science in Chemistry, Dec 2012 GPA: 3.88
Minor in Biology Honors College
Emphasis: Secondary Education

Research

Experience: **Investigation of Calcitroic Acid and Its Phase II Conjugates December 2014-May 2019**
University of Wisconsin—Milwaukee, Arnold Lab

- Tripled yield of challenging 13-step total synthesis of calcitroic acid by modifying route
- Synthesized novel phase II water-soluble conjugates of calcitroic acid
- Tested compounds using biochemical means: methods include Griess assay, HTRF assay, fluorescence polarization, PCR, etc.
- Maintained vacuums, pumps, columns, hoods and other laboratory equipment in good working condition
- Participated in regular presentation and discussion of work with laboratory personnel

Targeting Ovarian Cancer: Conjugating siRNA and hPL Protein June 2013-September 2013
The University of Chicago, Piccirilli Lab

- Synthetically conjugated siRNA to a recombinant polypeptide hormone that targets receptors on the surface of ovarian cancer cells
- Gathered initial promising results for siRNA silencing delivery in an ovarian cancer cell line

Modification of Phosphoramidites and Analysis by Crystallography May 2012-August 2012
University of Toledo, Bryant-Friedrich Lab
NSF REU Student Researcher

- Attained an NSF scholarship to do research as a guest student in a participating professor’s lab
- Modified DNA building blocks a sequence that was then analyzed by X-ray crystallography
- Received the National Science Foundation’s scholarship to do undergraduate research as a guest student in a participating professor’s laboratory.
- Learned about oxidative DNA damage and repair.

- Participated in small-molecule organic synthesis, DNA synthesis and analysis, and liquid crystal growth in the development and investigation of a xylose-sugar modified version of the Dickerson-Drew Dodecamer DNA sequence.
- Operated instruments including: Biotage automated column, temperature regulator, DNA synthesizer, MALDI-TOF, OPC columns, HPLC, Carey UV, and UV-Vis spectrometer.
- Received training for and implemented methods including: annealing, DNA synthesis, anaerobic conditions, ^{31}P -NMR, melting temperature analysis, and X-ray crystallography.

Organic Synthesis of TAAR Regulators

April 2011-June 2012

Grand Valley State University, Hart Lab

- Pursued the synthesis and purification of a proposed small molecule to investigate its properties as a regulator for the Trace Amine-Associated Receptor.
- Received instruction for and implemented: ^1H -NMR, ^{13}C -NMR, IR, gravity columns, refluxing, and recrystallization.

Organic Synthesis of Novel Antibacterials

January 2010-May 2010

GVSU Chemistry Department

- Worked from a general route to synthesize various small molecule antibiotics.
- Honed general laboratory procedural skills, such as filtration, dissolution, extraction, TLC, and basic characterization methods.

Instructional
Experience:

General Chemistry Teaching Assistant

August 2014-May 2019

University of Wisconsin—Milwaukee

- Taught numerous discussion and laboratory sections
- Revised laboratory manuals in Chemistry for Engineers class
- Implemented additional formative assessment measures for students
- Complied with restrictions for control and treatment classes employed by a professor for their educational research purposes

Organic Chemistry Teaching Assistant

September 2013-June 2014

The University of Chicago

- Worked closely with a small undergraduate class teaching their lecture and laboratory over the course of a school year
- Dealt with entitlement complexes in highly privileged young adults
- Adapted curriculum to suit the non-standard quarter system

Long-term Substitute Teacher

December 2012-March 2013

Freedom Christian School

- Diversified lesson format to better assist several students with accommodations
- Adapted lessons from the primary teacher to enhance student learning and meet benchmarks
- Motivated sophomores through seniors at small private high school on to higher achievement
- Followed along with the usual teachers' lessons, altering them to suit my teaching style
- Worked with very small classroom sizes
- Diversified lessons in high school physics and chemistry to suit several students with accommodations

Student Teacher**August 2012-December 2012***Union High School*

- Developed an understanding of the particular challenges facing inner-city and underfunded schools
- Created a hands-on curriculum for high school biology and chemistry classes
- Underwent many professional development sessions
- Worked with very large class sizes
- Developed trust and made peace in diverse classrooms during difficult racial tensions
- Perfected practice with classroom management techniques

Teacher Assistant**January 2012-April 2012***Grandville Middle School*

- Gained insight to the instruction, management, and atmosphere of a middle school classroom.
- Developed professional relationships with cooperating teachers, staff, and students.

Structured Learning Assistance Facilitator**August 2010-December 2011***Grand Valley State University*

- Managed a classroom of college freshmen.
- Created worksheets and walk-throughs conducive to helping struggling students master general chemistry.

Small Group Leader**August 2009-April 2012***InterVarsity Christian Fellowship, USA: Grand Valley Chapter*

- Co-led in-depth studies of scripture with college students of all ages.
- Fostered nurturing, caring, and supportive small group communities committed to building up leaders and reaching out to our campus and community.

In-Class Tutor**Summer 2011***Gerald R. Ford Job Corps Center*

- Assisted teacher with in-class one-on-one tutoring.
- Developed a respect for and an understanding of inner-city school culture.

Publications:

- Teske, K. A.; Bogart, J. W.; Sanchez, L. M.; **Yu, O. B.**; Preston, J. V.; Cook, J. M.; Silvaggi, N. R.; Bikle, D. D.; Arnold, L. A., "Synthesis and evaluation of vitamin D receptor-mediated activities of cholesterol and vitamin D metabolites." *European Journal of Medicinal Chemistry*, **2016**, 109, 238-246.
- Kelly A. Teske, **Olivia B. Yu**, and Leggy A. Arnold, "Inhibitors for the Vitamin D Receptor–Coregulator Interaction" *Vitamin and Hormones* **2016**, 100, 45-82.
- Gloria S. Forkuo, Margaret L. Guthrie, Nina Y. Yuan, Amanda N. Nieman, Revathi Kodali, Rajwana Jahan, Michael R. Stephen, Gene T. Yocum, Marco Treven, Michael M. Poe, Guanguan Li, **Olivia B. Yu**, Benjamin D. Hartzler, Nicolas M. Zahn, Margot Ernst, Charles W. Emala, Douglas C. Stafford, James M. Cook, and Leggy A. Arnold "Development of GABA_A Receptor Subtype-

Selective Imidazobenzodiazepines as Novel Asthma treatments” *Molecular Pharmaceutics* **2016**, 13, 2026-23038.

- **Olivia B. Yu** and Leggy A. Arnold, “Calcitroic Acid—A Review.” *ACS Chem. Biol.* **2016**, 11(10), pp 2665-2672
- Forkuo, G. S.; Nieman, A. N.; Yuan, N. Y.; Kodali, R.; **Yu, O. B.**; Zahn, N. M.; Jahan, R.; Li, G.; Stephen, M. R.; Guthrie, M. L.; Poe, M. M.; Hartzler, B. D.; Harris, T. W.; Yocum, G. T.; Emala, C. W.; Steeber, D. A.; Stafford, D. C.; Cook, J. M.; Arnold, L. A., “Alleviation of Multiple Asthmatic Pathologic Features with Orally Available and Subtype Selective GABA_A Receptor Modulators.” *Molecular pharmaceutics* **2017**, 14 (6), 2088-2098.
- Jahan, R.; Stephen, M. R.; Forkuo, G. S.; Kodali, R.; Guthrie, M. L.; Nieman, A. N.; Yuan, N. Y.; Zahn, N. M.; Poe, M. M.; Li, G.; **Yu, O. B.**; Yocum, G. T.; Emala, C. W.; Stafford, D. C.; Cook, J. M.; Arnold, L. A., “Optimization of substituted imidazobenzodiazepines as novel asthma treatments.” *European Journal of Medicinal Chemistry* **2017**, 126, 550-560.
- **Olivia B. Yu** and Leggy A. Arnold, "Modulating Vitamin D Receptor–Coregulator Binding with Small Molecules." *Vitamin D, Volume 2, Health, Disease, and Therapeutics, Fourth Ed.* **2018**, 90, 657-664
- Gloria S. Forkuo, Amanda N. Nieman, Revathi Kodali, Nicolas M. Zahn, Guanguan Li, M. S. Rashid Roni, Michael Rajesh Stephen, Ted W. Harris, Rajwana Jahan, Margaret L. Guthrie, **Olivia B. Yu**, Janet L. Fisher, Gene T. Yocum, Charles W. Emala, Douglas A. Steeber, Douglas C. Stafford, James M. Cook, and Leggy A. Arnold, “A novel orally available asthma drug candidate that reduces smooth muscle constriction and inflammation by targeting GABA_A receptors in the lung.” *Molecular Pharmaceutics* **2018**, 15, 1766–1777.
- Tania Mutchie, **Olivia B. Yu**, Elliot Di Milo, Leggy A. Arnold, “Alternative binding sites at the vitamin D receptor and their ligands.” *Molecular and Cellular Endocrinology* **2019**, 485, 1-8.

Awards and Presentations:

- “Apparent ζ -potential as a tool to assess mechanical damages to the milk fat globule membrane.” Junior Seminar. Padnos Hall of Science 225, Grand Valley State University. 3/22/2011. (oral presentation)
- "Synthesis of Antibacterial Compound Library." Olivia White, Hart & Winchester Lab. Padnos Hall, Student Scholars Day, Grand Valley State University. 04/13/2011. (poster)
- “Regioselective Nucleophilic Ring-Opening of Aziridines in the Synthesis of T1AM Analogues.” Olivia White and Jeremy Whitmore, Hart Lab. San Diego Conference Center, 243rd ACS National Meeting. 03/26/2012. (poster)
- “Regioselective Nucleophilic Ring-Opening of Aziridines in the Synthesis of T1AM Analogues.” Olivia White, Hart Lab. Manitou Hall 123, Grand Valley State University, Undergraduate Research Symposium. 04/02/2012. (presentation)
- National Science Foundation Research Experience for Undergraduates Scholarship Recipient: Awarded 04/17/2012, for Summer 2012, University of Toledo. (award)
- “Synthesis of 2'-Deoxyxylothymidine Phosphoramidite and Incorporation into Oligonucleotides for Crystal Structure Analysis.” Olivia White, Bryant-Friedrich Lab. Bowman-Oddy Hall, University of Toledo. 08/02/2012. (presentation)
- “Development of a Direct VDR Binding Assay Based on Fluorescence Polarization.” Olivia Yu, Arnold Lab. Union Ballroom, University of Wisconsin—Milwaukee, Chemistry and Biochemistry Research Symposium. 04/03/2015. (poster)
- “Organic Carbamates in Medicinal Chemistry and Drug Design.” Olivia Yu, Arnold Lab. Chemistry 180, University of Wisconsin—Milwaukee. 11/13/2015. (presentation)

- “Synthesis of Calcitroic Acid to Determine its Potential for Prevention of Colon Cancer.” Olivia Yu, Arnold Lab. University of Madison, International Chemical Biology Society. 10/25/2016. (poster)
- “Synthesis of Calcitroic Acid to Determine its Potential for Prevention of Colon Cancer.” Olivia Yu, Arnold Lab. Union Ballroom, University of Wisconsin—Milwaukee, Graduate Student Research Symposium. 10/28/2016. (poster)
- “Investigation of the Biological Function of Calcitroic Acid and Its Phase Two Metabolites.” Olivia Yu, Elliot Di Milo, Viktoriia Senych, Kelly A Teske, Leggy A Arnold. Rosen Center, Orlando, Vitamin D Conference. 03/31/2017 (poster)
- “Investigation of the Biological Function of Calcitroic Acid and Its Phase Two Metabolites.” Olivia Yu, Elliot Di Milo, Viktoriia Senych, Kelly A Teske, Leggy A Arnold. Union Ballroom, University of Wisconsin—Milwaukee, Chemistry and Biochemistry Research Symposium. 05/23/2017. (poster)
- “Calcitroic Acid and the Vitamin D Receptor.” Olivia Yu. Kenwood Interdisciplinary Research Complex, University of Wisconsin—Milwaukee, Nobel Graduate Student Symposium. 09/29/2017 (distinguished presentation)
- “Investigating Calcitroic Acid, Its Phase Two Metabolites, and Their Biological Function,” Olivia Yu, Elliot Di Milo, Leggy A Arnold. Barcelona International Convention Center, Barcelona, Spain. 05/17/2018. (poster)
- “Investigating Calcitroic Acid, Its Phase Two Metabolites, and Their Biological Function,” Olivia Yu, Elliot Di Milo, Leggy A Arnold. Kenwood Interdisciplinary Research Complex Hall, Milwaukee Analytical Chemistry Conference. 01/25/2019. (poster)
- “Investigating Calcitroic Acid and Its Phase Two Metabolites,” Olivia Yu. Kenwood Interdisciplinary Research Complex 2175, Final Dissertation Defense. 04/22/2019 (oral presentation)